Australian Government
Geoscience Australia

An assessment of the uranium and geothermal potential of north Queensland

Record
2010/14

DL Huston (editor) with contributions by
B Ayling, D Connolly, DL Huston, B Lewis, TP Mernagh, A Schofield, RS Skirrow, and SE van der Wielen

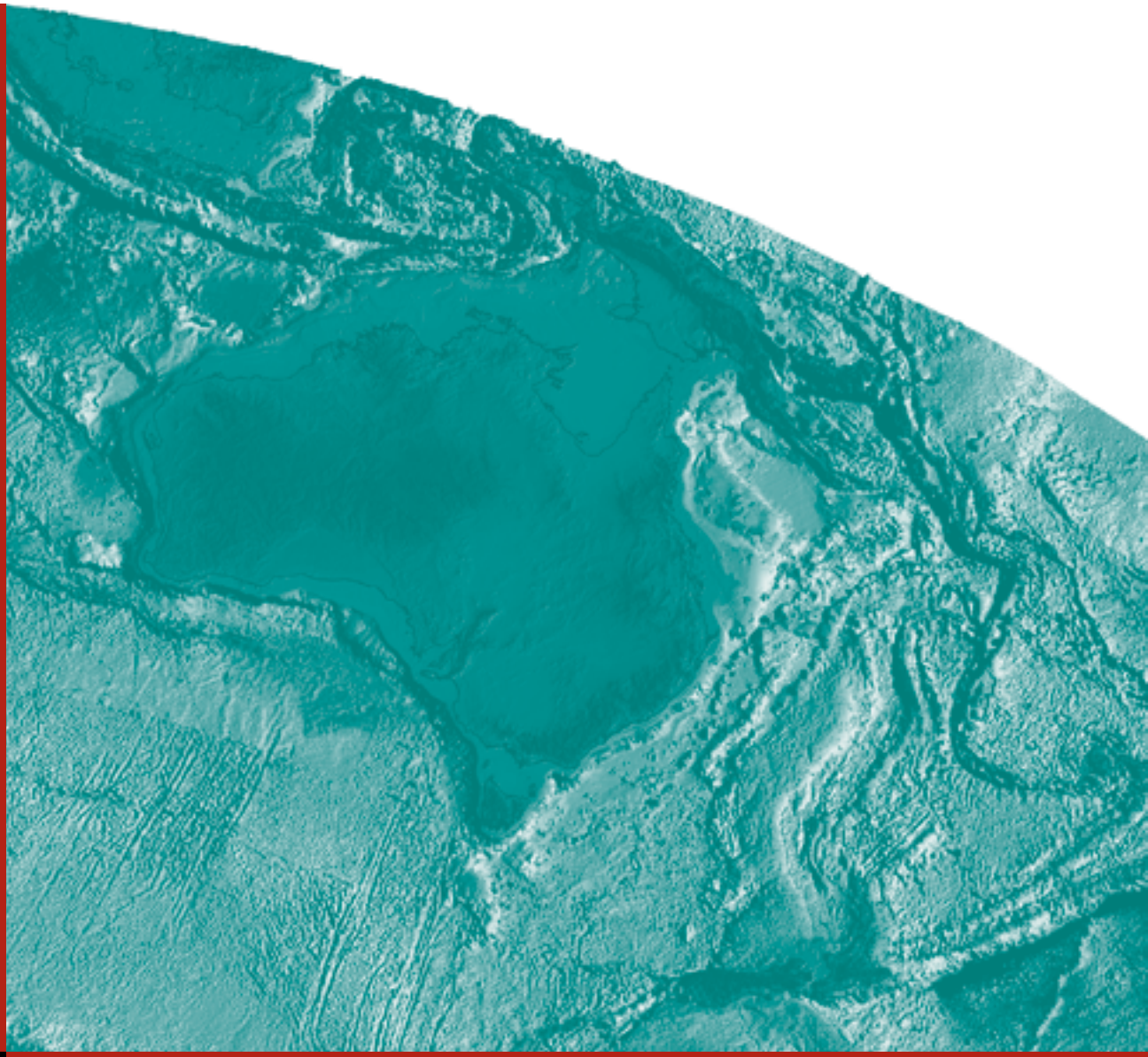

An assessment of the uranium and geothermal potential of north Queensland

GEOSCIENCE AUSTRALIA
RECORD 2010/14

Edited by

DL Huston

With contributions by B Ayling, D Connolly, DL Huston, B Lewis, TP Mernagh, A Schofield, RS Skirrow, and SE van der Wielen

1. Geoscience Australia, GPO Box 378, Canberra, ACT 2601

Department of Resources, Energy and Tourism
Minister for Resources and Energy: The Hon. Martin Ferguson, AM MP
Secretary: Mr John Pierce

Geoscience Australia
Acting Chief Executive Officer: Dr Chris Pigram

ISSN 1448-2177
ISBN 978-1-921672-82-8

GeoCat # 69711

Bibliographic reference: Huston, DL. (ed) 2010. An assessment of the uranium and geothermal potential of north Queensland. Geoscience Australia Record 2010/14.

Contents

EXECUTIVE SUMMARY 1

1. INTRODUCTION 2

2. REGIONAL GEOLOGY 2

2.1. Late Paleoproterozoic to early Mesoproterozoic 2
2.2. Late Neoproterozoic through Phanerozoic 6

3. URANIUM MINERAL SYSTEMS 7

3.1. Sandstone-hosted uranium systems 10
3.1.1. Regional geology and sandstone-hosted uranium systems 10
3.1.2. Sandstone-hosted uranium systems models 12
3.1.3. Results of assessment analysis for sandstone-hosted uranium systems 16
3.2. Unconformity-related uranium systems 17
3.2.1. Westmoreland uranium field 20
3.2.2. Maureen deposit 22
3.2.3. Ben Lomond deposit 24
3.2.4 Mineral system model for unconformity uranium systems 25
3.2.5. Results of assessment analysis for unconformity-related uranium systems 30
3.3. Metasomatic uranium systems 31
3.3.1. The Mount Isa uranium field 32
3.3.2. Mineral system model for Mount Isa uranium field 36
3.3.3. Results of assessment analysis for metasomatic uranium systems 41
3.4. Uranium-rich iron-oxide copper-gold systems 42
3.4.1. The Cloncurry district 42
3.4.2. The Einasleigh district 46
3.4.3. Mineral system model for uranium-rich iron oxide copper-gold systems 47
3.4.4. Results of assessment analysis for uranium-rich iron oxide copper-gold systems 53
3.5. Magmatic-related uranium systems 54
3.5.1. Orthomagmatic uranium systems 54
3.5.2. Magmatic-hydrothermal uranium systems 60

4. GEOTHERMAL SYSTEMS 68

4.1. Hot rock systems 70
4.1.1. Hot Rock Geothermal Model & Datasets 70
4.1.2. North Queensland Hot Rock Observations 76
4.1.3. Hot Rock Potential Analysis: Results & Interpretation 79
4.2. Hot sedimentary aquifer systems 80
4.2.1. Hot Sedimentary Aquifer Model and Datasets 80
4.2.2. North Queensland Hot Sedimentary Aquifer Observations 82
4.2.3. HSA Potential Analysis: Results & Interpretation for north Queensland 88

5. SYNTHESIS AND CONCLUSIONS 92

REFERENCES 95

APPENDIX A -- TABLES SUMMARISING CHARACTERISTICS OF URANIUM MINERAL SYSTEMS 104

SANDSTONE-HOSTED URANIUM ± VANADIUM 104

UNCONFORMITY-RELATED URANIUM 105

METASOMATIC URANIUM 106

URANIUM-BEARING IRON OXIDE COPPER-GOLD 106

ORTHOMAGMATIC URANIUM 108

MAGMATIC-HYDROTHERMAL URANIUM 108

Executive summary

The uranium and geothermal energy potential of north Queensland has been assessed using a geosystems approach as part of the Australian Government's Onshore Energy Security Program. Four types of uranium mineral systems are known to have produced significant uranium-bearing deposits in north Queensland: (1) unconformity-related deposits (Westmoreland), including deposits traditionally classified as volcanic-related (Maureen and Ben Lomond: see section 3.2), (2) metasomatic deposits (Mount Isa uranium field), (3) uranium-bearing iron oxide copper-gold deposits, and (4) magmatic-hydrothermal deposits (Mary Kathleeen). In addition, sandstone-hosted uranium mineral systems may have produced uranium accumulations in the Mesozoic to Cenozoic Eromanga and Carpentaria basins based on analogies with the Frome Embayment in South Australia. Based on the characteristics of known deposits and the geology of north Queensland, a modified pmd*CRC five-questions approach to mineral system analysis was used to identify areas considered to have potential for uranium mineralisation. This analysis identified known uranium districts and identified other areas as having significant potential.

Three areas were identified as having significant potential for sandstone-hosted deposits in the Eromanga and Carpentaria Basins:

- an area east of Cloncurry,
- an area 90 km north of Hughenden, and
- an area around the township of Richmond.

Parts of the Burdekin Basin and immediately underlying units were identified as having potential for unconformity-related deposits. Outside of known uranium districts, the following areas were identified as having greatest uranium potential within Proterozoic and Paleozoic rocks:

- extensions of the Mount Isa uranium field to the north and south along bounding faults to the Leichhardt River Fault Trough (for unconformity-related and metasomatic uranium deposits),
- extensions of the Cloncurry iron-oxide copper-gold district undercover to the south and, particularly, to the north along the inferred eastern boundary of the Mount Isa Province (for uranium-rich iron oxide copper-gold deposits), and
- a 50 km wide by 200 km long, northwest trending belt southwest of Cairns (for metasomatic and/or iron-oxide copper-gold deposits).

Although other areas were also identified in the analysis as having potential, those listed above are considered most prospective in that they either extend known districts under cover or were identified independently by analysis of more than one uranium system. As a check on the veracity of the process, our analysis also identified known uranium districts as having high potential.

A systems approach has also been applied to assess the geothermal potential of north Queensland. Although no geothermal systems have yet been commercially developed in north Queensland, theoretical considerations and analogies with systems in South Australia and elsewhere were used to identify essential elements for geothermal systems. Prospectivity assessments for Hot Rock and Hot Sedimentary Aquifer systems identified similar geographic areas with high potential, including:

- the Millungera Basin,
- the Eromanga Basin,
- the northwest part of the Carpentaria Basin, near Burketown,
- the north-central Drummond Basin, and
- the Galilee Basin.

1. Introduction

As part of the Onshore Energy Security Programme, Geoscience Australia has undertaken a series of energy potential assessments, both on a national scale and on a regional scale in association geological framework studies. These framework studies, which are designed to provide information on geodynamic and architectural controls on energy systems, are linked to the acquisition of deep seismic, magnetotelluric and airbourne electromagnetic data. The focus of fiscal year 2008-2009 was north Queensland, stretching from the Northern Territory border to the coast, between 17° and 22° south latitude[1]. In addition to the seismic data acquisition and interpretation, these framework studies have included geochronological studies as well as uranium mineral system and geothermal system studied in collaboration with the Uranium and Geothermal Projects. The main goal of these studies is to provide background data that can be used by industry for exploration, however the data also provide new information that can be used in assessing the potential of north Queensland for uranium and geothermal resources using geosystems (i.e. mineral and geothermal systems) methodologies in a GIS environment. This report provides such an assessment in a qualitative to semi-quantitative way. One of the goals of this analysis is to define the extent of areas or regions with known deposits; another goal was to define areas with previously unrecognised potential.

2. Regional geology

The geology of north Queensland (Fig. 1), though complex, can be simplified into two major periods: the late Paleoproterozoic to the early Mesoproterozoic (1900-1500 Ma), which involved the growth (and cratonisation of the Mount Isa and Georgetown Provinces, and the late Neoproterozoic through the Phanerozoic (800 Ma-present), which initiated with Rodinia break-up, followed by rifting and accretion to form the Tasman Orogen and the the development of the intracontinental Great Artesian Basin system. This section provides a brief overview of this history. Some of the following sections provide additional details where needed, and Kositcin et al. (2009) provide a comprehensive account of the geological history of north Queensland.

2.1. LATE PALEOPROTEROZOIC TO EARLY MESOPROTEROZOIC

The oldest dated rocks in north Queensland are granites within the basement (i.e. pre-1800 Ma basement: Fig. 2) rocks that for the most part are restricted to the Kalkadoon-Leichhardt Belt of the Mount Isa Province and the Murphy Inlier. This Kalkadoon-Leichhardt Belt, which consists of mostly of migmatitic to gneissic supracrustal rocks, was intruded by ~1860-1850 Ma granites (Bierlein et al., 2008) associated with felsic volcanics (Betts and Giles, 2006), providing a minimum age for this belt. These basement rocks are overlain by a series of three superbasins that form the Eastern and Western Foldbelts in the Mt Isa Province. The oldest superbasin, the Leichhardt Superbasin (Fig. 2), was deposited between ~1800 Ma and 1750 Ma (Page et al., 2000) and contains a rift fill dominated by a thick pile of continental tholeiites (Eastern Creek Volcanics) and fluvial to lacustrine siliciclastic and lesser carbonate rocks (Jackson et al., 2000). Gibson et al. (2008) inferred that this basin formed as a result of ENE-WSW-directed extension (see also Betts and Giles, 2006). In the western part of the Mount Isa Province (mostly to the west of the Kalkadoon-Leichhardt Belt), the Calvert Superbasin (Fig. 2), which overlies the Leichhardt Superbasin, was deposited between 1730 Ma and 1695 Ma (Page et al., 2000). The superbasin consists of continental to shallow marine

[1] This region includes geographically northwest Queensland and most of the north Queensland region of Bain and Draper (1997).

siliciclastic and carbonate rocks, including red beds, that are interlayered with intrusive and extrusive felsic and mafic volcanic rocks that were deposited in a rift environment (Jackson et al., 2000). The volcanic rocks are erupted over an extended time range from ~1730-1720 Ma in the Peters Creek Volcanics to ~1709 Ma for the Fiery Creek Volcanics. Gibson et al. (2008) inferred that this basin formed as a consequence of a NE-SW to ENE-WSW extension direction, possibly initiating with the Wonga extensional event that was accompanied by the emplacement of ~1740 Ma syn-kinematic granites (Holcombe et al., 1991; Gibson et al., 2008).

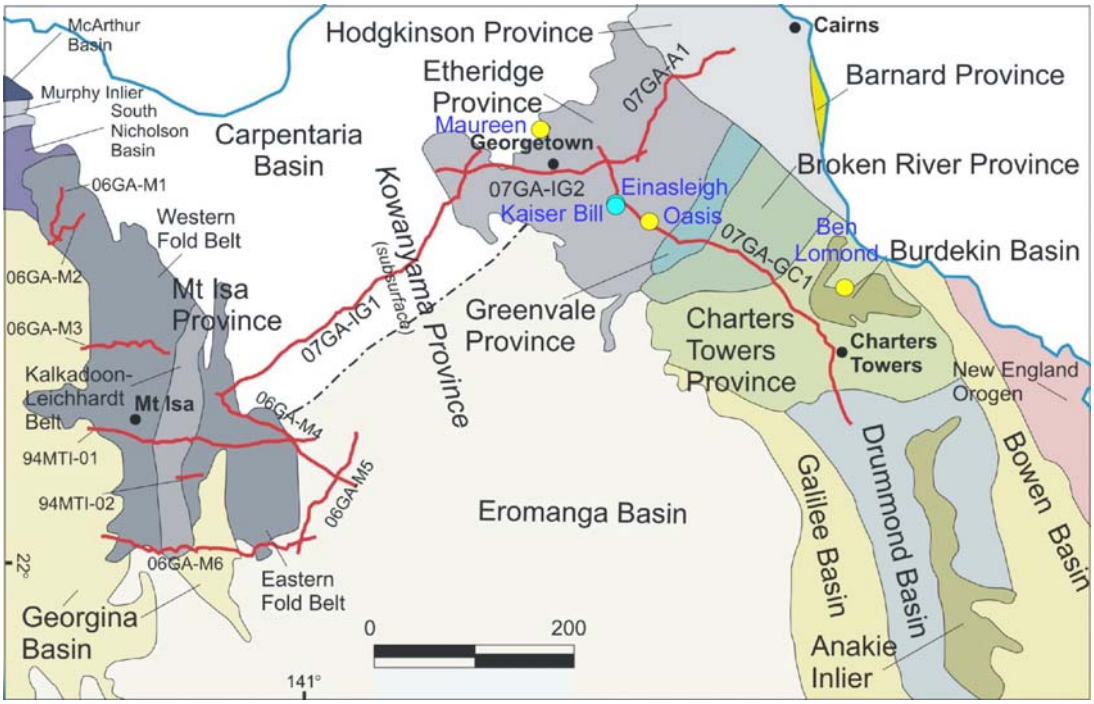

Figure 1: *Geological elements of north Queensland showing the locations of deep crustal land seismic traverses and selected uranium (yellowcircles) and uranium-bearing iron oxide copper-gold (light blue circles) deposits..*

However, the relationship of rocks in the eastern part of the Mount Isa Province (i.e. the Soldiers Cap Group: Fig. 2) to the Calvert Superbasin during Calvert-time is more complex. Rocks in this area, although generally included in the Calvert Superbasin (Murphy et al., 2008), are dominated by deep water turbidites that contain mafic intrusive and extrusive igneous rocks and minor felsic volcanic rocks (Beardsmore et al., 1988). These rocks, which form the Soldiers Cap Group, are, at ~1676 Ma (Page and Sun, 1998), younger than the shallow marine part of the Calvert Superbasin to the west and correspond in time with development of the Gun unconformity and the emplacement of the Sybella and related granites in the western Mount Isa Province (Neumann et al., 2009).

The third superbasin, the 1665-1595 Ma Isa Superbasin (Fig. 2: Page et al., 2000; Neumann et al., 2006; equivalent to the McArthur Basin), overlies the Calvert Superbasin and rocks of the Soldiers Cap Group. The older part of the basin contains fluviatile to shallow marine sandstone, siltstone and dolomite with subordinate black shale and minor felsic volcanism ("pinkites": tuffs and peperites), whereas the younger part of the superbasin comprises up to 8 km of turbidites, carbonaceous shales and stromatolitic dolostones deposited in a shallow to deep marine environment (Hutton and Sweet, 1982; Southgate et al., 2000; Betts and Giles, 2006). The South Nicholson Basin overlies the Isa Superbasin to the northwest.

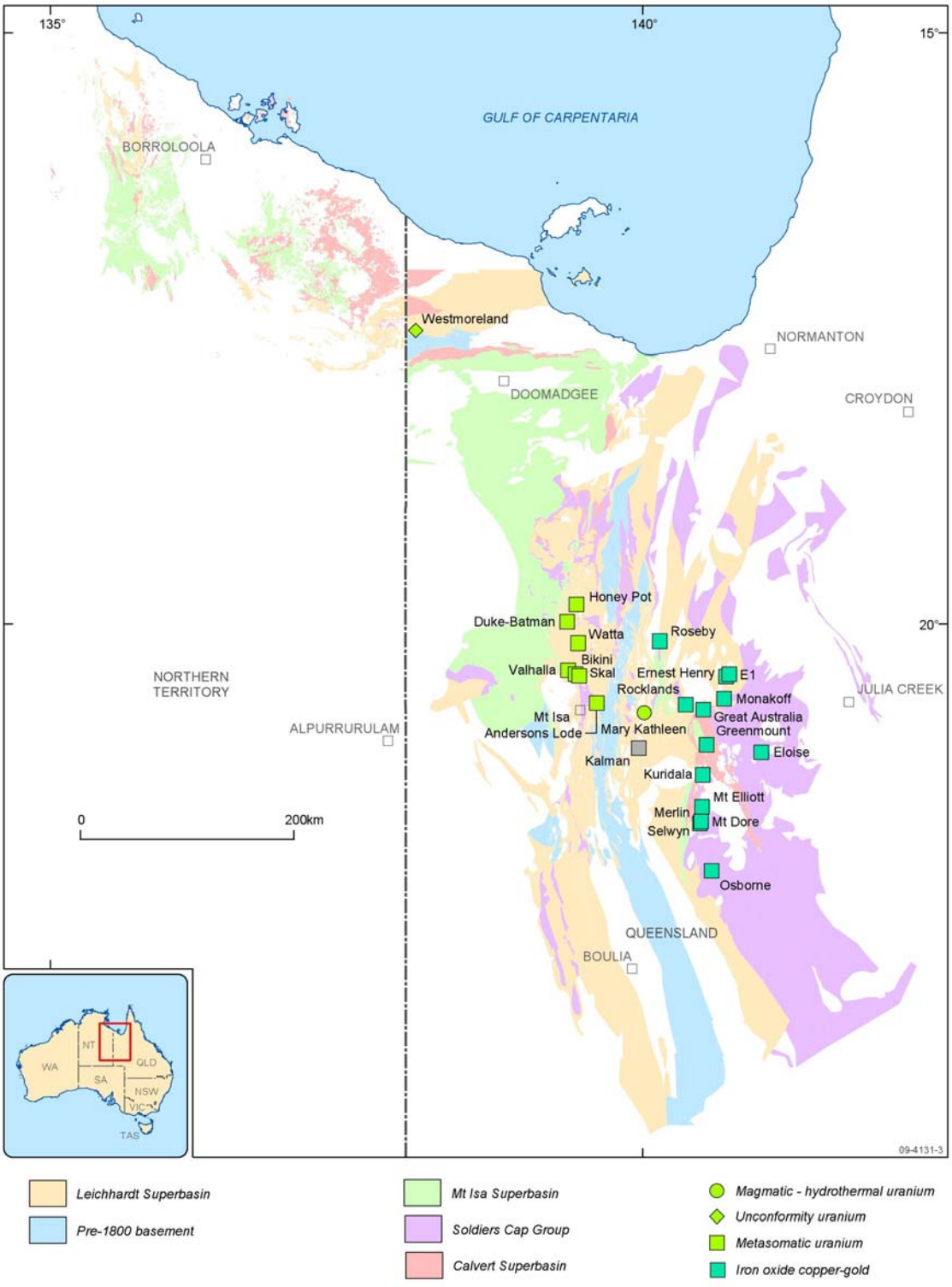

Figure 2: *Geological map of Paleo- to Mesoproterozoic basins of northeast Australia showing the locations of known uranium and iron-oxide copper-gold deposits and prospects.*

Rocks of the Mount Isa Province were subjected to four phases of contractional deformation associated with the 1640-1500 Ma Isan Orogeny. The earliest deformation (D_1[2]) began at ~1640 Ma and involved north-directed thin-skinned thrusting, possibly associated with the accretion of the Warumpi Province along the southern margin of the North Australian Craton (Scrimgeour et al., 2005). The main period of deformation (D_2) began at 1600 Ma, and extended to 1565 Ma (Connors and Page, 1995; Giles and Nutman, 2002; Hand and Rubatto, 2002; Rubenach, 2008). This event was characterised by thrust development within an east-west contractional regime (Murphy et al., 2008). This was followed by brittle D_3 structures formed under southeast-northwest contraction at ~1550 Ma (though poorly dated: Connors and Page, 1995; Hand and Rubatto, 2002; Betts and Giles, 2006) and then by localised D_4 deformation associated with the emplacement of the Naruku-Williams Granite Suite between 1530 and 1500 Ma (Rubenach, 2008).

The Etheridge Province forms the easternmost extent of Paleo- to Mesoproterozoic rocks in north Queensland, and is bound on the east by Neoproterozoic and younger rocks (Fig. 1). Based on similar lithologies and similar age data, the Etheridge Group, which forms the basal known unit in the Etheridge Province, has been correlated with the Soldiers Cap Group in the Mount Isa Province and interpreted to have formed in an extensional basin (Gibson et al., 2008). The Kowanyama Province (Fig. 1) is interpreted to link these two provinces underneath Mesozoic cover. Exposed rocks in the Etheridge Provinces have a large range in metamorphic grade, with rocks in the east (Einasleigh Metamorphics) characterised by high grade (amphibolite and granulite facies) whereas rocks to the west (Etheridge and Langlovale Groups) are of much lower (greenschist and sub-greenschist facies) grade. Lithological units within the lower Etheridge Group (Robertson River Subgroup) can be traced across metamorphic gradients into the Einasleigh Metamorphics, suggesting partial correlation (Withnall et al., 2009).

In the western part of the Etheridge Province, the Etheridge Group is overlain unconformably by sandstone, mudstone and shale of the ~1625 Ma (maximum depositional age) Langlovale Group (Withnall et al., 1997, 2009; N. Neumann, unpublished data). These rocks are overlain unconformably by felsic ignimbrites of the Croydon Volcanic Group, which has an age of ~1552 Ma (Black and McCulloch, 1990) and is coeval, with magmatic rocks of the 1560-1550 Ma Esmeralda and Forsayth Supersuites (Black et al., 1998, 2005).

The deformation history of the Etheridge Province is complex, and studies of this history have resulted in conflicting results in some cases. Based on a synthesis of available studies, Withnall et al. (2009) proposed the following Proterozoic geological history: (1) 1710-1675 Ma deposition of lower part of Einasleigh Metamorphics; (2) ~1675 Ma (possibly as old as 1695 Ma) deformation and metamorphism in the lower part of the Einasleigh Metamorphics; (3) 1665-1620 Ma deposition of the Roberston River Subgroup and uppermost Etheridge Group; (4) north-south shortening at ~1620 Ma (D_1); (5) 1625-1590 Ma deposition of the Langlovale Group; (6) east-west shortening at ~1590 Ma (D_2), (7) uplift and retrogressive metamorphism between 1590 and 1560 Ma, (8) northwest-southeast shortening accompanied by low pressure, high temperature metamorphism and emplacement of the Forsayth Supersuite at 1560-1550 Ma (D_3), (9) eruption of the Croydon Volcanic Group and emplacement of the Esmeralda Supersuite at ~1550 Ma, and (10) deformation at ~1510 Ma (D_4). The deformation history in many ways is similar to that seen in the Mount Isa Province.

[2] In this report we have adopted the structural nomenclature of Murphy et al. (2008), who recognised an earlier phase of deformation than previous workers (e.g. Betts and Giles, 2006).

2.2. LATE NEOPROTEROZOIC THROUGH PHANEROZOIC

With the exception of deposition of late Neoproterozoic sedimentary rocks in the Georgina Basin in the west (Fig. 1) and minor mafic magmatism, the period between 1500 and 600 Ma appears to have been geologically quiescent in North Queensland, with geological activity restarting at about 600 Ma with the initiation of the first of three orogenic systems associated with convergence from the east. The first of these, the Thomson Orogen, which includes the Greenvale and Charters Towers provinces and the Anakie Inlier, abuts Paleo- to Mesoproterozoic rocks of the Etheridge Province to the northwest (Fig. 1). Henderson and Withnall (2009) indicate that this orogen began with the development of a Neoproterozoic passive margin that initiated with the break-up of Rodinia. Beginning in the late Cambrian and continuing into the early Ordovician (500-460 Ma), this passive margin was overprinted by an active continental margin, resulting initially in contraction associated with the 520-490 Ma Delamarian Orogeny. Although this orogeny is better developed in southeastern Australia, it has been recognised in the vicinity of Charters Towers and Greenvale (Fergusson et al., 2007). Following the Delamarian Orogeny, the passive margin went into extension during west-dipping subduction. Subduction and associated extension to form backarc volcanosedimentary basins continued between 480 and 460 Ma and was accompanied by magmatism of the Macrossan Association (Henderson and Withnall, 2009). This period of extension was terminated by the ~430 Ma Benambran Orogeny.

Following the Benambran Orogeny, northeastern Queensland was characterised by extensive marine sedimentation dominated by siliciclastic rocks and carbonates, with local tholeiitic mafic volcanism in the Broken River and Hodgkinson Provinces, forming the Mossman (Henderson and Withnall, 2009), or North Queensland (Kositcin et al., 2009), Orogen. This sedimentation was contemporaneous with the emplacement of voluminous I- and S-type and lesser mafic magmatism of the 430-380 Pama Association (Bain and Draper, 1997). This magmatic assemblage forms a quasi-continuous belt around the Hodgkinson and Broken River Provinces (Kositcin et al., 2009). This phase of north Queensland evolution was terminated by the ~360 Ma Tabberraberran Orogeny.

The last major orogenic assemblage in north Queensland was the New England Orogen, which is widely developed along the eastern coast of Australia between north-central Queensland and northern New South Wales. In north Queensland, this orogen is associated with localised backarc basins that were developed upon the Thomson Orogen, including the early (Late Devonian to Early Carboniferous) Drummond and Burdekin basins and the later (latest Carboniferous to Late Triassic) Galilee and Bowen basins. The later basins overlapped in with time extensive magmatism of the Kennedy Association (Henderson and Withnall, 2009; Kositcin et al., 2009). The New England Orogen was affected by contraction during the 360-340 Ma Kanimblan Orogeny and was terminated by the 265-230 Ma Hunter-Bowen Orogeny (Kositcin et al., 2009). After the end of the Hunter-Bowen Orogeny, eastern Australia is charaterised by a series of backarc basins associated with subduction well offshore (Gurnis et al., 1998). The main basin developed during this time is the early Jurassic to mid-Cretaceous Carpentaria-Eromanga-Laura basin system. The Carpentaria and Eromanga basins form extensive, though generally thin, cover on Proterozoic rocks of the Isa and Etheridge Provinces.

3. Uranium mineral systems

Between 1958-1963 and 1976-1982, the Mary Kathleen mine in the eastern part of the Mt Isa Inlier (Fig. 2) produced 8.882 kt of U_3O_8 (with remnant ore containing 1.200 kt U_3O_8), making it Australia's largest U producer during these periods (McKay and Miezitis, 2001). Exploration during uranium booms between the 1950s and 1970s identified a number of other significant deposits (Table 1), including Valhalla and nearby deposits (Skal, Bikini, Duke Batman and Honey Pot: 43.5 kt U_3O_8) in the north-central Mt Isa Inlier, the Westmoreland group of deposits along the Murphy Inlier (23.6 kt U_3O_8), the Maureen deposit near Georgetown (4.5 kt U_3O_8), the Ben Lomond deposit (4.9 kt U_3O_8) west of Townsville, and several smaller deposits near Mt Isa (Andersons: 2.0 kt U_3O_8; and Watta: 1.7 Kt U_3O_8: Fig. 2). In addition to these established resources, some of iron-oxide copper-gold deposits in the Cloncurry district, in the eastern Mt Isa Province contain anomalous, though not ore grade, uranium concentrations. For example, the Ernest Henry deposit averages 50 ppm U (Ryan, 1998). Moreover, a large number of uranium-bearing mineral occurrences and prospects are known throughout north Queensland, including additional prospects in the Proterozoic Murphy, Mt Isa and Georgetown Inliers, in Paleozoic cover rocks and in the Mesozoic to Cenozoic Eromanga-Carpentaria Basin.

Table 1: Historical production and identified mineral resources of uranium deposits in north Queensland.

Deposit	Resource category	Tonnage (Mt)	Grade (% U_3O_8)	Total U_3O_8 (t)	Comment
Ben Lomond district					
Ben Lomond	Indicated	1.33	0.27	3591	NI43-101 compliant
Ben Lomond	Inferred	0.60	0.21	1260	NI43-101 compliant
Ben Lomond	Total	1.93	0.25	4851	NI43-101 compliant; non- NI43-101 compliant Mo grade of 0.15% estimated from previous work indicates ~2.90kt Mo
Georgetown district					
Maureen	Indicated	3.12	0.09	2808	NI43-101 compliant
Maureen	Inferred	1.54	0.11	1694	NI43-101 compliant
Maureen	*Total*	*4.66*	*0.10*	*4502*	*NI43-101 compliant*
Other Georgetown	*Inferred*	*2.90*	*0.10*	*2900*	*Pre-JORC/NI43-101*
Mount Isa uranium field					
Valhalla	Indicated	27.8	0.0891	24770	JORC compliant
Valhalla	Inferred	7.3	0.0799	5833	JORC compliant
Valhalla	Total	35.10	0.0872	30603	JORC compliant
Skal	Inferred	7.6	0.0508	3861	JORC compliant
Bikini	Inferred	10.10	0.0517	5222	JORC compliant
Duke Batman	Indicated	0.50	0.0780	390	JORC compliant
Duke Batman	Inferred	1.61	0.0630	1014	JORC compliant
Duke Batman	Total	2.11	0.0666	1404	JORC compliant
Honey Pot	Inferred	2.56	0.0700	2419	JORC compliant
Andersons	Inferred	2.00	0.1010	2020	JORC compliant
Watta	Inferred	4.20	0.0410	1722	JORC compliant
Westmoreland district					
Westmoreland	Indicated	8.0	0.09	7040	NI43-101 compliant
Westmoreland	Inferred	16.0	0.09	15040	NI43-101 compliant
Westmoreland	Total	24.0	0.09	22080	NI43-101 compliant
Mary Kathleen district					
Mary Kathleen	Production, 1958-1963	2.95	0.14	4080	
Mary Kathleen	Production,			4802	

	1958-1963				
Mary Kathleen	Remnant ore			1200	
Mary Kathleen	Total			10082	Includes production and remnant ore

The styles of U deposits in north Queensland are quite diverse, and these deposits have been assigned to quite different groups in the IAEA classification scheme (IAEA, 2009). However, some deposits have broad similarities suggesting linked genetic origins, and in the following discussion we use a combination of the IAEA classification along with a continuum classification presented by Skirrow et al. (2009). Following the classification of Skirrow et al. (2009), the mineral systems are discussed in the following order: (1) basin and surface-related uranium systems (including sandstone-related and unconformity-related systems); (2) metamorphic-related systems (including metasomatic systems), (3) hybrid systems (including iron-oxide Cu-Au systems), and (4) magmatic-related systems (including orthomagmatic and magmatic-hydrothermal systems). This schema links a number of IAEA deposit types together and progresses from basin-related processes of diagenesis and early fluid flow, through basin inversion and metamorphism to magmatism and related hydrothermal activity. In our analysis we consider that so-called volcanic-related deposits in north Queensland are basinal systems in which volcanic units within the basin have provided a source of uranium (see section 3.2). Figure 3 shows the location of the north Queensland deposits on the ternary classification of Skirrow et al. (2009), which highlights similar processes and possible continua between uranium systems, and provides broader, more genetic, descriptions for some systems. Based on these systems descriptions and on the six-question approach to mineral systems analysis (see below), a series of essential components (Appendix A) and mappable characteristics were identified (see individual sections for tabulations) and used in subsequent uranium assessments.

Following the success of a systems approach to understanding and discovering petroleum accumulations (Magoon and Dow, 1994) and previous process-based analyses of mineral deposits (e.g. Lacy, 1974), Wyborn et al. (1994) first formalised a construct for analysing processes linked to the accumulation of mineral resources. Wyborn et al. (1994) proposed that a "mineral system" had seven geological factors:

(1) sources of the mineralising fluids and transporting ligands;
(2) sources of the metals and other ore components;
(3) migration pathway;
(4) thermal gradient;
(5) energy source;
(6) a mechanical and structural focussing mechanism at the potential depositional site; and
(7) chemical and/or physical mechanisms for ore precipiation.

The original mineral systems approach was adapted by the Australian Geodynamics Cooperative Research Centre into a set of five questions (Walshe et al., 2005), later adopted by the Predictive Mineral Discovery Coopertative Research Centre (Barnicoat, 2008). In this analysis, we have adapted these and added an additional questions to determine "essential components" and "mappable criteria" that can be used in a GIS environment to indicate uranium potential. The mineral systems questions used in this analysis are:

(1) What are the geodynamic and P-T histories (including timing of mineralisation) of the system?
(2) What is the structural and lithological architecture of the system?
(3) What and where are fluid reservoirs and metal sources for the mineral system?
(4) What are the fluid flow drivers and pathways?
(5) What are the metal (and ligand) transport and depositional processes?
(6) What are the effects of post-depositional processes on metal accumulations?

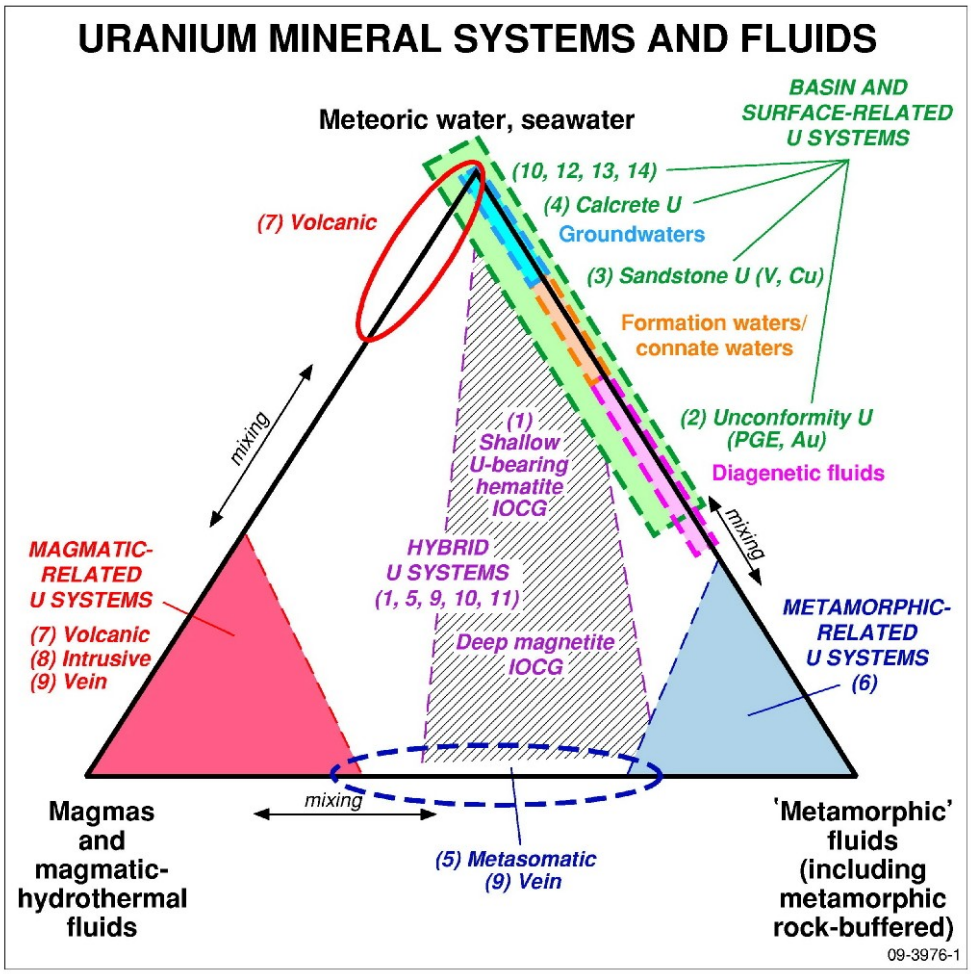

Figure 3: *Ternary diagram illustrating the location of uranium deposits in north Queensland (sandstone, unconformity, metamorphic-related, iron oxide-copper gold and magmatic-related) on the continuum classification of uranium deposits of Skirrow et al. (2009).*

Essential components and mappable criteria determined through consideration of these have been further assessed based on scale. In our analysis we have emphasised regional- to district-scale parameters, hence the assessments provided in this report must be considered at this scale and have little, if any, direct application at the deposit or prospect scale. Finally, where relative and/or absolute data were available, temporal constraints were considered in the analysis.

We have adopted the methods described in Czarnota et al. (2008) for assessing uranium potential. These authors identified both conceptual and empirical controls on the localisation of lode gold mineral systems and the resultant gold deposits in the Yilgarn Craton of Western Australia using a mineral system approach. From this mineral system analysis, they identified a series of parameters that could be mapped using geological, geophysical and geochemical data in a GIS environment. For each parameter, areas were assigned scores dependent upon the presence and intensity of that parameter. For all parameters these scores ranged from zero to three, with a value of three indicating the most favourable characteristics for the parameter. In areas that lacked information, a value of zero was assigned. In some cases, favourable features were given buffers, with the values decreasing away from the favourable feature. A total of twelve parameters were used in the analysis and the

potential score for an area was the sum of the scores for all parameters. This analysis, which did not use known gold deposits as a parameter, successfully predicted the location of known deposits in most cases, and, in addition, identified several areas of high potential with only minor prospects known (Czarnota et al., 2008).

In the analysis of both uranium and geothermal potential, a similar methodology was adopted, although the parameters used in assessing potential differed from the lode gold system. For uranium potential, conceptual and empirical controls described by Skirrow et al. (2009), as adapted for north Queensland, were used to identify parameters for potential analysis. As metasomatic and magmatic systems had not been considered by Skirrow et al. (2009), a set of controls were identified for these mineral systems as part of this study. Details parameters used to analyse each uranium system are provided below along with a description of known deposits in the study area.

3.1. SANDSTONE-HOSTED URANIUM SYSTEMS (S VAN DER WIELEN)

Sandstone-hosted uranium mineral systems are an important type of uranium deposit as they account for a quarter of the world uranium production and a third of global resources (OECD Nuclear Energy Agency, 2008). In Australia there is only one operating sandstone-hosted uranium deposit, the Beverley uranium mine, which accounts for 7% of Australia's uranium production (McKay, 2008) with several other deposits coming into production in the near future. Due to a combination historically low uranium prices and political policy Australian Phanerozoic Basins remain relatively under explored for sandstone-hosted uranium deposits. This section will assess the potential for sandstone-hosted uranium mineralisation within north Queensland by (1) describing sandstone-hosted uranium system models, (2) documenting relevant aspects of the regional geology, and (3) outlining essential components and mappable criteria used in mineral system assessment.

3.1.1. Regional geology and sandstone-hosted uranium systems

Two Mesozoic intracratonic basins have been recognised in the assessment area, the Carpentaria Basin to the north and the Eromanga Basin in the south. The Eromanga Basin covers 1,200,000 km^2 of central, eastern Australia and is underlained by older sedimentary basins as well as Proterozoic basement (Fig. 4). The Carpentaria Basin covers 700,000 km^2 of northeastern Australia. Both basins have a broad northeast-southwest structural trend that controls the location of major depocentres and basement highs such as the Euroka Arch, which separates the two basins (Fig. 4).

Previous workers (Gravestock et al., 1986; Radke et al., 2000 and Cotton et al., 2006) have compiled a detailed stratigraphic framework for the Eromanga and Carpentaria basins (Fig. 5). The Eromanga Basin has been subdivided into three main stratigraphic sequences: a lower non-marine sequence, a middle marine sequence and an upper non-marine sequence. The lower non-marine sequence consists of medium-grained sandstone (i.e. Hutton and Precipice Sandstones) that was deposited in a braided fluvial environment, followed by fine grained lacustrine sandstone, siltstone and shale of the Injune Group. The middle marine sequence comprises basal sandstone (i.e. Cadna-owie Formation, Algebuckina Sandstone, Hooray Sandstone and others) that prograde into deeper water shale and mudstone (the Bulldog Shale, Allaru Mudstone, Toolebuc Formation and others). Of importance to this study, the Toolebuc Formation has significant organic content and has previously been investigated for oil shale potential (Gravestock et al., 1986). The upper non-marine sequence (the Winton Formation) comprises a ~1,000 m thick package of sedimentary rocks (sandstones, shales and siltstones) that was deposited in a low-energy fluvial to lacustrine environment. The correlatives of the older Eromanga sediments (i.e. lower non-marine sequence) are missing from the Carpentaria Basin but the younger sequences can be mapped across the two basins.

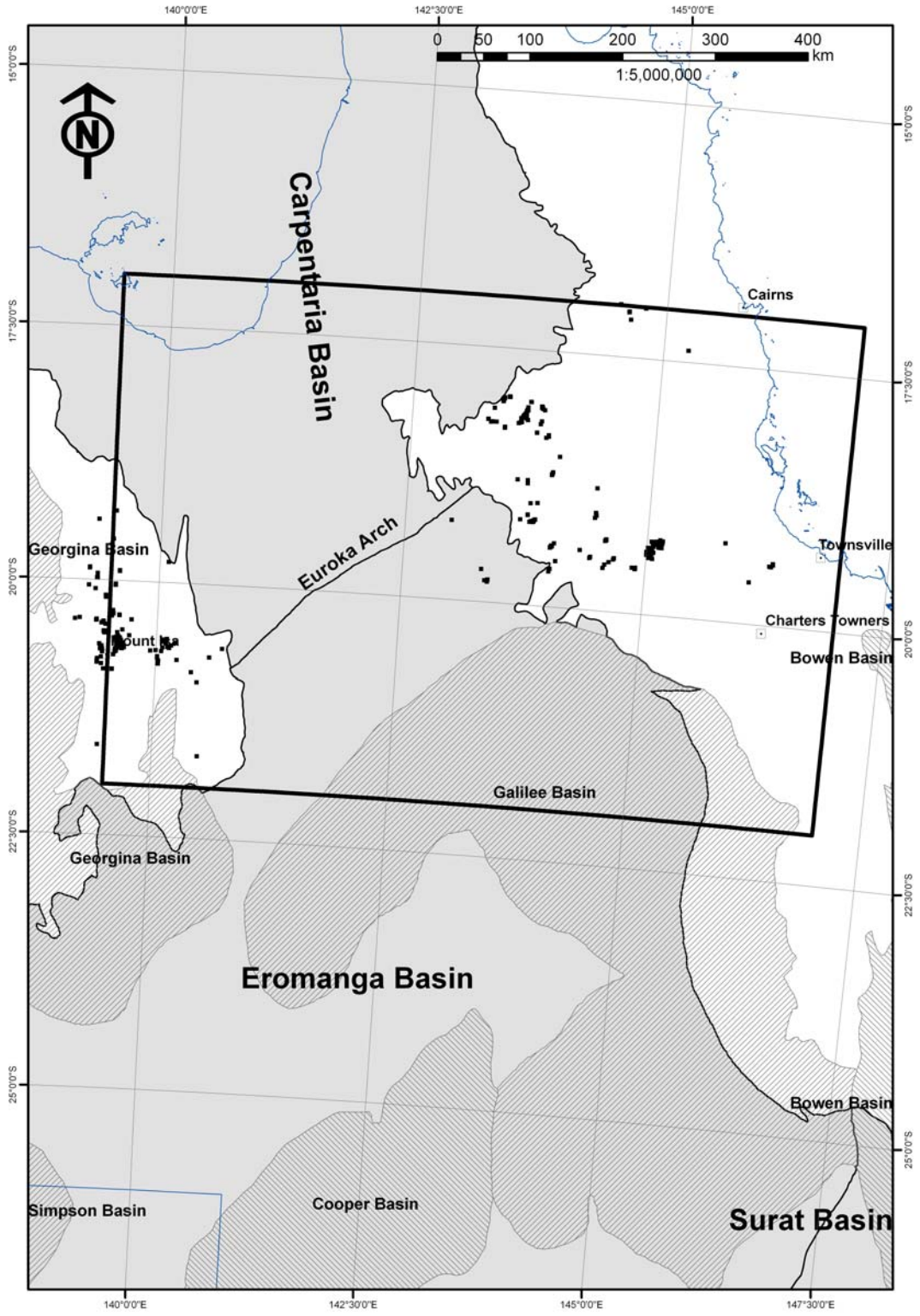

Figure 4: *Map showing the energy assessment area (bold rectangle), the extent of the Eromanga Basin, Carpentaria Basin and underlying Palaeozoic Basins (diagonal hatching). Known uranium occurrences and deposits are represented by black squares.*

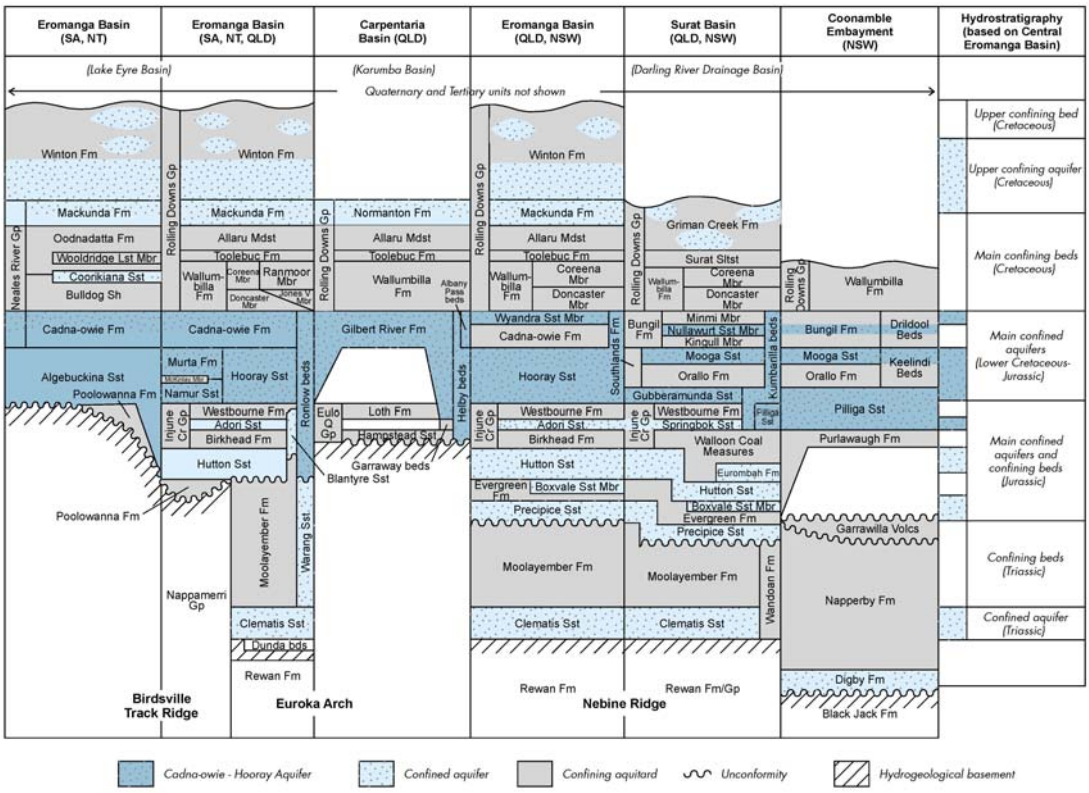

Figure 5: *Time-space plot showing the correlation between the Eromanga and Carpentaria Basins. Main sandstone aquifers and confining aquitards for the Great Artesian basins are marked (from Radke et al., 2000).*

3.1.2. Sandstone-hosted uranium systems models

There are currently no known sandstone-hosted uranium deposits within north Queensland although anomalous uranium values have been recorded in the Toolebuc Formation (Ramsden et al., 1982), a Mesozoic black shale that has previously been investigated as potential oil shale source (Dickson and Ramsden, 1986; Riley and Saxby; 1982; Glikson et al., 1985).

Two models have been proposed for the formation of sandstone-hosted uranium deposits (Fig. 6): a single-fluid model and a two-fluid model (Jaireth et al., 2008). In the single-fluid model, oxidised meteoric water migrates through a confined reduced sandstone aquifer progressively oxidising and dissolving uranium from the sandstone. The uranium is subsequently deposited and concentrated at the redox roll front (Fig. 6a). In the two-fluid model (Fig. 6b), oxidised meteoric water migrates through a clean sandstone aquifer dissolving uranium from the sandstone. A reduced basinal fluid (hydrocarbon- and/or H_2S-bearing) from underlying petroleum basins migrates upwards along faults, mixes with the oxidised fluid resulting in the precipitation of uranium adjacent to the fault. It is important to note in the two-fluid model that there are little to no in situ reductants so that uranium bearing oxidised fluids can migrate much deeper into the basin where there is greater opportunity of interaction with a reduced fluid. Based on these two broad models, the following discussion considers the sandstone-hosted system using the "six questions" approach (Appendix A).

The sandstone-hosted system produces two broad deposit types, sandstone-hosted deposits in which uranium deposition occurs within a laterally continouous sandstone aquifer at depth in a basin, and paleochannel-related deposits in which uranium deposition occurs within laterally restrictive fluvial channels. The following discussion considers these two sub-types together (collectively referred to as sandstone-hosted uranium systems) as they share many mineral system critical components.

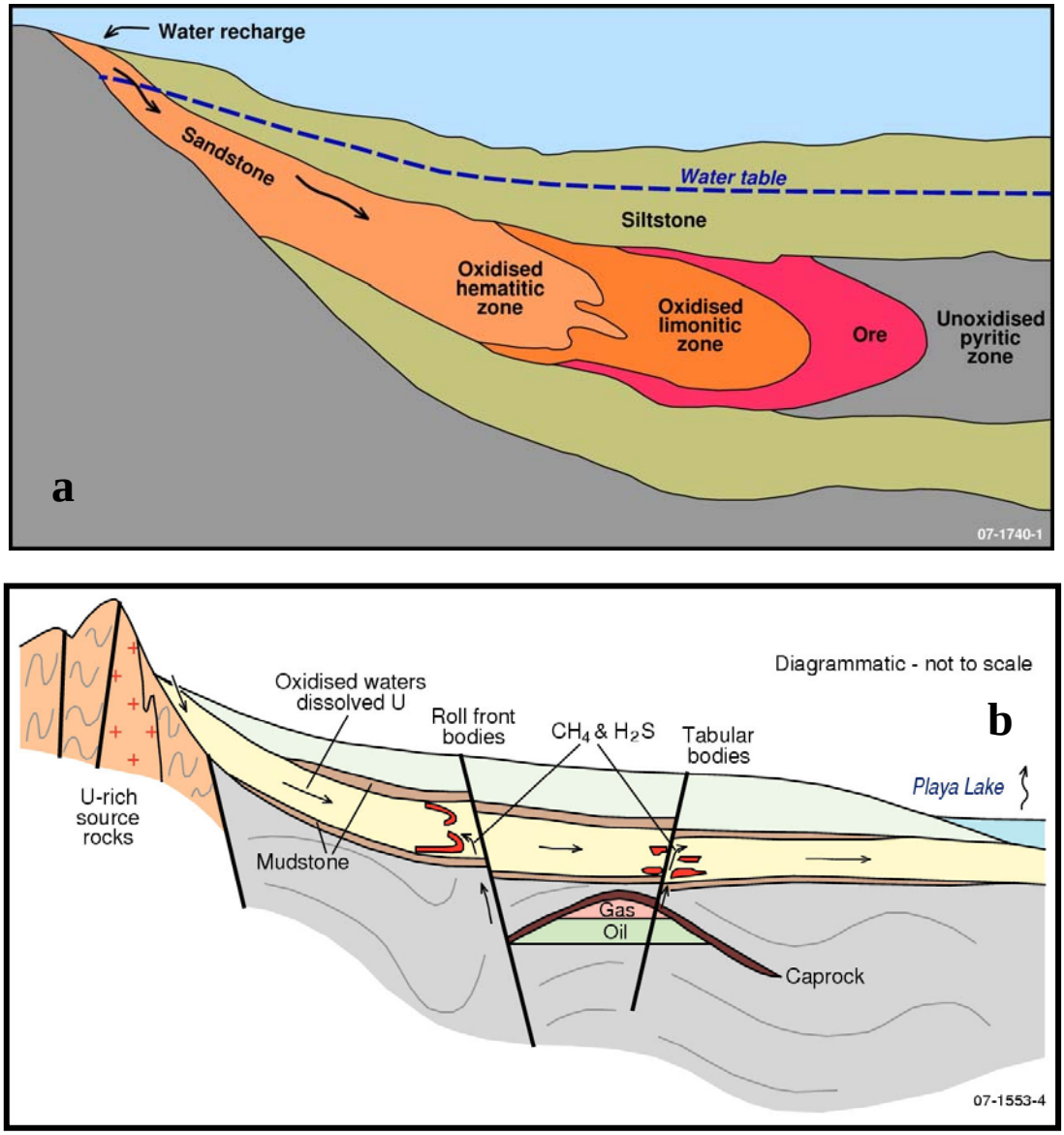

Figure 6: *Conceptual models that have been proposed for sandstone-hosted uranium deposits: (a) a single fluid model, and (b) two fluid model (after Jaireth et al., 2008).*

Q1. What is the geodynamic and P-T history (including timing of mineralisation) of the system?
Sandstone-hosted uranium systems are found in intercontinental, continental or intermontane basins that contain large packages of fluvial and/or mixed fluvial-marine sandstones. This setting juxtaposes sandstones with underlying uranium-rich basement rocks. Known sandstone-hosted uranium deposits are restricted to late Devonian or younger sedimentary basins, leading to the interpretation that terrestrial plant material is required for precipitation of uranium from solution. However, in older basins, hydrocarbons moving into the basin may have fullfilled the role of wood as a reductant (c.f. Fig. 6b and section 3.1.3). If reductants are not present in the basin, oxidised fluids would have continued migration until meeting reductants in basement rocks as in the unconformity-related sandstone system (section 3.2). The other important geodynamic factor in sandstone-hosted uranium systems is the uplift history of the region as this provides a mechanism for fluid drivers (question 4) as well as being important in preservation of the system (question 6).

Based on this discussion, the following criteria were considered in the potential assessment:

- Intercontinental, continental or intermontane basins
- Large packages of fluvial and/or mixed fluvial-marine sandstones

Q2. What is the structural and lithological architecture of the system?

In all mineral systems architecture is important for the following reasons:

- It provides a container in which the mineral system can develop.
- In creates variation in permeability and porosity for focusing fluid flow.
- It provides a spatial link between fluid, sources of metals, ligands and sulphur as in the case of an onlaping sedimentary sequence where there can be juxtaposition of sandstone lithologies against uranium rich basement.
- In certain circumstances it may be important in driving fluids as in the case of basin inversion or in embayments where groundwater flow paths can be focused.

Growth and basin margin faults are important in sandstone-hosted uranium systems as they can they control the distribution and shape of sandstone lithologies (i.e. wedge shape sandstone lithologies proximal to permeable faults and/or uranium rich basement), paleochannels and basin morphology. Variations in permeability and porosity play a role in controlling fluid flow regime for sandstone-hosted uranium system (i.e. permeable sandstone units that are confined by less permeable fine grain lithologies). Empirical evidence suggest that topographic gradient of 5° to 10° is required for the formation of a sandstone-hosted uranium system (Skirrow et al., 2009). Topographic gradient provides a hydraulic head and mechanism for fluid flow. Topographic gradient can be achieved by:

- Primary deposition dip.
- Tilting of the sequence due to the reactivation of basin margin faults.
- Change in continental stress fields.
- Basin subsidence.
- Basinal doming.

Based on this discussion, the following criteria were considered in the potential assessment:

- Embayments.
- Onlapping sedimentary sequence.
- Basin controlling faults.
- Distribution of paleochannels.

Q3. What and where are fluid reservoirs and metal sources for the mineral system?

In sandstone-hosted uranium systems the third question is mostly concerned with sources of uranium, reductants and fluids. In particular, Australian Proterozoic rocks are elevated in uranium compared to crustal averages (Budd et al., 2001) and as such they are likely to be the primary source of uranium. There are two potential sources of uranium for this system:

- Leached uranium from the hinterland.
- Leached uranium from detrital uranium minerals within basin sediments or paleochannels. In this scenario weathering and erosion of uranium rich basement rocks are deposited into a basin or paleochannel, from where it is subsequently leached.

Organic materials are the primary source of reductants for this type of uranium system. They can take the form of an *in situ* carbonaceous material within the sediments as in the case of the single fluid model or as a hydrocarbon and/or H_2S-bearing fluid. In the latter case locations of known hydrocarbon fields will be important in determining sandstone-hosted uranium prospectivity. Meteoric water is the main fluid involved in these systems. They are typically low temperature (20-60°C) and are initially highly oxidised (air saturated), weakly acidic to neutral (pH 4-7) but are progressively buffered by wallrock interaction to become reduced and alkaline. In the two fluid model, hydrocarbon and/or H_2S rich connate water may be the source of reductants and are likely to be highly reduced, warm (60-100°C) and have variable pH.

Based on this discussion, the following criteria were considered in the potential assessment:

- Proterozoic basement with elevated uranium concentrations.
- Presence of reduced organic material (solid, gas or aqueous) within or underlying the basin.
- Meteoric water.

Q4. What are the fluid flow drivers and pathways?

As mentioned above, topographic gradient is the main driver for fluids in sandstone-hosted uranium systems. Meteoric water migrates by gravitational pull until it reaches hydraulic equilibrium. In the case of the two fluid model, where a hydrocarbon and/or H_2S rich fluids is involved, then natural buoyancy of the fluid may be an important driver for the migration of fluids. An example of this would be hydrocarbons migrating up dip along permeable lithologies and faults. Other possible drivers for fluids movement include convection and deformation-related forcing.

Variations in permeability and porosity play a role in controlling fluid flow pathways. Likely fluid flow pathways include:

- High permeability faults.
- Permeable sandstone units that are confined by low permeability lithologies.
- Palaeochannels.

Based on this discussion, the following criteria were considered in the potential assessment:

- Hydrologically connected, highly permeable, immature (feldspathic-arkosic) sandstones.
- Palaeochannels.

Q5. What are the metal (and ligand) transport and depositional processes?

Changes in redox state of the uranium-bearing fluid are the primary depositional mechanism for sandstone-hosted mineral system. Changes in redox state can be achieved by either by wall rock interactions (i.e. single fluid model with an *in situ* reductant) or mixing of two fluids (i.e. and oxidised fluid carrying uranium in solution and a second reduced, hydrocarbon and/or H_2S-bearing fluid). Other potential deposition processes may include:

- Changes in silica saturation.
- Presence of vanadium and/or phosphate rich lithologies.
- Changes in pH.

Based on this discussion, the following criteria were considered in the potential assessment:

- Changes in redox state by either fluid-rock interaction or fluid mixing
- Changes in pH by fluid-rock interaction

Q6. What are the effects of post-depositional processes on metal accumulations?

As with any mineral system, denudation and exhumation can destroy mineralisation by eroding host lithologies. Changes in the hydrologic regime that originally formed the sandstone-hosted uranium system can either degrade or enrich mineralisation depending on circumstances. Factors that can change hydrologic regime include:

- Change in continental stress fields – changes in stress fields may have a major influence on a hydrologic regime resulting in a completely different fluid flow regime (i.e. tilting of the sequence due to the reactivation of basin margin faults).
- Changes in climate (i.e. rainfall) – high rainfall will increase the watertable and fluid flow rates resulting in uranium dissolution whereas low rainfall will have the opposite effect and likely help preserve the system.
- Sea-level changes – a sea-level fall may drop the water table resulting in uranium remobilisation during subsequent weathering periods.
- Changes in vegetation – Changes in vegetation type can affect the chemistry of meteoric waters. For instance, increased biomass in tropical forests increases the acidity of the water due to the formation of humic acid caused by the natural breakdown of vegetation.

- Diagenetic effects – Diagenetic effects can either increase or decrease permeability and can therefore change the hydrologic regime. Silica dissolution will increase permeability of a sandstone, resulting in an increase fluid flow and potentially remobilise uranium mineralisation. In the case of silicification and/or clay development, pore spaces may become clogged, reducing permeability, resulting in a decrease in fluid flow and potentially sealing mineralisation from other post-depositional processes.
- Post mineralisation uplift – Post mineralisation uplift is likely to destroy this system by eroding host lithologies or remobilising uranium by weathering processes.

Based on the above discussion and existing data sets, Table 2 and 3 summarise mappable criteria used in the assessment of the north Queensland area for both sandstone and paleochannel-related uranium systems.

3.1.3. Results of assessment analysis for sandstone-hosted uranium systems

The assessment for sandstone-hosted mineral systems have highlighted three prospective regions (Plates 1 and 2):

A. The area east of Cloncurry. The western margin of the Eromanga Basin where it abuts the Mt Isa inlier is prospective for sandstone-hosted uranium systems. The Naraku and Williams Suites in the Eastern succession have elevated concentrations of uranium (i.e. Joplin, 1963; Pollard et al., 1998; Wyborn, 1998 and Mclaren et al., 2003) and are possible primary uranium source for sandstone-hosted systems in this region. The eastern succession of the Mt Isa Inlier is a region of high topographic relief and likely the principal driver for fluids. The Toolebuc Formation in the Eromanga Basin is an organic-rich shale that contains elevated uranium concentration (van der Wielen et al., 2009) although the overlying sand dominated lithologies (i.e. Mackunda and Normanton Formations) and the underlying sandstones (Cadna-owie and Hooray Sandstones) would be the likely host lithologies for this system. This area has been highlighted due to it's proximity to a uranium source and basin margin as well as containing elevated uranium concentrations within sediments (i.e. radiometric, natural gamma logs).
B. The area 90 km north of Hughenden. In this region the eastern margin of Eromanga Basin forms a discrete embayment and is surrounded by Proterozoic basement of the Georgetown Inlier. The Proterozoic Einasleigh Metamorphics have elevated uranium concentrations (Withnall, 1985) and are the likely to be the probable source of uranium in this region. This area has been highlighted due to it's proximity to a uranium source and basin margin as well as containing elevated uranium concentrations within sediments (i.e. radiometric only).
C. Area around the township of Richmond. This area has been highlight in the analysis due to an radiometrics anomaly in the Mesozoic sediments (potential uranium depositional site) corresponding with a change in pH of groundwater.

Within the assessment area there is no known economic accumulation of hydrocarbons (Radke, 2009) as a result the presence of hydrocarbon were not used in the assessment for sandstone hosted uranium systems. Although, minor occurrences of hydrocarbons have been recorded within the area and include:

- At Ernest Henry Cu-Au deposit hydrocarbons have been responsible for forming native copper at the base of the Eromanga Sediment (pers comm. Robert Dennis, 2001)
- Stratigraphic drilling by Bureau of Mineral Resources (currently Geoscience Australia) in the Eromanga and Carpentaria Basins intercepted flowing hydrocarbons (i.e. Jericho 11; Ozimic, 1981) from the Toolebuc Formation. The Tololebuc Formation was not believed to be the source of the hydrocarbons as geochemical analysis showed that the fluid was mature

hydrocarbon of terrigenous origin unlike the typical marine-type kerogen found within the Toolebuc Formation (Ozimic, 1981).

- The Toolebuc Formation has been previously investigated as potential oil shale play (Radke, 2009) as it has high TOC. As Radke (2009) points out the Toolebuc Formation is an ideal hydrocarbon source rock but has not been through the maturation process to any significant extent. The Toolebuc Formation would make an ideal *in situ* reductant due to its high TOC and as a result been used in the assessment.

- Devonian or older basins are thought to have low potential for sandstone hosted uranium systems due to the lack of vegetation. If no reductant is present in the basin any soluble uranium is free to migrate and is only likely to be precipitated in the basement (i.e. form an unconformity uranium system). The one exception could be if you have an old (pre-Devonian) hydrocarbon source acting as a mobile reductant. The scenario has not been investigate as part of this assessment but the Neoproterozoic to Devonian Georgina Basin, and Millungera Basin of unknown age may have some potential for sandstone hosted uranium systems. The Galilee Basin could also contain sandstone hosted uranium systems but lacked the required publicly available datasets needed to conduct an assessment.

3.2. UNCONFORMITY-RELATED URANIUM SYSTEMS (TP MERNAGH)

Unconformity uranium systems produce the largest known high-grade uranium deposits, currently sourcing about 25% of the world's mined uranium production (Wall, 2006). According to the classification of Skirrow et al. (2009: Fig. 3), these deposits are hybrid systems, involving mixtures of meteoric water and diagenetic fluids. Uranium deposition typically occurs at or below an unconformity between a thick cover of sedimentary rocks and a reduced crystalline basement.

Current models for the formation of unconformity-related uranium deposits can be divided into two general types. The first involves the basement as the source of uranium and the basins as the source of the fluids (e.g. Johnson and Wall, 1984; Mernagh et al., 1994; Cuney et al., 2003; Derome et al., 2005). The second involves the overlying basin as a source for both the uranium and fluid (e.g. Hoeve et al., 1980; Ruzicka, 1993; Kyser, 2007). The first model sources uranium from the breakdown of monazite along fault zones as basinal brines interact with the basement. Uranium is precipitated when the oxidised fluid carrying uranium interacts with a reduced basement lithology (Hoeve et al., 1980), or encounters reductants in the basin such as volcanic units (Ahmad and Wygralak, 1990), or mixes with reduced fluids derived from the basement (Johnson and Wall, 1984; Mernagh et al., 1994). In some cases, fluid interaction with feldspathic or calcareous rocks may cause only a moderate increase in pH and a decrease in the oxidation state (fO_2), leading to precipitation of other metals (e.g. gold and platinum group metals), but little or no uranium (e.g. the Coronation Hill deposit).

In the basin model the source of uranium is from the breakdown of U-bearing detrital minerals, such as monazite, zircon, phosphates, tourmaline and uraninite by basinal fluids in deep basin paleoaquifers (e.g. Hoeve et al., 1980; Ruzicka, 1993; Kyser, 2007). These fluids flow laterally along paleoaquifers but may also flow downward due to the density of the highly saline fluid. Some models allow part of the fluid to enter faults and fracture zones in the basement rocks and thus become reduced before ascending again along faults and fractures, where they mixed with laterally moving oxidised fluids. Precipitation of the uranium (and other metals) takes place at the interface between the oxidising and reducing fluids (i.e. at the redox front). High-grade uranium or polymetallic mineralisation forms directly at the unconformity. Medium-grade uranium mineralisation may form below the unconformity and low-grade uranium mineralisation may form within the overlying sediments at some distance above the unconformity.

Table 2: Mappable criteria used for potential assessment of sandstone uranium systems hosted in Mesozoic sediments

MINERAL SYSTEM QUESTION	CRITERIA	SCORE	DATASET & REFERENCE	COMMENTS
1, 2	*Distribution of Mesozoic sedimentary basins* Within 10 km of basin margin Within 30 km of basin margin Within 100 km of basin margin	 3 2 1	Basement Relief Image of Australian Onshore and Offshore Sedimentary Basins (ANZCW-0703002747)	Mesozoic and younger basins polygons were extracted from the Australian onshore sedimentary basins shape file
3	*Uranium source* 10 km buffer around U-enriched basement rocks 30 km buffer around U- enriched basement rocks 100 km buffer around U-enriched basement rocks	 3 2 1	Radiometric Map of Australia (Minty et al., 2009)	Uranium values greater than and equal to 10 ppm were extracted from the filtered uranium band and converted to a polygon shape file. A spatial query was used to select values for crystalline basement only.
5	*Uranium deposition – evidence from radiomentric maps* Uranium enrichment (>10 ppm) within Mesozoic and younger basins 10 km buffer around U-enriched basin rocks 20 km buffer around U-enriched basin rocks 30 km buffer around U-enriched basin rocks	 4 3 2 1	Radiometric Map of Australia (Minty et al., 2009)	Uranium values greater than and equal to 10 ppm were extracted from the filtered Uranium band and converted to a polygon shape file. A spatial query was used to select values for Mesozoic and younger sedimentary basins.
5	*Uranium deposition – evidence from drill hole gamma logs* Natural gamma logs >250 API Natural gamma logs >200 API Natural gamma logs >150 API	 3 2 1	GABLOG Database (Habermehl et al., 2001)	Gridded natural gamma logs. Contours (250, 200, 150 API) were extracted and converted to a polygon shape file.
3, 4	*REDOX gradient* Gradient in Eh potential determined from groundwater data 5 km buffer around Eh gradient 15 km buffer around Eh gradient	 3 2 1	Hydrochemistry (Radke et al., 2000)	Gridded Eh field (hydrochemistry). Contours (0 mv) were extracted and converted to a polyline shape file
3, 4	*pH gradient* Gradient in pH potential determined from groundwater data 5 km buffer around pH gradient 15 km buffer around pH gradient	 3 2 1	Hydrochemistry (Radke et al., 2000)	Gridded pH field (hydrochemistry). Contours (pH 7) were extracted and converted to a polyline shape file

Table 3: Mappable criteria used for potential assessment of paleochannel-related sandstone-hosted uranium systems

MINERAL SYSTEM QUESTION	CRITERIA	SCORE	DATASET & REFERENCE	COMMENTS
1, 2	*Distribution of Mesozoic sedimentary basins*	3	Basement Relief Image of Australian Onshore and Offshore Sedimentary Basins (ANZCW-0703002747)	Mesozoic and younger basins polygons were extracted from the Australian onshore sedimentary basins shape file
2, 4	*Distribution of Cainozoic alluvium and/or fluvial units*	3	Surface geology of Australia 1:1,000,000 scale (Whitaker et al., 2007)	Cenozoic alluvium and/or fluvial units extracted from the 1:1,000,000 scale surface geology of Australia
3, 5	*Distribution of organic/carbonaceous rich sediments*	3	Surface geology of Australia 1:1,000,000 scale (Whitaker et al., 2007) and GABLOG Database (Habermehl et al., 2001)	Interpreted distribution of the Toolebuc Formation for drilling and surface geology (1:1,000,000 scale surface geology of Australia).
3	*Uranium source* 10 km buffer around U-enriched basement rocks 30 km buffer around U- enriched basement rocks 100 km buffer around U-enriched basement rocks	 3 2 1	Radiometric Map of Australia (Minty et al., 2009)	Uranium values greater than and equal to 10 ppm were extracted from the filtered uranium band and converted to a polygon shape file. A spatial query was used to select values for crystalline basement only.
5	*Uranium deposition – evidence from radiomentric maps* Uranium enrichment (>10 ppm) within Mesozoic and younger basins 10 km buffer around U-enriched basin rocks 20 km buffer around U-enriched basin rocks 30 km buffer around U-enriched basin rocks	 4 3 2 1	Radiometric Map of Australia (Minty et al., 2009)	Uranium values greater than and equal to 10 ppm were extracted from the filtered Uranium band and converted to a polygon shape file. A spatial query was used to select values for Mesozoic and younger sedimentary basins.

Wall (2006) has suggested that the Westmoreland deposits at the southern end of the McArthur Basin and perhaps also the Maureen (see also Mathison and Hurtig, 2009), Ben Lomond and other U-Mo deposits in the Georgetown region are unconformity-related uranium systems. Although the interpretation of Wall (2006) is preferred, it must be noted that the Maureen and Ben Lomond deposits are traditionally classified as volcanic-related deposits using the IAEA classification. All three of these deposits are described in more detail below, along with a discussion regarding the classification of the Maureen deposit using recent data and observations of Wall (2006) and Mathison and Hurtig (2009).

3.2.1. Westmoreland uranium field

The Westmoreland mineral field is located near the south-eastern margin of the Paleoproterozoic-Mesoproterozoic McArthur Basin. The northern and southern ends of the McArthur basin share numerous geological attributes including similar stratigraphic rock types and metal inventories. The Westmoreland uranium field comprises at least 50 uranium prospects of various size and grade (Ahmad and Wygralak, 1990), but the three largest deposits are Redtree, Huarabagoo and Junagunna (Fig. 7). These three deposits have a collective inferred and indicated resource of 23.6 kt U_3O_8 (Laramide Press Release 23/04/2009: Table 1).

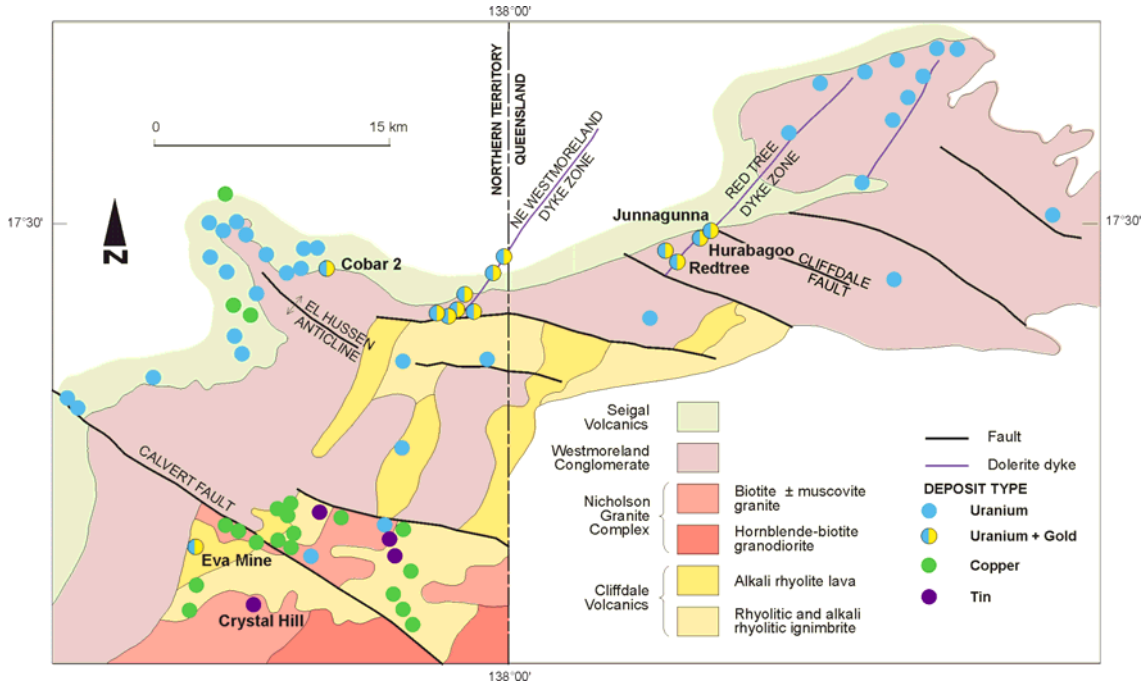

Figure 7: *Geological setting of mineral deposits and mineral occurrences in the Westmoreland uranium field (modified from Lally and Bajwah, 2006).*

The oldest rocks in the Westmoreland region are Palaeoproterozoic quartz-feldspar-mica schists and gneisses of the Murphy Metamorphics (not shown in Figure 7), which are only exposed in the Northern Territory. Palaeoproterozoic acid lavas and ignimbrites (Cliffdale Volcanics) unconformably overlie the metamorphic rocks. The upper units of the Cliffdale Volcanics and the Nicholson Granite have been dated at ~1840 Ma (M. Ahmad, Northern Territory Geological Survey, personal communication). Multiphase intrusions of the Nicholson Granite Complex (granites and adamellites) intrude the metamorphics and Cliffdale Volcanics. These rocks are unconfomably overlain by rocks of the McArthur Basin.

The basal unit of the McArthur Basin, the Westmoreland Conglomerate, is a fluvial deposit, more than 1200 m thick, and comprises arkose, conglomerate and quartz arenites. This unit, which corresponds to basal unit of the Leichhardt Superbasin, has been subdivided into four stratigraphic units (Ahmad and Wygralak, 1990). Most of the uranium mineralisation is within the upper unit (Ptw4 unit), which is porous, coarse-grained sandstone, conglomeratic in part, and 80 - 90 m thick. Basalt of the Seigal Volcanics conformably overlies the Westmoreland Conglomerate. These rocks are followed by dolomite, sandstone and mafic and felsic volcanic rocks of the upper part of the Tawallah Group, which corresponds to the Calvert Superbasin.

Aphyric, medium-grained, dolerite dykes intrude along north-east trending fault and fracture zones which intersect the Westmoreland conglomerate. The most significant of these are the Redtree and the Northeast Westmoreland dyke zones (Fig. 7). The Redtree dyke zone is over 15 km long and has been intruded by a complex series of dykes, with individual dykes generally less than 20 m thick. The Westmoreland uranium deposits (Redtree, Junnagunna and Huarabagoo) lie along the Redtree dyke zone. Faults in the Westmoreland uranium field developed at low strains, apparently in response to WNW-ESE directed compression. They transect and postdate Isan D_2 and D_3 fold systems but in part reactivate older basement faults.

The Redtree deposit flanks the Redtree dyke zone immediately north of the northwest-trending Namalangi fault (Fig. 7). It comprises stratiform and discordant uranium mineralisation with grades ranging from 0.15 to over 2 % U_3O_8 in four lenses. Stratiform mineralisation up to 15 m thick is hosted entirely within the Westmoreland Conglomerate just below the Seigal Volcanics. Vertically discordant mineralisation occurs in the Westmoreland Conglomerate and dolerite of the Redtree dyke zone and may be up to 40 m thick.

The Junnagunna deposit occurs at a fault intersection west of the Redtree dyke zone and south of the north-west trending Cliffdale fault (Fig. 7). Uranium mineralised zones in the Junnagunna deposit are predominantly flat-lying and concentrated within the upper unit of the Westmoreland Conglomerate, just below the Seigal Volcanics. Minor discordant mineralisation occurs within the Westmoreland Conglomerate adjacent to the Redtree dyke. The stratiform mineralisation is 0.5 to 10 m thick and grades from ~0.3 to 1 % U_3O_8. Limited mineralised zones also occur on the northern side of the Cliffdale fault and the eastern side of the Redtree dyke zone.

The Huarabagoo deposit is located approximately 3 km north-east of the Redtree deposit (Fig. 7) and is a zone of vertical mineralisation in a structurally complex area of the Redtree dyke zone. In this zone there were multiple injections of smaller dykes (steeply dipping and horizontal) associated with the two main vertical dykes. Most of the mineralisation is within the Westmoreland Conglomerate adjacent to the dykes and the remainder is in the dykes. No grades are available for Huarabagoo but it is said to be geologically similar to the Redtree deposit (Laramide Press Release 23/04/2009).

Pitchblende is the main economic mineral in these deposits, but secondary uranium minerals of the phosphate, vanadate, silicate, arsenate and sulphate groups are dominant in the weathered parts. In horizontal orebodies that are open to surface oxidation secondary mineralisation is associated with hematite, chlorite and sericite, and forms grain coatings and interstitial fillings. Uranium and gold mineralisation coexist in places and this association is the youngest mineral phase. Parts of the Junnagunna horizontal-type mineralisation and of the vertical type mineralisation at Huarabagoo contain gold; values of up to 80 g/t have been obtained, but more commonly the gold assays about 0.2 - 7.0 g/t.

Polito et al. (2005) suggest that $^{40}Ar/^{39}Ar$ dating of illite in the Westmoreland uranium field shows that fluid migration began as early as 1680 ± 18 Ma and continued beyond 1645 ± 40 Ma. $^{207}Pb/^{206}Pb$ ages of uraninite (Polito et al., 2005) indicate that mineralisation formed around 1655 Ma but was later overprinted by fluids at 878 Ma. Thus, the mineralogy, age, and geochemistry of the Westmoreland uranium deposits is similar to that of the uranium deposits of the Alligator Rivers uranium field in the northern McArthur basin suggesting that these deposits are also unconformity uranium systems.

3.2.2. Maureen deposit

The Maureen deposit is located 35 km northwest of Georgetown. Uranium-fluorine-molybdenum mineralisation forms irregular stratabound zones in a sequence of conglomerate, sandstone, siltstone and overlying volcanics (Fig. 8). Miller and Mortimer (1974) noted that 98% of the uranium at Maureen occurred within the lower part of the conglomerate (within 100 m of the basal unconformity) with 2% in the underlying basement.

The Mesoproterozoic Lane Creek Formation forms the basement to the Maureen deposit (Fig. 8). The original sediments consisted of laminated, highly carbonaceous mudstone and siltstone, interbedded with pale grey to white mudstone and siltstone. In places, the mudstone and siltstone were calcareous, as rare, thin, relatively pure recrystallised limestone beds occur locally. Metamorphism of the Lane Creek Formation has produced mainly mica schists with some quartzite and calc-silicate rocks (Withnall et al., 1997). The carbonaceous schists are generally finer grained than the non-carbonaceous ones. Andalusite and cordierite occur in rocks of higher metamorphic grade (amphibolite facies). Locally these rocks are migmatitic.

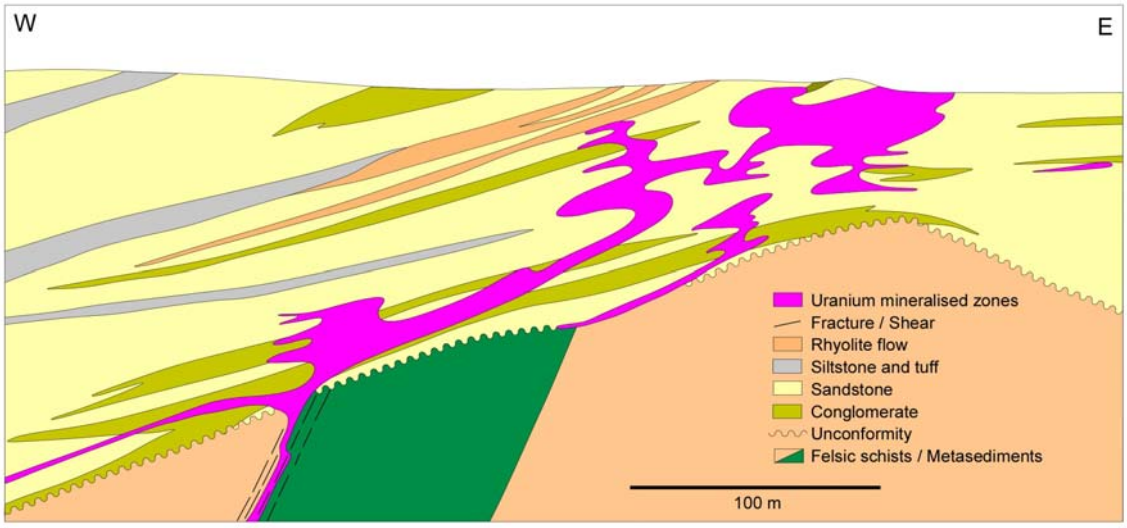

Figure 8: *Schematic longitudinal section of the Maureen deposit (modified from Jones, 2006).*

A basal conglomerate overlies the Lane Creek Formation and, in places, a thin bed of black or dark grey carbonaceous and pyritic siltstone lies between the basal conglomerate and the unconformity. The lower clastic sequence (up to 150 m thick) sits above these rocks and is composed of variably micaceous conglomerate, pebbly sandstone, muddy feldspathic sandstone and haematitic fine grained sandstone and siltstone. The lower clastic sequence grades upwards into an upper clastic sequence of volcaniclastic sandstone with rhyolite clasts, red micaceous muddy sandstone and tuffaceous siltstone and haematitic mudstone. These sediments are considered by Mathison and Hurtig (2009) to be part of the Late Carboniferous to Early Permian Maureen Volcanic Group. This

is consistent with recent dating where the youngest zircon from a sedimentary unit near the base of the clastic sequence yielded an age of 336 ± 6 Ma (2σ: N Kositcin, pers. comm., 2009), which is interpreted as a maximum depositional age of this unit. This analysis is inconsistent with the interpretation that the rocks form part of the Devonian Gilberton Formation, as suggested by Denaro et al. (1997), *although it must be stressed that it is only a single analysis and must be treated with caution*.

Mineralised zones in the clastic sediments occur as irregular layers roughly parallel to bedding of the host sediments. They branch off near irregularly shaped vertical zones which plunge westwards along the unconformity. Molybdenum mineralisation generally coincides with uranium mineralisation but patches of uranium- and molybdenum-only mineralisation also occur (Mathison and Hurtig, 2009). Some thin shear-hosted and vein-style, sulphide-rich, U-Mo mineralisation extends below the unconformity into the underlying metamorphic basement. All uranium and molybdenum mineralisation is replacement-style and ranges from total replacement where the original host rock is totally replaced by fluorite, clays, and sulphides (including molybdenite and uranium) to partial replacement, disseminations and thin veins. The fine-grained carbon in the mineralised zone is described as precipitated carbon rather than as a remnant carbonaceous material deposited during sedimentation (Mathison and Hurtig, 2009).

The primary mineralogy consists of very-fine-grained uraninite, purple fluorite and fine-grained complex molybdenum minerals. The molybdenum (including uranium-molybdenum) minerals include molybdenite, ferrimolybdite, umohoite, wolfenite, powellite, ilsemannite and iriginite (Bain, 1977). In the oxidised zone, the uranium minerals are mainly complex uranium phosphates, including saleeite, renardite, meta-uranocircite, autunite and meta-autunite (Bain, 1977). Associated minerals include fluorite, arsenopyrite, arsenian pyrite, dickite, chamosite, goyazite anatase, precipitated carbon and minor sphalerite (Mathison and Hurtig, 2009). Alteration halos of fluorite, dickite, chamosite and disseminated pyrite surround higher grade zones. The estimated in situ resources for the Maureen deposit are 2.9 kt U_3O_8 and 1.9 kt Mo (Table 1: Mega Uranium Ltd, Press Release 07/07/2008).

As mentioned above, the Maureen and Ben Lomond deposits were traditionally classified as volcanic deposits according to the IAEA classification (McKay and Miezitis, 2001). However, Wall (2006) has alternatively suggested that they are of the unconformity-related type.

The Maureen and nearby deposits are localised within 100 m stratigraphically of the unconformable contact between Paleozoic siliciclastic rocks and Mesoproterozoic basement, but they are spatially associated with felsic volcanic rocks most likely of the Maureen Volcanic Group (Mathison and Hurtig, 2009). Hence, the deposits have characteristics of both volcanic and unconformity-related deposits using the IAEA classification. Based on petrographic and fluid inclusion studies by Hurtig (2008), Mathison and Hurtig (2009) interpreted that mineralisation occurred as the result of the mixing of downward or laterally moving, uraniferous oxidised fluids with ascending, methane-bearing fluids. The uraniferous fluids were interpreted to have moderate salinities (3-16 eq wt % NaCl) and temperatures between 210 and 300°C. These fluid characteristics are very similar to those that formed unconformity-related deposits, hence the preferred interpretation is that these deposits are unconformity-related.

It is possible (probable?) that spatial associations to the unconformity and felsic volcanic rocks are both important features that control the location of mineralisation. The unconformity provides the redox boundary for uranium deposition whereas the volcanics are a readily-leachible, uranium-rich source. In the analysis the distribution of felsic volcanic rocks and unconformities have been used to

assess potential for deposits such as Maureen and Ben Lomond (see below). The analysis for orthomagmatic uranium systems (section 3.5.1) also highlighted the felsic volcanic rocks as having high potential.

3.2.3. Ben Lomond deposit

The Ben Lomond deposit is located in the Burdekin Basin, 60 km west-southwest of Townsville. Uranium-molybdenum mineralisation forms steeply dipping zones associated with east-west-trending fault-fracture systems below an angular unconformity between Carboniferous volcanics and older volcanic-volcanoclastic successions (Fig. 9). Ben Lomond was discovered by Pechey (Australia) Exploration Pty Ltd in 1975 and later explored by Minatore Australia Pty Ltd. During delineation of the ore-body, approximately 3500 t ore averaging 0.21% U_3O_8 was mined and this ore was stockpiled on the lease. Exploration drilling carried out along the Ben Lomond Ridge to the east indicated that the mineralised structure and host rock extend well beyond the delineated deposit.

Ben Lomond (Fig. 9) occurs in a fault-bounded block of Carboniferous, calc-alkaline volcanics within the St James Volcanics, part of the Glenrock Group. These overlie Keelbottom Group sediments of Late Devonian to Early Carboniferous age, and older basement rocks consisting of sediments and volcanics of the Neoproterozoic Argentine Metamorphics. Unconformably overlying the St James Volcanics is the Early Carboniferous Watershed North Rhyolite, a crystal-rich to lithic-rich rhyolitic ignimbrite at least 400 m thick, which is thought to have been deposited in a cauldron subsidence event (Hutton et al., 1997).

In the vicinity of the deposit, the youngest non-intrusive rocks exposed are carbonaceous/pyritic shales and sandstones of the Late Carboniferous Insolvency Gully Formation, which unconformably overlies the St James Volcanics and Watershed North Rhyolite. The Insolvency Gully Formation is intruded by the Late Carboniferous to Early Permian age Speed Creek Granite.

The uranium-molybdenum mineralisation is in a complex system of subparallel, steeply-dipping veins and fractures associated with a wide shear zone. The upper limit of the mineralised vein system is a few metres below the unconformity at the base of the Watershed North Rhyolite. The fracture system does not extend into the overlying Watershed North Rhyolite. Mineralisation is best developed 10-50 m below the unconformity. The vein system is mineralised over a length of more than 750 m, a maximum width of 150 m and vertical depth of 100 m. The mineralised zone is parallel to the axial plane of a shallow plunging syncline in the host rhyolitic tuff. The primary mineralogy includes pitchblende, coffinite and molybdenite, with minor amounts of uranium phosphate (torbernite and metatorbernite) and jordisite (amorphous MoS_2). Minor amounts of galena, sphalerite, pyrite, marcasite and arsenopyrite also occur in the ore. Quartz is the main vein mineral with minor sericite, chlorite and tourmaline, all of which also occur as disseminations in the wallrock. The mineralised zone is characterised by strong silicic and hematitic wallrock alteration assemblages and is associated with peripheral zones of chloritisation and pervasive dolomitisation.

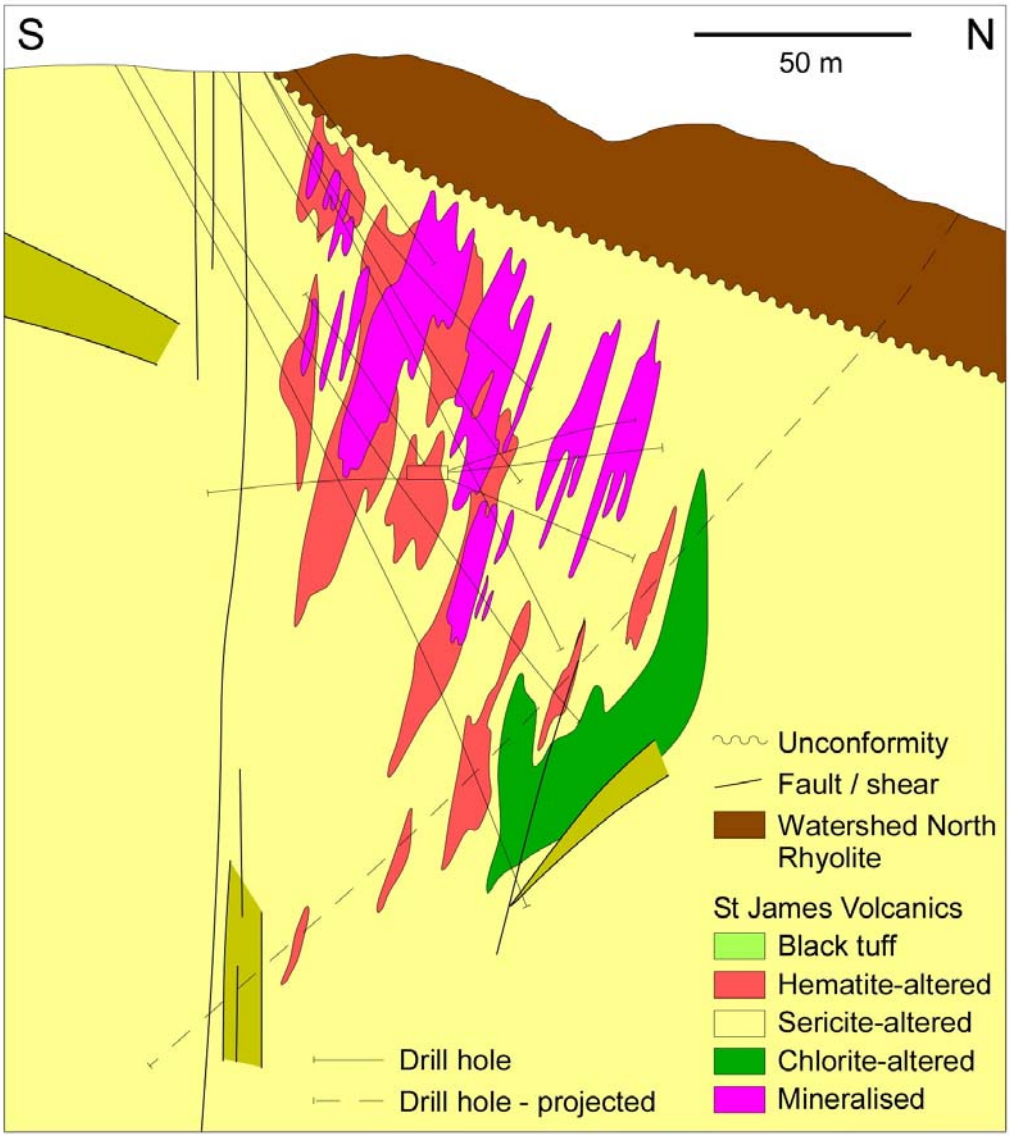

Figure 9: *North-south cross-section through the western part of the Ben Lomond deposit (modified from Vigar and Jones, 2005).*

The estimated in situ resources for the Ben Lomond deposit are 4.9 kt U_3O_8 and 2.9 kt Mo (Table 1). On the basis of its relatively high average U_3O_8 grade (0.25%) and its substantial molybdenum content, Ben Lomond is one of the highest value per tonne uranium resources outside the Athabasca Basin in Canada.

3.2.4 Mineral system model for unconformity uranium systems

Mernagh et al. (1998) have previously defined the essential components associated with some of the unconformity-related uranium deposits in the Alligator Rivers and South Alligator Valley uranium fields in the Northern Territory. The interpretation of the Maureen and Ben Lomond deposits as unconformity-related deposits (Wall, 2006) and the general acceptance of the Neoproterozoic

deposit (Western Australia) as an unconformity-related deposits (McKay and Miezitis, 2001) indicates that unconformity uranium systems may not be restricted to the Mesoproterozoic and that they also occur in younger rocks. A generalised model for unconformity-related uranium systems is shown in Figure 10. The mineral system model uses the "six questions" approach which has been developed to ensure that all aspects of the system, including its broad geological context, are considered and that attention is paid to system parameters across scales (Appendix A).

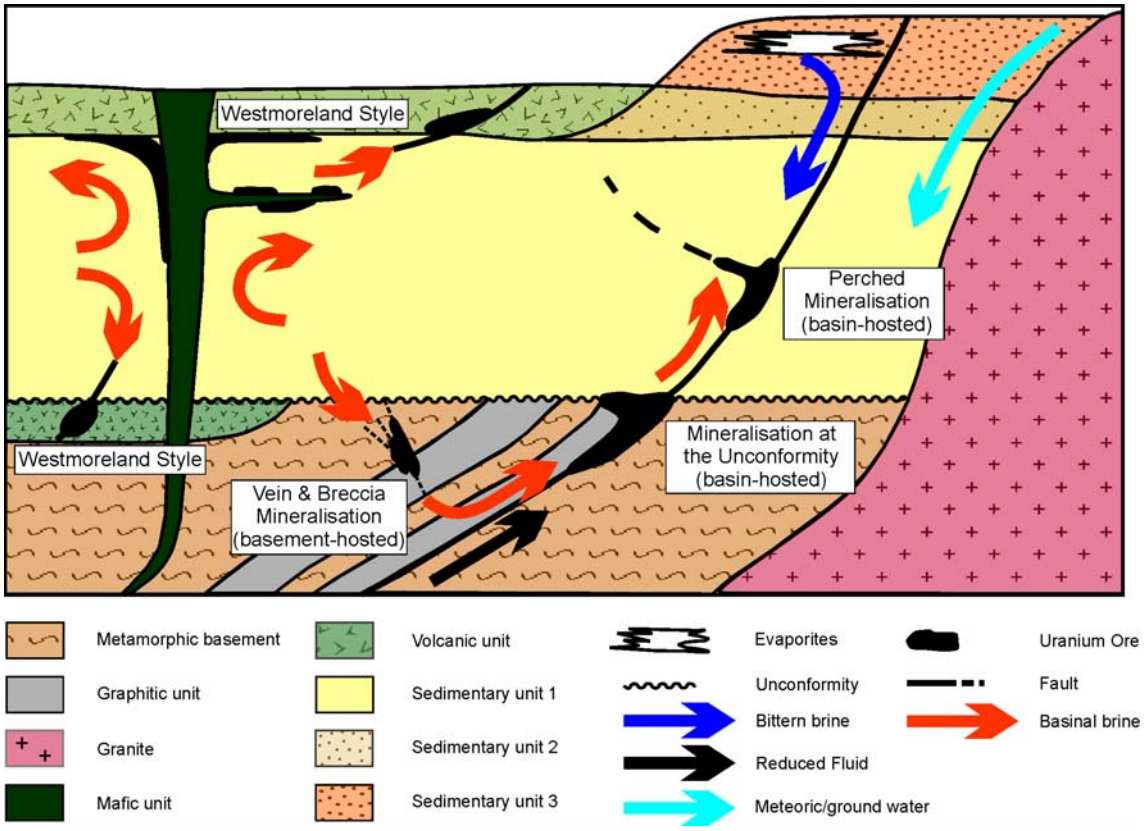

Figure 10: *Mineral system model for unconformity-related uranium deposits.*

Q1. What is the geodynamic and P-T history (including timing of mineralisation) of the system?

These systems are generally located in intracratonic, epicontinental or foreland basins which unconformably overly uranium-rich basement rocks. The basement may consist of granite-gneissic domes and/or inliers or it may contain felsic (meta)sediments or mixtures of the two. The basement typically has a clock-wise P-T-t metamorphic path. External changes in plate stress may lead to basin inversion and enhanced fluid flow. Polito et al. (2005) report that uraninite from the Westmoreland deposits experienced almost complete Pb loss between ca. 1100 and 750 Ma. These ages respectively coincide with the assemblage and break up of Rodinia whereas ages around 497 Ma are most likely related to the formation of the Georgina basin that covered much of northern Australia.

Based on this discussion, the following criteria were considered in the potential assessment:

- Distribution of fluid source and potential depositional sites.

Q2. What is the structural and lithological architecture of the system?

As the name implies, these systems typically require a major disconformity (generally an unconformity) between the basement containing relatively reduced rocks and the overlying basin which contains oxidised, highly permeable sedimentary rocks. There is often an onlapping relationship between the basin and basement. Periodic reactivation of basement faults during and after basin development creates the faults and architecture for later fluid flow pathways. The faults generally exhibit relatively small displacement (less than a few hundred metres) and form conjugate networks but may include fault strands with strike lengths of 10s to 100s of kilometres. The deposits sometimes also show a close association with gravity highs and/or ridges which may reflect major structures in the basement that control later fluid flow in the system.

Based on this discussion, the following criteria were considered in the potential assessment:

- Distribution of unconformities, sedimentary basins as well as fundamental fault sets.

Q3. What and where are fluid reservoirs and metal sources for the mineral system?

The uranium and other associated metals (e.g. Ni, Co, Cu, Pb, Zn, Au, PGE, and Mo) are thought to be leached from U-rich rocks by oxidised fluids. This could be uranium-rich felsic rocks either rimming or underlying the basin, or from the breakdown of U-bearing detrital phases, such as monazite, zircon, uraninite, phosphates and tourmaline, in the basin sediments or from felsic volcanic rocks within and/or in close proximity to the aquifer.

The uranium-bearing fluids are typically moderate temperature (~150 – 200°C), saline, and highly oxidised. Such temperatures imply the prior existence of a thick, sedimentary cover sequence. The sources of these saline fluids are not well defined and they may be diagenetic fluids buffered by evaporites, or evolved meteoric waters, or connate brines, or seawater. However, it is the chemistry of the fluid that is of most importance as these fluids have to preserve a high redox state in order to maintain high uranium solubility. Therefore the source rocks, fluid flow pathways and reservoirs must have a low abundance of reductants.

Based on this discussion, the following criteria were considered in the potential assessment:

- Uranium-rich source rocks such as felsic rocks underlying the basin, lithic fragments of felsic rocks in the aquifers, uranium-rich minerals (e.g. zircon, monazite, allanite, apatite etc.) within the basin sediments, or felsic volcanic rocks in close stratigraphic proximity to the aquifers.

Q4. What are the fluid flow drivers and pathways?

Fluid flow drivers are typically those found in most sedimentary basins such as topographic flow, diagenesis, deformation events and temperature variations. Fluid flow pathways are influenced by the formation of aquifers and aquitards during diagenesis, and other lateral and vertical variations in permeability caused by faulting and shearing during episodes of basin extension and basin inversion. The aquifers are typically defined by illite-kaolinite alteration or hematite-bearing oxidised assemblages or aquitards with intense silicification. Basement penetrating faults are often defined by illite-kaolinite and/or chloritic alteration.

Polito et al. (2005) have suggested that several phases of fluid overprinting have occurred in the Westmoreland region between 1159 and 497 Ma. This indicates that the fluid flow pathways remain active over an extended period of time and this may enable significant remobilisation of the uranium ore.

Based on this discussion, the following criteria were considered in the potential assessment:

- Inversion of early extensional faults during D_1 (distribution of faults active during D_2)
- Demagnetisation resulting from the formation of hematite at the expense of magnetite during interaction with oxidised fluids.
- The distribution of sericite and kaolinite alteration haloes which are indicators of fluid flow.

Q5. What are the metal (and ligand) transport and depositional processes?

Uranium has the ability to complex with a large number of ligands depending on the pH and oxidation state of the fluid. It can be transported as oxy-hydroxy, chloride, fluoride, sulphate, phosphate, carbonate, etc. complexes. Uranium ions in aqueous solution can form very complex species due to the four possible oxidation states as well as hydrolytic reactions that lead to the formation of polymeric ions. For example, in oxidised aqueous fluids, U^{6+} readily forms the linear polar uranyl ion, UO_2^{2+}. Uranium is deposited when these oxidised fluids come in contact with reductants in the basin or in the basement rocks. Examples of possible reductants include carbonaceous shales, Fe^{2+}-rich rocks, hydrocarbons and H_2S in reduced fluids. Zones of faulting and brecciation, particularly in the basement, are important for focusing the fluids and enhancing their interaction with reduced rock assemblages. There is also a general association of calcareous rocks with reduced rocks in the basement which may indicate that changes in pH are also important during the depositional process.

Based on this discussion, the following criteria were considered in the potential assessment:

- Uranium occurrences will indicate potential for a uranium mineral system.
- The distribution of Fe-rich or carbonaceous rich rocks will indicate areas of potential reductants.
- Uranium enrichment as indicated by gamma-ray spectrometric images of uranium, U/Th.

Q6. What are the effects of post-depositional processes on metal accumulations?

$^{207}Pb/^{206}Pb$ and $^{40}Ar/^{39}Ar$ dating of mineralisation in the Westmoreland region (Polito et al., 2005) indicate several episodes of fluid flow occurred after the original mineralisation event and may have remobilised some of the ore. Fluid overprinting occurred between 1159 and 497 Ma and the uraninite experienced almost complete Pb loss between ca. 1100 and 750 Ma (Polito et al., 2005). These fluid overprints were most likely responsible for the precipitation of late Fe-(±Cu) and Pb sulphide minerals that occur with, and cut the uraninite (Polito et al., 2005).

As most deposits of this type occur close to the basal unconformity between the sedimentary basin and the basement rocks there is a good chance of preservation for this style of mineralisation. Most of the basins that still exist are 1 – 3 km thick, flat-lying and essentially unmetamorphosed. However, in some cases, the basin fill can be absent, having been removed by erosion, leaving the basement rocks outcropping at the surface and exposing the ore to possible leaching by surface waters.

Based on this discussion, the following criteria were considered in the potential assessment:

- Enrichment of thorium relative to uranium and potassium in radiometric data, this may indicate mineralisation at depth. Thorium enrichment has been observed at higher structural levels in some unconformity-related deposits and is generally associated with higher concentrations of rare-earth elements and Zr (Mernagh et al., 1998).

These criteria are presented in more detail in Table A6 of Skirrow et al. (2009). Based on these features and available datasets, a series of mappable criteria were identified and are summarised in Table 4. These criteria have been used as the basis for uranium potential analysis. Table 4 also indicates the weightings used in the analysis.

Table 4: Mappable criteria used for potential assessment of unconformity-related uranium deposits.

MINERAL SYSTEM QUESTION	CRITERIA	SCORE	DATASET & REFERENCE	COMMENTS
1, 2	*Distribution of unconformities* 1 km buffer 5 km buffer 10 km buffer 15 km buffer	 4 3 2 1	Solid geology (Liu, 2009)	Unconformities interpreted from the solid geology map.
2,3	*Distribution of fluid source and potential depositional sites* Leichhardt Superbasin 5 km buffer around Leichhardt Superbasin	 3 1	Surface geology of Australia (Whitaker et al., 2007)	Basal units of Leichhardt Superbasin are known hosts to U mineralisation. Fluid source possibly basinal brines.
3	*Uranium source* 10 km buffer around U-enriched basement rocks 30 km buffer around U-enriched basement rocks 100 km buffer around U-enriched basement rocks	 3 2 1	Radiometric Map of Australia (Minty et al., 2009)	Uranium values greater than and equal to 10 ppm were extracted from the filtered uranium band. A spatial query was used to select values for crystalline basement only.
3	*Felsic volcanic rocks* Felsic compositions	 3	Solid geology (Liu, 2009)	Compositional classification is taken from geological unit descriptions.
4	*Fluid flow – demagnetisation* One standard deviation (σ) below mean 2σ below mean	 1 3	Magnetic Map of Australia	
4	*Fluid flow – sericite alteration* 1 σ above mean 2 σ above mean	 1 3	ASTER data for North Queensland	
4	*Fluid flow – kaolinite alteration* 1 σ above mean 2 σ above mean	 1 3	ASTER data for North Queensland	
4	*Fluid flow – faults* 1 km buffer around D_1 faults 1 km buffer around D_2 faults	 2 3		
5	*Distribution of potential depositionals sites -- mapped geology* Mafic rocks	 3	Surface geology of Australia (Whitaker et al., 2007)	Compositional classification is taken from geological unit descriptions.
5	*Uranium deposition – evidence from U^2/Th radiomentric maps* 1 σ above mean 2 σ above mean	 1 3	Radiometric Map of Australia (Minty et al., 2009)	

5	*Uranium deposition – evidence from thorium enrichment* 1 σ above mean 2 σ above mean	 1 3	Radiometric Map of Australia (Minty et al., 2009)	Thorium enrichment has been observed at higher structural levels in unconformity-related deposits

3.2.5. Results of assessment analysis for unconformity-related uranium systems

Plate 3 shows the results of the potential analysis for unconformity-related uranium systems in North Queensland. Note however that the availability of datasets is not uniform over the study area. There is also limited information on the distribution of key alteration minerals such as hematite, kaolinite and sericite. A key component of these systems is the presence of an unconformity and the juxtaposition of oxidised and reduced assemblages. With these considerations, the assessment has highlighted known areas of unconformity-related mineralisation, as well as identifying areas with potential but without known mineralisation:

A. The Westmoreland region. The major unconformity-related deposits in northern Queensland occur in this region which is highlighted by the presence of unconformities, reduced-rocks of the Leichhardt Basin, uranium source rocks, mafic potential depositional sites and a Th anomaly which may indicate mineralisation at depth.
B. The Mount Isa Inlier. This region has the highest potential for unconformity-related uranium partly due to the fact more data is available for this area. However, it contains many of the key elements including faults and unconformities, suitable uranium source rocks, mafic potential depositional sites and Th anomalies. Furthermore, an area of very high potential occurs along the eastern margin of the Kalkadoon-Leichhardt Belt which corresponds with a zone of intense demagnetisation. There is also considerable potential in the region south of Mount Isa as well.
C. The Esmeralda Supersuite. This region is highlighted by the presence of unconformities, uranium source rocks, mafic potential depositional sites and a strong Th anomaly. It is interesting to note that the Esmeralda Supersuite has strong similarities to the Hiltaba Supersuite of the Gawler Craton.
D. Area around and to south of Maureen. This region contains numerous unconformities, including the one associated with the Maureen U-Mo-F deposit, as well as igneous rocks with anomalours uraniums contents. The sediments of the Carpentaria Lowlands Region also onlap onto the margin of the Georgetown Region and may provide the oxidised, basinal brines commonly associated with unconformity-related uranium systems.
E. The Paleozoic magmatic belt southwest of Cairns. This region contains numerous unconformities and igneous rocks with anomalous uranium contents, mafic volcanic rocks and a strong Th anomaly. The sediments of the Carpentaria Lowlands Region also onlap onto the margin of the Georgetown Region and may provide the oxidised, basinal brines commonly associated with unconformity-related uranium systems.
F. The Northern Charters Towers Region. Similar to regions D and E above, this region contains numerous unconformities, uranium source rocks, mafic potential depositional sites and a strong Th anomaly. Within this region the Burdekin Basin, which hosts the Ben Lomond uranium deposit, is highlighted as having higher potential due to the presence of uranium-bearing source rocks, the Fe-rich volcanics of the Glenrock Group and the carbonaceous sediments of the Insolvency Gully Formation.

3.3. METASOMATIC URANIUM SYSTEMS (D HUSTON)

Using the IAEA classification, McKay and Miezitis (2001) interpreted uranium deposits in the Mount Isa uranium field (Fig. 11), to the north of Mt Isa, as metasomatite deposits. This group of deposits, which also includes deposits in the Kivroy Rog Basin in the Ukraine, the Lagoa Real district in Brazil and smaller districts in Brazil, northern Sweden and Guyana, is unified by the close association of the ores with sodic-calcic alteration assemblages that typically contain abundant albite (Polito et al., 2009; Cuney and Kyser, 2009). According to the continuum classification of Skirrow et al. (2009), these deposits are hybrid systems, involving mixtures of magmatic-hydrothermal and metamorphic fluids. The association with albitic alteration assemblages may suggest links to IOCG systems (Hitzman and Valenta, 2005; Skirrow et al., 2009).

Although not as well documented as IOCG, unconformity-related or sandstone-hosted deposits, metasomatite deposits are economically significant, with deposits in the Kivroy Rog Basin containing up to 50 kt U_3O_8 (Cuney and Kyser, 2009), and the Mount Isa uranium field collectively containing 47.2 kt U_3O_8 (Table 1). In addition to the close association with albite-dominated proximal alteration assemblages, these deposits share a number of other similarities. Most importantly, the deposits appear to be spatially associated with major shear zones. For instance, in the Mount Isa uranium field the Valhalla deposit is near the Mt Isa-Twenty-nine Mile Fault system (Fig. 11: Polito et al., 2009), and in the Kivroy Rog district in the Ukraine, all major deposits are localised along north-trending, deeply-rooted continental-scale structures (Cuney and Kyser, 2009). In at least some cases, the deposits appear to be hosted by subsidiary structures or sedimentary units near the main structures, but not the main structures themselves. These structures commonly have a ductile early history, followed by a brittle later history: the uranium appears to be associated with the brittle later history (e.g. Kivroy Log and Skuppesavon: Cuney and Kyser, 2009).

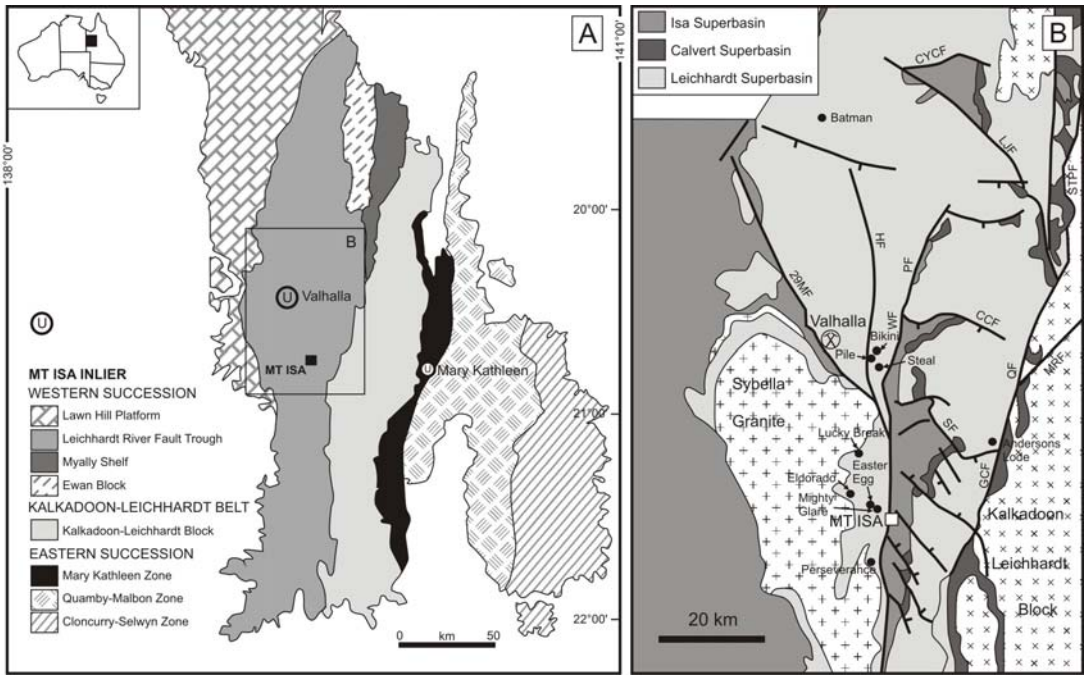

Figure 11: Geology *of the Mt Isa uranium field (modified after Polito et al., 2009). 29MF = 29-Mile Fault; HF = Hero Fault; PF = Paroo Fault; WF = Western Fault; CCF = Conglomerate Creek Fault; GCF = Gorge Creek Fault; QF = Quilarlar Fault; STPF = Saint Paul Fault; LJF = Lake Julius Fault; CYCF = Crystal Creek Fault.*

In addition to albite, most proximal alteration zones associated with metasomatic uranium deposits are characterised by the presence of sodic amphibole (e.g. riebeckite) or pyroxene (e.g. aegerine), along with calcite. Another ubiquitous characteristic is that alteration was accompanied by desilicification (Cuney and Kyser, 2009; Polito et al., 2009). In many of the deposits U-bearing titanates (e.g. brannerite and davidite) and zircon, as well as uraninite, host uranium. Garnet and, in some cases, epidote accompany the albitic alteration assemblage. Iron oxide minerals, particularly hematite, typically accompany the albitic assemblage. In several of the described examples late stage sulphide minerals, including pyrite, galena, chalcopyrite and bornite are present. Proximal albitic alteration assemblages grade to less altered wall rocks mostly through replacement of K-feldspar in the wall rock by albite (Cuney and Kyser, 2009). Where estimated, the earliest alteration assemblage is relatively high temperature (250-500°C), with later, lower temperature (150-200°C) assemblages identifed in some deposits (e.g. Kivroy Rog: Polito et al., 2009).

One of the most significant differences between metasomatic uranium deposits is the wide variety of host rocks. Host rocks to these deposits vary from siliciclastic lenses within a basalt dominated package (Valhalla and Andersons: Gregory et al., 2005; Polito et al., 2009), through mica schist, gneiss, amphibolite, siltstone and mafic volcanic (Kivroy Rog, Ukraine), granite, syenite, orthogneiss and paragneiss (Lagoa Real, Brazil; Epinharas, Brazil; and Kurupung, Guyana) and felsic metavolcanic rocks (Skuppesavon, Sweden: Polito et al., 2009). This variability of host rock suggests that fluid-host rocks interaction is not an essential component in the depositional processes associated with the formation of these deposits, and other depositional processes such as fluid mixing or phase separation may be important.

3.3.1. The Mount Isa uranium field

One of the two most significant repositories of uranium in north Queensland are metasomatic deposits in the Mount Isa uranium field. Over 100 uranium deposits, prospects and occurrences are known in this field, with a major deposit at Valhalla and smaller deposits at Skal, Bikini, Duke, Batman, Honey Pot, Andersons and Watta (Table 1). Collectively these deposits contain total resources of 47.2 kt U_3O_8. These deposits are hosted within the Leichhardt River Fault Trough, to the north of Mt Isa. This trough is filled by rocks of the 1790-1755 Ma (Page et al., 2000; Neumann et al., 2006) Leichhardt Superbasin. In the Mt Isa uranium field this superbasin is dominated by tholeiitic basalt of the ~1780 Ma Eastern Creek Volcanics that overlie fluvial to shallow marine siliciclastics and volcanic rocks of the Bottletree Formation and Mt Guide Quartzite. The Bottletree Formation overlies basement of the >1850 Ma Kalkadoon-Leichhardt Belt (Bierlein et al., 2008; Neumann, 2007). The Eastern Creek Formation is overlain by coarse- to medium-grained siliciclastics of the Myally Subgroup and fine-grained siliciclastics and dolostone of the Quilalar Formation, the uppermost unit of the Leichhardt Superbasin. These rocks are overlain by siliciclastic sedimentary rocks and bimodal volcanic rocks of the 1730-1690 Ma Calvert Superbasin and then by siliciclastic and dolomitic sedimentary rocks the 1665-1590 Ma Isa Superbasin (Neumann et al., 2009).

In the Mount Isa uranium field the Leichhardt River Fault Trough is bound by the Mount Isa-Twenty-nine Mile-Mount Gordon fault system against Isa Superbasin rocks to the west and by the Quilalar-Gorge Creek-St Paul Fault system against the Kalkadoon Leichhardt Fault to the east (Fig. 11). Based on a seismic traverse across the field (Hutton et al., 2009), these faults are interpreted as original extensional faults that defined the extent of the Leichhardt River Fault Trough. As discussed in section 2.1, rocks of the Mount Isa uranium field were then subjected to four phases of deformation associated with the 1640-1520 Ma Mount Isa Orogeny. The earliest period of thin-skinned deformation (D_2) began at 1600 Ma, and became widespread at 1585-1565 Ma (Connors

and Page, 1995; Giles and Nutman, 2002; Hand and Rubatto, 2002). This was followed by thick-skinned east-west contraction between 1550 and 1500 Ma, which included D_3 and D_4. In the Mount Isa area, these events are constrained to between 1550 and 1530 Ma (Connors and Page, 1995; Hand and Rubatto, 2002; Betts and Giles, 2006).

Rocks in the Leichhardt River fault Zone, between the Mount Isa-Twenty-nine Mile-Mount Gordon and Quilalar-Gorge Creek-St Paul fault systems underwent peak metamorphism under greenschist facies during D_3, with rocks in the Mount Isa uranium field within the chlorite zone at peak temperatures of 300-350°C (Foster and Rubenach, 2006). An age of metamorphism for this event of 1532 ± 7 Ma is suggested by the age of a syn-kinematic pegmatite (Connors and Page, 1995).

However, to the west of the Mount Isa Fault, the grade increases rapidly to amphibolite facies, beginning in the biotite zone, through the cordierite and sillimanite zones and into the sillimanite-K-feldspar zone over a distance of 15 km (Foster and Rubenach, 2006). Electron microprobe (Gibson et al., 2008) analyses of metamorphic monazite indicate multiple periods of metamorphic monazite growth, with growth at ~1636 Ma, ~1599 Ma (major peak), ~1542 Ma and ~1521 Ma. The major peak corresponds broadly with a regional 1600-1575 Ma timing for peak metamorphism and D_2 across the Mount Isa Inlier (Giles and Nutman, 2002; Hand and Rubatto, 2002), whereas the ~1542 Ma peak corresponds to the D_3 event recorded on the eastern side of the Mount Isa-Twenty-nine Mile-Mount Gordon fault system.

The eastern margin of the Mount Isa uranium field is also marked by a jump in metamorphic grade across the Quilalar-Gorge Creek-St Paul Fault system into the Kalkadoon-Leichhardt Belt, where basement rocks and rocks of the Leichhardt Superbasin have been metamorphosed to amphibolite facies. The age of metamorphism, however, is not known (Foster and Rubenach, 2006).

Schofield (2009), in an analysis of uranium contents in igneous rocks across Australia, has compiled uranium analyses of igneous rocks in the Mount Isa Inlier, including rocks from the Mount Isa uranium field. This analysis identifies the Sybella Granite, which forms a belt just to the west of the Mount Isa-Twenty-nine Mile fault system, as highly uranium enriched (mean 8.4 ppm based on 302 analyses with total range of 2-40 ppm) with a large proportion of analyses exceeding 20 ppm. In contrast, granites in the Kalkadoon-Leichhardt belt, to the east of the Quilalar-Gorge Creek-St Paul Fault system are closer to global average uranium contents (mean 5.3 ppm based on 304 analyses with total range of 1-35 ppm). Schofield (2009) also indicated that mafic igneous rocks from the Eastern Creek Volcanics are depleted in uranium relative to the granites (mean 2.2 ppm based on 29 least-altered analyses with total range of 0.5-6 ppm), though enriched relative to typical basalts.

3.3.1.1. Regional alteration in the Mount Isa uranium field

Regional alteration assemblages affecting basaltic rocks in the Mount Isa uranium field (Fig. 11) have been described as a part of studies on uranium and copper mineral systems (Wyborn, 1987; Bain et al., 1992; Heinrich et al., 1995; Gregory et al., 2005). Wyborn (1987) identified four regional alteration assemblages that have affected basaltic rocks in the vicinity of the Mount Isa copper deposit and the Mount Isa uranium field.

The earliest assemblage, which affects uncleaved rocks with relict igneous textures involves progressive replacement of igneous minerals by the assemblage albite-actinolite-chlorite with minor epidote, sphene, K-feldspar, biotite and chalcopyrite, the last mineral present in amygdales and veins. As rocks altered by this assemblage retain high magnetic susceptibility (Wyborn, 1987), it is likely that magnetite was stable during this alteration, which Heinrich et al. (1995) interpreted to

have developed as the peak metamorphic assemblage. This early assemblage was characterised by gains in K_2O and local enrichment of Cu, particularly within vesicular flow tops (Wyborn, 1987).

The second assemblage described by Wyborn (1987) involved progressive replacement of the earlier assemblage by an epidote-quartz-sphene assemblage with variable actinolite, chalcopyrite, pyrite and hematite (Hannan et al., 1993; Heinrich et al., 1995). This assemblage not only formed epidosites (locally >50% epidote), but also veins that cut metamorphic textures but are also boudinaged within the regional fabric, suggesting a syn-D_3 timing (Heinrich et al., 1995). This alteration resulted in an increase in Fe_2O_3/FeO, CaO and SiO_2 contents, but decreases in Na_2O, K_2O, MgO and copper and very little change in uranium (Heinrich et al., 1995). To the north and east of Mount Isa, the epidote-quartz-sphene assemblage has been mapped using HYMAP (Yang et al., 2000), with some uranium prospects showing an association with this assemblage (cf. Gregory et al., 2005).

The third assemblage of Wyborn (1987), which replaces and veins the earlier assemblages, is dominated by calcite, albite, chlorite and magnetite with minor biotite and K-feldspar. This assemblage is extensive in comparison with a texturally-similar calcite-albite-hematite assemblage that is restricted to north-south-trending fracture zones that cross-cut earlier D_3 faults (Heinrich et al., 1995). This alteration involved increases in Na_2O, CaO, Fe_2O_3/FeO and CO_2 but decreases in K_2O and magnesium, with no significant changes in uranium content. It is spatially associated with uranium prospects to the northeast of Mount Isa (Bain et al., 1992; Heinrich et al., 1995).

The last assemblage described by Wyborn (1987) was dominated by chlorite, albite and rutile, with variable sphene, pyrite, pyrrhotite, ilmenite and tourmaline and with biotite in K-rich rocks. This assemblage is most extensively developed in basaltic rocks below the Paroo Fault in the vicinity of the Mount Isa copper orebodies (Hannan et al., 1993; Heinrich et al., 1995). This assemblage is described as progressively removing Ca-bearing phases, suggesting that it post-dated the carbonate-Fe-oxide assemblage (Heinrich et al., 1995). Leaman (1991) estimated that this assemblage has affected ~30 km^3 of basalt in this area. A similar assemblage is developed in higher grade rocks to the west of the Mount Isa fault (Heinrich et al., 1995) and in an area 11 km south of the Cu orebody (Wyborn, 1987). Geochemically, this assemblage is associated with increases in SiO_2, MgO, but decreases in Na_2O, CaO, CO_2, Fe_2O_3/FeO and, importantly, copper.

Of the regional alteration assemblages described in the literature, metasomatic uranium deposits in the Mount Isa uranium field are most closely associated with the epidote-quartz-sphene assemblage and, particularly the calcite-albite-hematite assemblage, the latter developed along north-trending fractures that also host uranium prospects. Temporally, these assemblages are synchronous or slightly postdate peak-metamorphic conditions and D_3. The earlier albite-actinolite-chlorite assemblage appears to be a regional metamorphic assemblage, whereas the chlorite-albite-rutile assemblage appears to later and possibly unrelated to the uranium deposits. Although well developed in basalt of the Eastern Creek Volcanics, regional alteration assemblages do not appear to have an expression in siliciclastic sedimentary rocks, either in sedimentary lenses intercalated with basalt or in the underlying Mount Guide Quartzite and Bottletree Formation. This may suggest that the ore fluids were in equilibrium with these rocks.

3.3.1.2. Deposits of the Mount Isa uranium field

Most of the deposits, prospects and occurrences in the Mount Isa uranium field are hosted by the Eastern Creek Volcanics, although a few prospects are present in rock of the underlying Mt Guide Quartzite (Leander Quartzite) and the overlying Myally Subgroup and Surprise Creek Formation of the Calvert Superbasin (Brooks, 1975). The most significant deposit, Valhalla, consists of two lenses

hosted by a clastic sedimentary lens within tholeiitic basalt of the Eastern Creek Volcanics (Fig. 11). The larger, northern lens strikes NNW and plunges ~50° to the south (Eggers, 1999). Least altered host sedimentary rocks consist of fine-grained quartzo-feldspathic sandstone and gritty siltstone with accessory biotite, muscovite and variable amounts of Fe and Mg- silicates, hematite and magnetite (Polito et al., 2009). The deposit is located ~800 m east of the Twenty-nine Mile Fault (Fig. 11).

The ores are associated with a zone of variably albite-calcite-riebeckite-hematite altered sandstone/siltstone. This zone is commonly brecciated, with the ore zones mostly characterised by sub-angular to angular clasts of intensely altered sandstone/siltstone (to 20 mm) infilled by a matrix comprising the assemblage brannerite-apatite-zircon-calcite-hematite. The highest grade zones are marked by uraninite-hematite-dolomite-chlorite veins (Polito et al., 2009). The uranium-mineralised interval is also marked by LREE (to 500 ppm total LREE) and, particularly, zirconium (to 4%) and HREE (to 140 ppm total HREE) enrichment. Both margins of the mineralised zone appear to have low-grade (to 0.4%) copper enrichment (Fig. 3 of Polito et al., 2009). Polito et al. (2009) reported pyrite and lesser chalcopyrite and bornite as paragenetically late stage minerals, probably accounting for the localised copper enrichment.

Descriptions of other deposits in the Mount Isa uranium field are limited, with the best description of Anderson's Lode. Like Valhalla, this deposit is hosted by a sedimentary lens within tholeiitic basalt of the Eastern Creek Volcanics. The deposit has an irregular, tabular form, with dimensions of ~20 m × 60 m at surface that increase with depth (Brooks, 1975; Gregory et al., 2005). The body trends east-west, with a steep northerly plunge, parallel to the intersection between a north-striking fracture cleavage (local S_2) and an earlier penetrative cleavage (local S_1; Bain et al., 1992). The uranium is preferentially enriched in siltstone beds (sandstone beds are generally barren), where it is closely associated with fluorapatite and lesser chlorite, biotite and magnetite. The ore assemblage includes brannerite and associated anatase, quartz and galena. Magnetite and titanite overgrow all earlier ore-related phases (Gregory et al., 2005). Gregory et al. (2005) also noted a correlation between uranium and gold. Although Anderson's Lode has some similarities to the Valhalla deposit, it also has some important differences to the Valhalla deposit, the most notable being the lack of an albite-riebeckite-bearing assemblage. Another important difference is the association with the Quilalar-Gorge Creek-St Paul Fault system along the eastern margin of the Mount Isa uranium field.

In addition to deposits in the low metamorphic grade Leichhardt River Fault Trough, a number of uranium occurrences and prospects are present in higher metamorphic grade rocks to the west of the Mount Isa-Twenty-nine Mile fault system (Fig. 11). Gregory et al. (2005) described two of these prospects, at Eldorado and Lucky Break, as being hosted within or at the contact between amphibolite of the Eastern Creek Volcanics and muscovite-bearing schists. Uranium mineralisation is associated with hornblende-rich layers in the amphibolite where it has not been affected by epidote alteration. They interpreted that the uranium was emplaced during or before peak metamorphism based on the observation that uraninite is contained within peak metamorphic hornblende and titanite. However, inspection of their Figure 4C suggests that titanite and uraninite infill and, therefore, postdate hornblende.

3.3.1.3. Timing of mineralisation in the Mount Isa uranium field

At the Valhalla deposit, LA-HR-ICPMS analysis of brannerite yielded a range in ^{207}Pb-^{206}Pb ages between ~584 Ma and 1543 ± 15 Ma, with the latter age within error of an upper discordia intercept age of 1564 ± 27 Ma (Polito et al., 2009). These ages also overlap with a $^{40}Ar/^{39}Ar$ plateau age for riebeckite of 1551 ± 7 Ma (Polito et al., 2009). These results collectively suggest an age for the Valhalla deposit of 1550-1540 Ma, an age that corresponds in time with the early part of the third

phase (D_3) of the Isa Orogeny (Betts and Giles, 2006; Murphy et al., 2008). Based on textural relationships, Gregory et al. (2005) suggested a pre- to syn-metamorphic timing for mineralisation at the Andersons deposit. ^{40}Ar-^{39}Ar dating of one uranium-mineralised biotite separate from biotite-chlorite-magnetite-hematite altered basalt yielded a plateau-like age of 1534 ± 4 Ma. A second sample yielded single step ages of between ~1554 Ma and 1524 Ma (Perkins et al., 1999). The plateau-like age is probably the best age estimate for the age of mineralisation, an age similar to the likely age of Valhalla and consistent with a syn-metamorphic (D_3) timing of mineralisation.

Based on textures at Anderson's Lode and Eldorado-Lucky Break, Gregory et al. (2005) interpreted these deposits as metamorphosed unconformity-related uranium deposits, an interpretation quite different to that advanced by Polito et al. (2009) at Valhalla. Although there are significant differences between these deposits vis-à-vis ore and alteration assemblages and geological setting, we consider it unlikely that two different styles of mineralisation were involved. Based on the textures at Eldorado-Lucky Break and the ^{40}Ar-^{39}Ar data at Anderson's Lode, we consider these deposits, as well as Valhalla, to be most likely metasomatic deposits formed during D_3.

3.3.2. Mineral system model for Mount Isa uranium field

Based on the above synthesis and discussion, we interpret uranium deposits in the Mount Isa uranium field formed as part of an oxidised U(V-Zr-REE-P) mineral system that developed during the third phase (D_3) of the Isan Orogeny in response to basin inversion. Figure 12 illustrates essential components of this mineral system. In the deeper part of the Leichhardt Superbasin, metamorphic fluids and or connate brines equilibrated with oxidised, shallow water sediments, including red beds, under greenschist conditions, leading to the development of an oxidised, moderately saline, sodic ore fluid with temperatures of 300-350°C. Because this fluid formed in equilibrium with the lower part of the Leichhardt Superbasin, it did not produce significant regional alteration zones in these rocks.

This ore fluid then acquired uranium from not only the lower part of the Leichhardt Superbasin, but also uranium-rich rocks from the walls and basement to the Leichhardt River Fault Trough. This process was enhanced by the presence of uranium-rich source rocks, particularly those that underwent prior high-grade metamorphism.

Inversion of the Leichhardt River Fault Trough during east-west contraction associated with the third phase (D_3) of the Isan Orogeny between 1550 and 1530 Ma expelled these U-rich fluids up inverted extension faults and faults that initiated as reverse faults during D_3. Chemical gradients set up as these oxidised fluids encountered the reduced, Fe-rich Eastern Creek Volcanics caused the fluids to become reduced and the volcanics to become oxidised. This produced the epidote-quartz-sphene regional alteration assemblage and the calcite-albite-iron oxide, particularly the calcite-albite-hematite, fracture-related alteration assemblage. Small uranium occurrences were deposited as part of these reactions. Copper was leached during these reactions.

The deposition of uranium from these fluids was enhanced within siliciclastic lenses within the Eastern Creek Volcanics. These permeable lenses allowed the oxidised uranium-bearing fluids to mix with reduced fluids in equilibrium with the basaltic rocks surrounding the lenses. This process enhanced uranium precipitation as the reduced fluids accessed a greater volume of rock than would have been accessed through fluid-rock reactions alone. Reaction of the uraniferous oxidised fluids would have produced a zoned deposit, with uranium minerals, which precipitate under relatively oxidised conditions (Skirrow et al., 2009), depositing near the core of the mineralised zone and copper and possibly zinc and lead depositing along the margin. Given this model, the following section addresses the six mineral system questions to determine mappable criteria used in potential

assessment. More details of the metasomatic mineral system are presented in Appendix A, and Table 5 summarises the mappable criteria and weightings used in potential assessment of the metasomatic uranium mineral system.

Q1. What is the geodynamic and P-T history (including timing of mineralisation) of the system?

Evidence from the Mount Isa uranium field, together with evidence from other global systems, suggest the systems form relatively late in the active geological history of an area, associated with contraction and post-peak metamorphism. Alteration assemblages and temperature estimates suggest greenschist facies conditions at the time of mineralisation. Mineralisation appears to be associated with inversion of pre-existing extensional faults during D_3, suggesting that not only the metamorphic and contractional history of the province is important, but also the early extensional history is important. In the case of the Mount Isa metasomatic system, the architecture of the system was set up by extension early in the geodynamic history and the reactivated later in the history by contraction associated with D_3 deformation. In addition, the eruption of voluminous mafic volcanic rocks during the early extension also set up the redox gradients that caused uranium deposition (see below). Based on this discussion, the following criteria were considered in the potential assessment:

- Greenschist facies metamorphism at time of mineral system activity (metamorphic grade).
- Inversion of basin, juxtaposing higher metamorphic grade source rocks against lower grade basinal rocks and setting up a metamorphic gradient (metamorphic gradient).

Q2. What is the structural and lithological architecture of the system?

Key aspects of the architecture of the metasomatic uranium system include extensional faults developed during basin development and the associated rock sequence. These faults were conduits for uraniferous fluids during basin inversion. They also juxtaposed basinal rocks against granites and basement that sourced uranium. The depositional sequence was characterised by fluviatile, lacustrine and shallow marine sequences prior to the eruption of voluminous mafic volcanics. The contrast between these highly oxidised sedimentary rocks against mafic volcanics became a very effective redox gradient for uranium deposition during fluid flow associated with later basin inversion. Based on this discussion, the following criterion was considered in the potential assessment:

- Distribution of sedimentary and volcanic facies (distribution of Leichhardt Superbasin) as well as fundamental faults set up during initial extension to form Leichhardt Superbasin.

Q3. What and where are fluid reservoirs and metal sources for the mineral system?

Unlike some other mineral systems, a uranium-enriched source appears to be essential for metasomatic uranium systems. As discussed by Schofield (2009), Proterozoic granites in the Mount Isa Province, particularly the ~1670 Ma Sybella Granite, are enriched in uranium relative to crustal averages. Spatially, the majority of deposits and prospects as well as virtually all mineral resources, are proximal (i.e. within 5 km) to exposed portions of the Sybella Granite (Fig. 11). Mobilisation of uranium in granite sources and then transport of this uranium to depositional sites requires highly oxidised fluids. This fluid was most likely either a basinal fluid or a fluid which had equilibrated with magmatic rock (cf. Polito et al., 2009). A likely fluid source was either basinal brines expelled during basin inversion, or metamorphic fluids that have equilibrated with regional magmatic rocks or a hybrid between these end-members. Another possiblity is magmatic-hydrothermal fluids; however, granites coeval with mineralisation (1550-1540 Ma) are not known in the Mount Isa uranium field. Based on this discussion, the following criteria were considered in the potential assessment:

- Uranium-rich rocks within the source region (i.e. basement and rift margins) at the time of mineral system activity (distribution of uranium-rich basement rocks and granites).
- Sourcing of oxidising, moderate to high temperature (300-500°C) fluids from basal part of Leichhardt Superbasin during regional greenschist facies metamorphism (distribution of Leichhardt Superbasin).

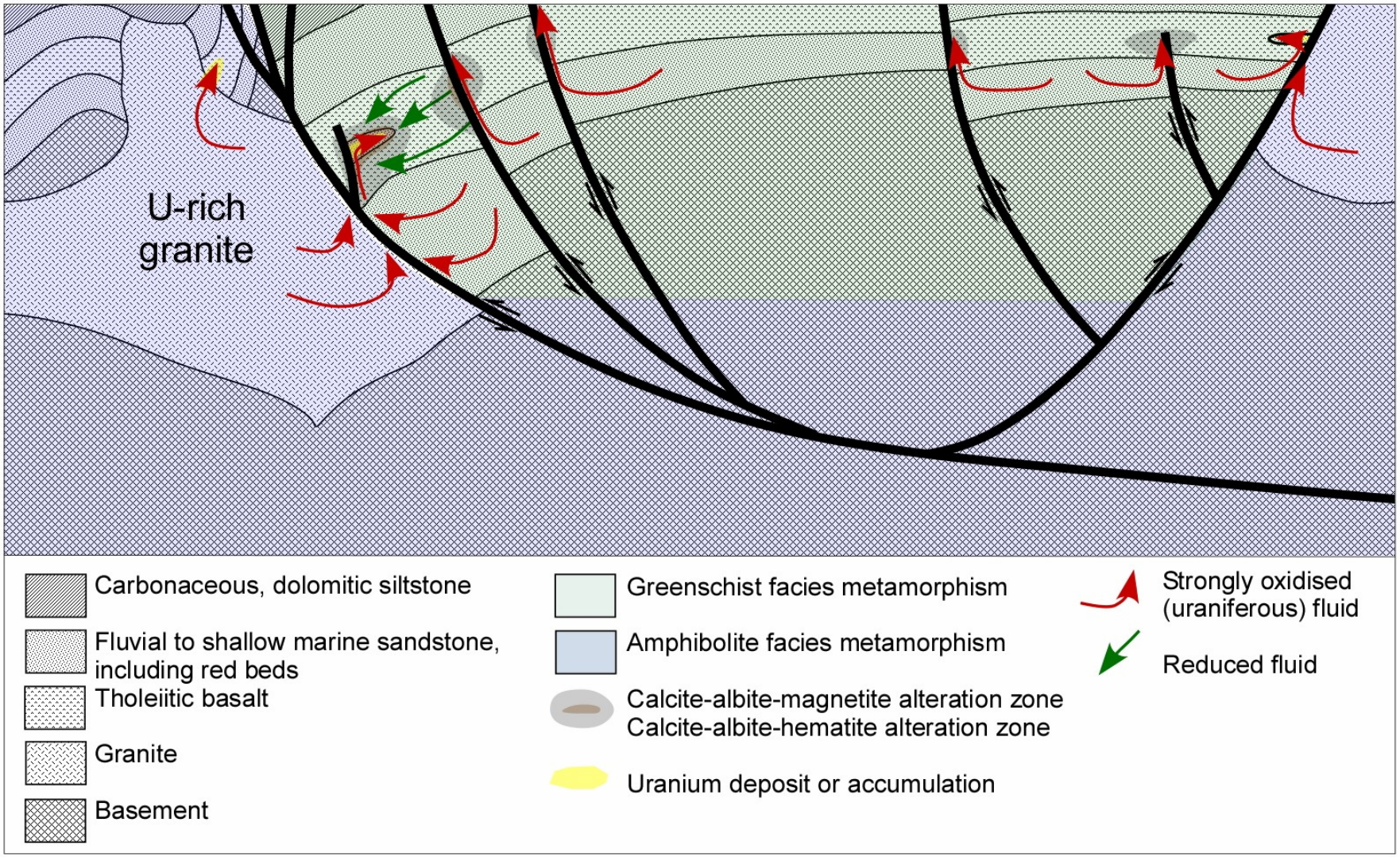

Figure 12: *Mineral system model for metasomatic uranium deposit in the Mt Isa district.*

Table 5: Mappable criteria used for potential assessment of metasomatic uranium deposits.

MINERAL SYSTEM QUESTION	CRITERIA	SCORE	DATASET & REFERENCE	COMMENTS
1	*Metamorphic grade* Greenschist facies Amphibolite facies	 3 1	Rubenach (2008)	Restricted to Mt Isa Province
1	*Metamorphic gradient (greenschist → amphibolite)* 5 km buffer on greenschist side of gradient 2 km buffer on amphibolite side of gradient	 3 1	Rubenach (2008)	Restricted to Mt Isa Province
2, 3	*Distribution of fluid source and potential depositional sites* Leichhardt Superbasin 5 km buffer around Leichhardt Superbasin	 3 1	Surface geology of Australia (Whitaker et al., 2007)	
3	*Uranium source -- radiometric data* 0-10 km buffer around U-enriched basement rocks 10-30 km buffer around U-enriched basement rocks	 3 1	Radiometric map of Australia (Minty, 2009)	Uranium values greater than or equal to 10 ppm were extracted from the filtered uranium band and converted to a polygon shape file. A spatial query was used to select values for crystalline basement only
3	*Uranium source -- granite data* 5 km buffer around granite analyses with >6 ppm U 5 km buffer around granite analyses with 3-6 ppm U 5 km buffer around granite analyses with 1-3 ppm U	 3 2 1	Schofield (2009)	High solubilities allow uranium to become highly concentrated with progressive magmatic evolution
4	*Fluid pathways -- structural conduits* 0-2 km buffer around D_3 faults 2-4 km buffer around D_3 faults 4-6 km buffer around D_3 faults	 3 2 1	Northwest Queensland GIS	
4	*Fluid pathways -- regional alteration assemblages* 2 km buffer around carbonate-albite-hematite assemblages	 2	Heinrich et al. (1995)	Data restricted to southern part of Mt isa uranium field
5	*Uranium deposition -- evidence from radiometric data* Uranium enrichment (>10 ppm) within Leichhardt Superbasin 10 km buffer around U-enriched rocks 20 km buffer around U-enriched rocks	 3 2 1	Radiometric map of Australia (Minty, 2009)	Uranium values ≥10 ppm were extracted from the filtered uranium band and converted to a polygon shape file. A spatial query was used to select values for Leichhardt Superbasin rocks.

5	*Distribution of potential depositional sites -- mapped geology* Mafic rocks	3	Surface geology of Australia (Whitaker et al., 2007)	No buffer
5	*Distribution of U-related mineral deposits* 0-2 km buffer around vanadium deposits 2-4 km buffer around vanadium deposits 4-6 km buffer around vanadium deposits	3 2 1	MINLOC	

Q4. What are the fluid flow drivers and pathways?

Geological and timing relationships suggest that hydrothermal fluid migration occurred during greenschist facies metamorphism associated with southeast-northwest-directed contraction during D_3. This contractional event expelled the hybrid basinal brine-metamorphic fluid along pre-existing extensional faults during inversion. Movement of these fluids along these faults is recorded by a epidote-quartz-sphene assemblage and, particularly a calcite-albite-hematite assemblage. Uranium occurrences are commonly associated with these assemblages. Based on this discussion, the following criteria were considered in the potential assessment:

- Inversion of early extensional faults during D_3 (distribution of faults active during D_3).
- Movement of fluids through mineral system along inverting structures and into upper parts of basin (distribution of carbonate-albite-hematite alteration assemblages).

Q5. What are the metal (and ligand) transport and depositional processes?

As discussed above, uranium is interpreted to have been transported by oxidised fluids that formed oxidised epidote- and hematite-bearing mineral assemblages. Deposition of uranium from such fluids requires reaction either with a reduced rock package or mixing with fluids in equilibrium with such a package. Both processes appear to have been important in the Mount Isa uranium field. A number of the smaller prospects, such as Eldorado and Lucky Break, are hosted by amphibolite at the contact with muscovite schist, suggesting that reaction with the amphibolite was the main depositional mechanism. In contrast, the Valhalla and Anderson's Lode deposits are hosted by sandstone lenses with Eastern Creek Basalt. At Valhalla, Polito et al. (2009) suggested two fluids were involved in ore deposition. The first is the hybrid basinal brine-metamorphic fluid, as discussed above, but the second was likely a reduced local fluid in equilibrium with the Eastern Creek Volcanics. Mixing of these two fluids in sandstone resulted in uranium deposition. Based on this discussion, the following criteria were considered in the potential assessment:

- Deposition of uranium (evidence of uranium deposition) as a consequence of fluid reduction caused by interaction with Fe^{2+}- (distribution of mafic rocks) or reduced-carbon-rich rocks or fluids in equilibria with such rocks.
- Deposition of redox-sensitive elements, such as vanadium (distribution of mineral deposits/occurrences with redox-sensitive elements such as vanadium).

Q6. What are the effects of post-depositional processes on metal accumulations?

Although U-Pb analyses of brannerite define an upper intercept at ~1564 Ma, which is interpreted to approximate the age of mineralisation, similar analyses for uraninite define a discordia with upper and lower intercepts of ~1222 Ma and 107 Ma, respectively. Polito et al. (2009) interpret the older age to indicate fluid flow during the assembly of Rodinia. The significance of the younger intercepts

is unclear, although they may relate to fluid flow associated with formation of the Eromanga Basin. The 175 Ma age just post-dates the initiation of the basin, whereas the ~107 Ma age corresponds with the deposition of the Toolebuc Formation, which signifies the maximum flooding surface of the basin (Radke et al., 2000; S van der Wielen, pers. com., 2009). Other that resetting the ages, these events do not appear to have affected the deposits. Consequently, no criteria relating to this question were included in the potential assessment.

3.3.3. Results of assessment analysis for metasomatic uranium systems

Plate 4 shows the results of potential analysis for metasomatic uranium systems in North Queensland. As the availability of some datasets was not uniform over the study area, the potential threshold was set lower for the Georgetown Inlier, the Tasman Orogen and the southern Macarthur Basin. This assessment has highlighted known areas of metasomatic uranium mineralisation, as well as identifying areas with potential but without known mineralisation:

A. Mount Isa uranium field. As expected, the analysis has highlighted the Mount Isa uranium field as having high potential.
B. Extension of Mount Isa uranium field to the south and west. The results suggest that high potential for metasomatic uranium deposits extends south of the Mount Isa uranium field along the western margin of the Leichhardt River Fault trough, particularly adjacent to the exposed and inferred extent of the Sybella Granite. The analysis also suggests potential along D_3 structures where they cut the Leichhardt River Fault Trough, particularly where Eastern Creek Volcanics are present.
C. Eastern margin of Leichhardt River Fault Trough. The analysis suggests high potential for metasomatic uranium deposits along with eastern margin of the Leichhardt River Fault Trough, along the boundary with the Kalkadoon-Leichhardt Belt.
D. East of Mary Kathleen. Another area of high potential in the Isa Province include the area to the south and east of the Mary Kathleen deposit in with Eastern Fold Belt.
E. Naruku Suite Plutons. Another prospective area identified is associated with metamorphic aureoles around Naraku Suite plutons in the Eastern Fold Belt, particularly where D_3 structures have been identified.
F. South of Mary Kathleen. The analysis has identified high potential in a north-trending belt 40 to 200 km south of Mary Kathleeen associated with the eastern margin of the Leichhardt Superbasin.
G. Westmoreland area. Outside of the Mount Isa Inlier, the analysis has highlighted moderate potential in the Westmoreland area, an area of significant unconformity-related deposits (see above).
H. Southwest of Cairns. Nearer the Pacific coast, the analysis has highlighted a 50 km wide zone to the southwest of Cairns associated with a number of uranium prospects.
I. Croydon area. Another area of moderate potential is the exposed Proterozoic near Croydon, particularly the Croydon Volcanics.
J. Len Lomond area. The analysis has highlighted the area to the north of the Ben Lomond deposit as having moderate potential.

An area about 120 km to the east of Georgetown highlighted by this analysis is not considered prospective as the assessed potential is based mostly on the distribution of Tertiary basalt.

3.4. URANIUM-RICH IRON-OXIDE COPPER-GOLD SYSTEMS (R SKIRROW AND D HUSTON)

In recent years, many historical and recently discovered copper-gold deposits in north Queensland have been classified as iron-oxide copper-gold deposits. In particular, these deposits include copper-gold deposit in the Cloncurry district and also some deposits near Einasleigh. The giant Olympic Dam deposit in South Australia, the largest known iron oxide copper-gold deposit, also is a major repository of uranium, and other iron oxide copper-gold deposits around Australia and the world commonly have anomalous uranium concentrations (Hitzman and Valenta, 2005).

3.4.1. The Cloncurry district

After the Olympic Dam iron-oxide copper-gold Province, the Cloncurry district in the eastern part of Mount Isa Province (Fig. 2) is the largest iron-oxide copper-gold mineral province in Australia. Exploration over the last 25 years has resulted in a number of significant Cu-Au discoveries, which are continuing with the outlining of a major deposit at Mount Elliott and a new style of Mo-Re deposit at Merlin in the Mount Dore system in the last five years. In addition to these deposits, other important deposits include Ernest Henry, Starra, Osborne, Monakoff, Eloise, and Greenmount (Fig. 2). Of these, the Ernest Henry and the Mount Elliott deposits are known to contain significant uranium grades and a number of prospects in the vicinity of the Mount Elliott deposit and in the Kuridala area also contain elevated to locally ore-grade uranium. This section describes the geology of known uranium-bearing systems and the relationship of the uranium to other commodities. A summary of the characteristics of deposits in which anomalous uranium has not been identified is presented in Kositcin et al. (2009).

3.4.1.1 Ernest Henry deposit

The Ernest Henry deposit (Fig. 2) is hosted largely by variably altered andesitic rocks that may correlate with ~1745 Ma metavolcanic rocks at surface to the west (Page and Sun, 1998). Mark et al. (2006) described the following alteration assemblages at Ernest Henry: (1) sodic (albitic) and/or sodic-calcic (albite-actinolite-diopside-magnetite-scapolite-pyrite) → (2) pre-ore (biotite-magnetite-garnet-K-feldspar) → (3) ore-stage (K-feldspar-quartz-rutile-calcite-magnetite-pyrite-biotite-barite-chalcopyrite-hematite) → (4) post-ore (calcite-dolomite-quartz-biotite-actinolite-pyrite-magnetite). The ores are hosted by breccias with clasts of K-feldspar-altered andesite infilled by the ore-stage assemblages. Other minor to accessory minerals include molybdenite, coffinite and scheelite among others (Mark et al., 2006), suggesting that the ores are enriched in molybdenum, tungsten and uranium in addition to gold and copper. The ores average 50 ppm U, with anomalous cobalt, rare earth elements, arsenic, fluorine and barium (Ryan, 1998). The pre-ore and ore-stage assemblages distinctly overprint the sodic and sodic-calcic assemblages (Mark et al., 2006).

3.4.1.2. Mount Elliott deposit

Recent drilling in the vicinity of the old Mount Elliott mine (Fig. 2) by Ivanhoe Australia has identified significant new (mostly primary) resources totaling 475 Mt grading 0.5% Cu and 0.3 g/t Au (Ivanhoe Australia 2008 annual report) in addition to previous production. The Mount Elliott system consists of four discrete lenses (Mount Elliott, Swan, Swell and Courbould) that are hosted by carbonaceous phyllites and quartz-mica schist that are part of the Kuridala Formation. The lenses are located within the NW-trending, composite Mount Elliott Fault Zone, with mineralized zones bound by steeply-dipping reverse faults (Fortowski and McCracken, 1998).

The carbonaceous phyllites were initially altered to an albitic alteration assemblage that was subsequently overprinted by a later skarn assemblage (Fortowski and McCracken, 1998; Garrett, 1992). The albitic assemblage is characterized by initial bleaching of the phyllites, resulting from destruction of graphite and biotite and the growth of the assemblage quartz-albite-sericite±pyrite,

with minor to trace pyrrhotite and fluorite, followed by progressive hematite dusting along fractures and foliation planes (Fortowski and McCracken, 1998). The skarn assemblage is characterized by the assemblage K-feldspar-calcite-clinopyroxene with local sphene and scapolite. This assemblage is overprinted by veins and breccias that are characterized by a chalcopyrite-pyrrhotite-pyrite-magnetite-clinopyroxene-scapolite-calcite assemblage, with pyrrhotite dominant over magnetite in the upper part of the system and grading to a deep, barren magnetite core. Chalcopyrite is associated with both pyrrhotite and magnetite (Fortowski and McCracken, 1998).

3.4.1.3. Uranium mineralisation

Although the main commodities in the Cloncurry district are copper, gold and, most recently, molybdenum, uranium is present at anomalous, though uneconomic, levels in several of the iron-oxide copper-gold deposits. These deposits include the Ernest Henry deposit, which averages 50 ppm U, and the Swan lens in the Mount Elliott system, which, based on assays released in a 2007 Ivanhoe Mines press release (http://www.ivanhoe-mines.com/i/pdf/2007-01-18_NR.pdf), has grades between 20 and 400 ppm over long intersections, and spot grades up to 2200 ppm. Plotting of these data, however, indicate that the uranium and copper assays do not correlate (Fig. 13a).

Uranium is present as a stand alone commodity at several prospects in the Cloncurry district in the vicinity of Kuridala, although public domain literature about these prospects is limited. The following descriptions are based largely on the Ivanhoe Mines (www.ivanhoe-mines.com) and Ivanhoe Australia (www.ivanhoeaustralia.com) websites. The most significant results have been at the Robert Heg prospect, which has historical assays of up to 9300 ppm U_3O_8 over 11 m. At this deposit, uranium is hosted by a chloritic shear zone, with low grade, possibly disseminated uranium within granite and calc-silicate rocks. Other nearby prospects include Dairy Bore, Old Fence and U2.

In the Mount Elliott area, uranium has been detected at the Amethyst Castle and Metal Ridge prospects. At Amethyst Castle, high grade, chalcocite mineralised breccias were intersected in several drill holes. These breccias are polylithic with a hematite matrix and chalcocite present both in the matrix and clasts. Elsewhere chalcocite-bornite-chalcopyrite-carbonate veins and vein breccias are present. Alteration assemblages include silica, albite and hematite, and the hosts include biotite schist and granite. Uranium grades typically range between X0-X00 ppm, with a maximum grade (over 1 m) of 1800 ppm. Like other deposits in the Cloncurry district, published assays suggest that copper and gold are correlated, but there is not a correlation between copper and uranium (Fig. 13b).

3.4.1.4. Summary of characteristics of iron-oxide copper-gold deposits in the Cloncurry district

As described above and in Kositcin et al. (2009), iron-oxide copper-gold deposits in the Cloncurry district are quite diverse, although there are some unifying themes. Despite varying in abundance, magnetite is present in all deposits, as are chalcopyrite and pyrite. In most deposits, there is an early albitic alteration assemblage that is overprinted by later K±Fe-bearing or skarn assemblages. The ore assemblage overprints these latter assemblages, largely as veins and/or breccias. Typically these deposits are characterized by a Cu-Au-Co-(Mo-W-U-Sn) assemblage with some deposits also containing Ba, F, Zn, Pb and/or Ni, and in most cases, the ores were introduced during regional D_4.

These deposits are hosted by a variety of rocks, ranging from epigenetic and syngenetic ironstone, through carbonaceous phyllite, quartz-mica schist, black shale and meta-arkose through to intermediate metavolcanic rocks and amphibolites. Another diverse characteristic is the Fe-S-O assemblage, with the relative abundance of pyrrhotite and hematite apparently governing Cu/Au ratios. At Osborne, pyrrhotite-rich zones are copper-rich, whereas hematite-rich zones are gold-rich. The main metal assemblage present in these deposits is Cu-Au; in some deposits Co is also important, Silver and Zn are associated with this assemblage. At the Merlin deposit, a Mo-Re assemblage is also present, although within an overall Cu-Au dominated system. In addition, where

assayed, uranium also appears to be an important component of these systems, although the lack of correlation between it and the Cu-Au assemblage may suggest different depositional settings and may indicate uranium potential beyond Cu-Au-mineralised zones in these deposits.

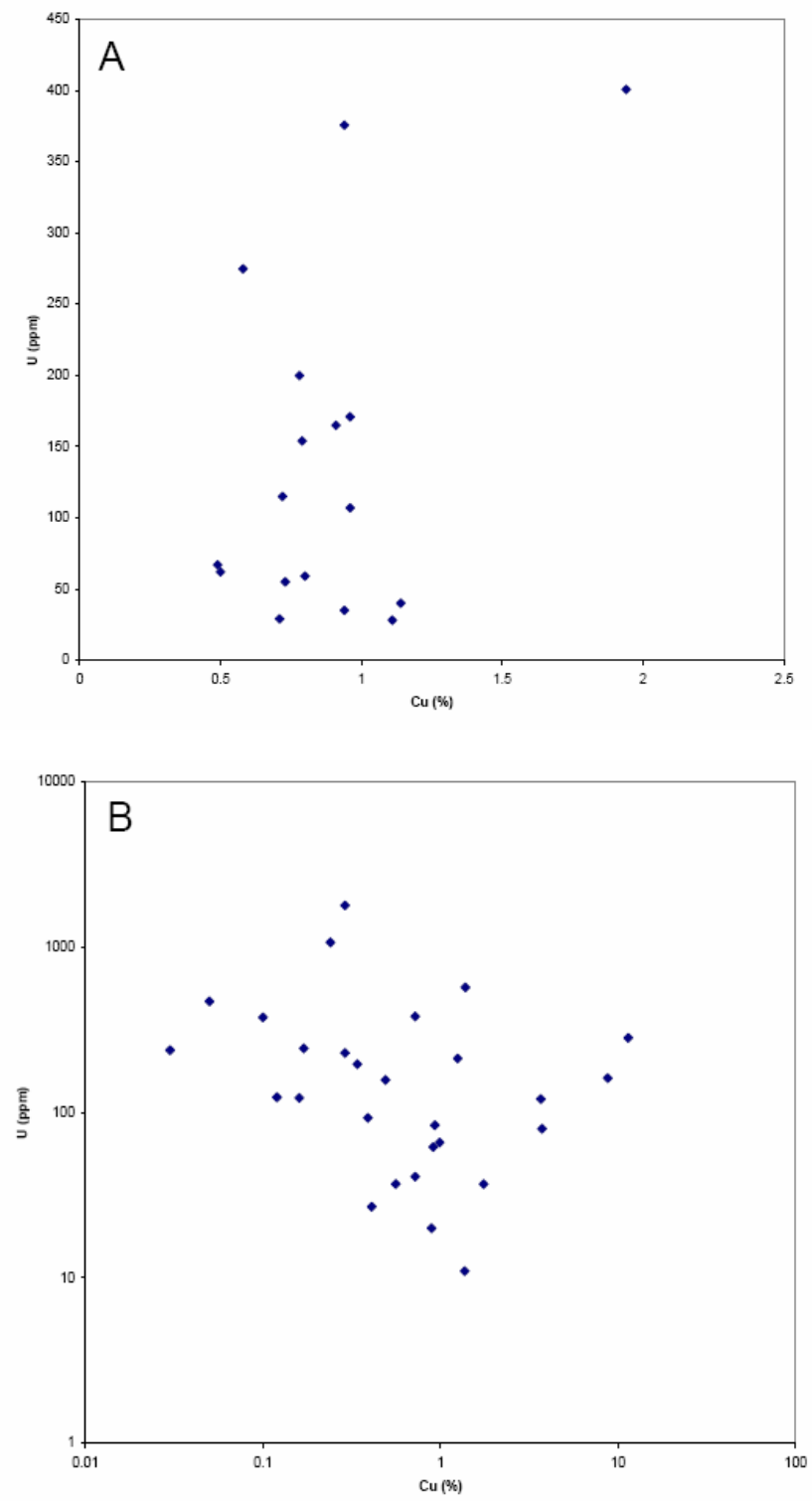

Figure 13: *Scattergrams showing the relationship between uranium and copper assays at the (a) Swan orebody of the Mount Elliott depost and (b) the Amethyst Castle deposit (data from www.ivanhoe-mines.com and www.ivanhoeaustralia.com).*

3.4.1.5. Regional alteration assemblages

Although not directly associated with copper-gold ore, early sodic and sodic-calcic alteration assemblages are a characteristic shared by many iron-oxide copper-gold deposits in the Cloncurry district and elsewhere around the world (Williams et al., 2005). Regionally, sodic and sodic-calcic alteration assemblages are widespread in the eastern part of the Mount Isa Province, affecting the rocks east of the Kalkadoon-Leichhardt Belt, particularly the Soldiers Cap Group. Oliver et al. (2004) recognized three episodes of albitic alteration, with the last the most extensive and most likely associated with iron-oxide copper-gold deposits of the Cloncurry district. This episode is interpreted to have formed between 1550 and 1500 Ma, coeval with emplacement of the Williams-Naruku Granites, which are also locally albite altered. In addition to albite, the regional alteration assemblage may include minor to trace titanite, amphibole, clinopyroxene, biotite, apatite, epidote, magnetite, hematite and pyrite (Oliver et al., 2004). The altered zones are typically crosscutting, commonly occurring along D_4 high-strain zones, in vein and in breccias. Where exposed these regional assemblages are typically interpreted to have formed between 400° and 600°C, at pressures of 200-450 MPa (Oliver et al., 2004).

3.4.1.6. Age of mineralisation

Studies of several deposits in the Cloncurry district indicate a syn- to late-D_4 mineraliastion timing. More recent geochronology has begun to clarifiy the absolute timing of mineralization. A summary of recent age data by Kositcin et al. (2009) suggests that, excepting the Osborne deposit, all deposits formed in the range 1530 to 1500 Ma. This range overlaps the likely age of regional albitic alteration and also the emplacement ages of granites that form the Williams-Naruku granite suite.

3.4.1.7. Regional controls on iron-oxide copper-gold mineralisation in the Cloncurry district

The results of the 2006 Mt Isa and 2007 Cloncurry-Georgetown-Charters Towers seismic surveys suggest that the eastern margin of the Mount Isa Province is bounded by a west-dipping suture juxtaposing this province with a two layered crustal block to the east, comprising the Numil Seismic Province and the Kowanyama-Etheridge Province (Korsch et al., 2009; Henson et al., 2009; Huston et al., 2009). This suture, also imaged by magnetotelluric data and inversions of aeromagnetic data (Chopping et al., 2009), is interpreted to be old, possibly the consequence of subduction and accretion of the Numil Province prior to 1850 Ma (Korsch et al., 2009; Huston et al., 2009).

When projected onto line 07GA-IG1 (using the trend of magnetic anomalies), the Ernest Henry deposit is located in the hangingwall of the crustal discontinuity (Huston et al., 2009), in a similar position to that inferred for the uranium-rich Olympic Dam iron oxide copper-gold deposit above a boundary zone between inferred Archean and Proterozoic crust that is visible in both seismic and MT data (Lyons and Goleby 2005). Other deposits in the eastern Mt Isa province appear to be situated a similar position relative to the inferred suture. In the northern part of the district, the surface projection of this suture is marked by the eastern margin of a gravity ridge and a major change in magnetic character (Fig. 14). In the southern part of the district, the suture follows either the position of a less pronounced change in magnetic character that projects onto the approximate position of the Cloncurry Fault (solid line: Fig. 14a), or the edge of the position of this suture corresponds approximately with the eastern margin of a gravity high (dashed line: Fig. 14b). This suture also appears to correspond with the western margin of the Carpentaria conductance anomaly of Lilley et al. (2001).

With the exception of the Eloise deposit, all iron-oxide copper-gold deposits are localised in the hangingwall of the suture, approximately 20-50 km west of its projection to surface (Fig. 14).

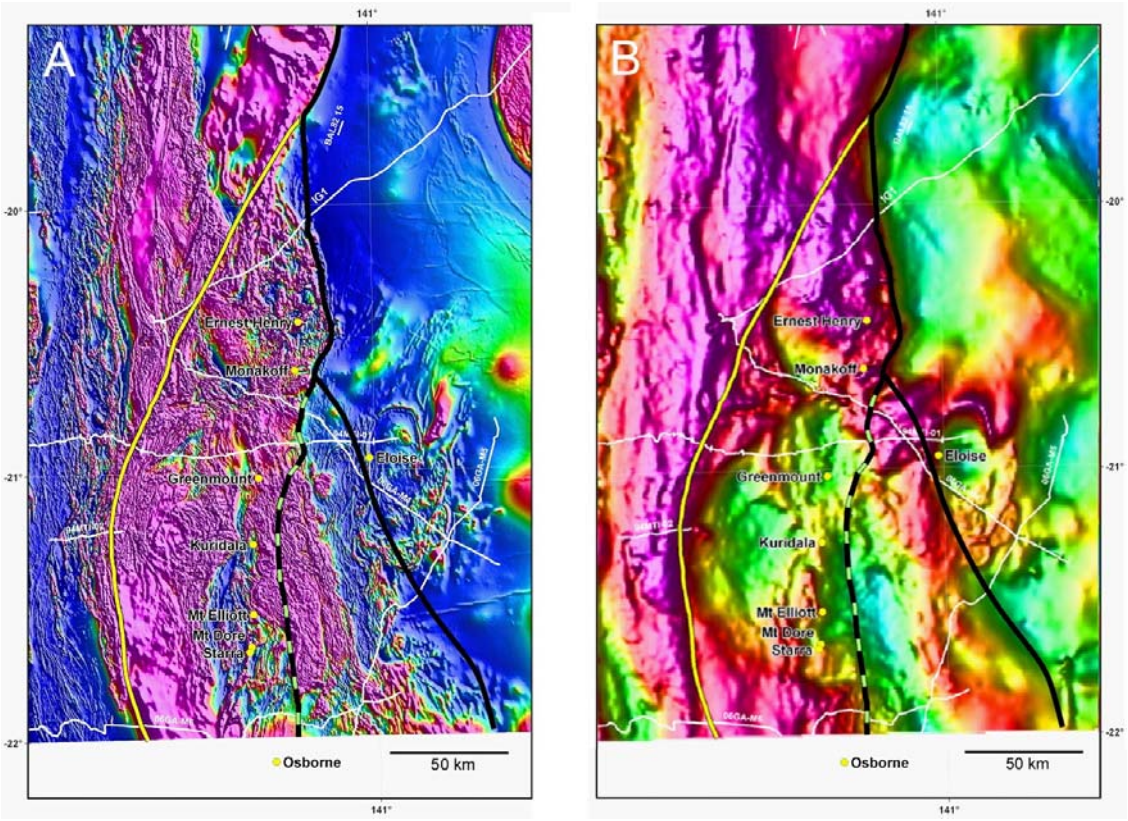

Figure 14: *Images of the eastern part the Mount Isa Province showing inferred position of Isa-Numil suture (black lines) and locations of known iron-oxide copper-gold deposits of the Cloncurry district: (A) reduced-to-pole aeromagnetic data; and (B) Bouger-normalised gravity data. The solid line is the inferred position based on the edge of magnetic and gravity gradients. The dashed line is an alternative position of the southern extension based on seismic data and a subtle change in magnetic character. The yellow line in the inferred extension of the Pilgrim fault system.*

3.4.2. The Einasleigh district

In addition to Broken Hill-type deposits (Kositcin et al., 2009), calc-silicate gneisses of the Einasleigh Metamorphics host copper-silver-gold deposits, which include the Einasleigh (Fig. 1), and nearby Kaiser Bill and Teasdale deposits (Denaro et al., 1997). These deposits, particularly Kaiser Bill and Teasdale, are associated with magnetic anomalies caused by the presence of magnetite and pyrrhotite in the ores. In general, these deposits are characterised by an ore assemblage of pyrrhotite-chalcopyrite-pyrite with accessory to trace molybdenite, sphalerite and galena (Lees and Buckle, 2009). Like other iron oxide copper-gold mineral systems, there is a broad spatial association with sodic-calcic alteration assemblages, in this case semi-regional albitic assemblages (I. Withnall, pers. comm., 2005).

At Einasleigh, Lees and Buckle (2009) recognised two types of mineralisation: (1) higher-grade tabular bodies of semi-massive to massive pyrrhotite-chalcopyrite-pyrite with magnetite, and (2) lower grade, skarn-like tabular bodies with barite and stringer to disseminated sulphide minerals. The main massive sulphide bodies are structurally controlled and contain marginal breccias and relic fragments of host rocks. These bodies also contain accessory to minor cubanite, uraninite, monazite and allanite (Denaro et al., 1997; Evins et al., 2007), and are interpreted as iron-oxide copper-gold deposits; the baritic body is interpreted as a Broken Hill-type deposit (Kositcin et al., 2009).

The Kaiser Bill deposit comprises disseminated to semi-massive sulphide and magnetite within metasediments near the contact with granite gneiss. In detail, the sulphide minerals comprise replacements, breccia infill, veins and stringers in silica-chlorite±epidote±actinolite altered biotite gneiss, amphibolite and pegmatite (Lees and Buckle, 2009). At surface the Teasdale prospect is characterised by two bands of gossanous quartz-magnetite gneiss (Denaro et al., 1997).

As discussed by Kositcin et al. (2009), the age and timing of mineralisation is complex, with up to three discrete events. The Einasleigh baritic bodies are interpreted to have formed at ~1685 Ma (lead isotope model age: Kositcin et al., 2009), whereas the copper-gold bodies are interpreted to have formed at either ~1590 Ma, which corresponds to the peak of monazite ages (Evins et al., 2007) and a lead isotope model age (Kositcin et al., 2009), or ~1400 Ma (Re-Os age from molybdenite and monazite ages: Evins et al., 2007). This mineralisation was overprinted by molybdenite-bearing assemblages at ~410 Ma (Re-Os age of molybdenite: Kositcin et al., 2009).

3.4.3. Mineral system model for uranium-rich iron oxide copper-gold systems

Figure 15 shows a model for uranium-bearing iron oxide-copper-gold mineral systems. Based on the empirical spatial relationship between major crustal boundaries and the distribution of iron oxide-copper-gold deposits seen in the Olympic Dam Province (Goleby and Lyons, 2005), and in north Queensland (Huston et al., 2009), these inferred sutures are interpreted to be fundamental controls on the distribution of these deposits, with the deposits localised in the hangingwall to the sutures. This relationship is consistent with the model of Oliver et al. (2008) that proposed that Williams-Naruku magmatism, which is temporally and spatially linked with iron oxide copper-gold mineralisation, was produced by the melting of enriched mantle lithosphere metasomatised during an earlier period of subduction. According to Korsch et al. (2009), this mantle metasomatism would have occurrred prior to ~1860 Ma in association with subduction related to convergence between the Isa Province and the Numil-Abingdon Seismic Province.

Melting of this enriched mantle, possibly associated with mafic underplating during extension resulted in production of the high-temperature A- and I-type melts temporally and spatially linked to iron oxide copper-gold deposits in the Olympic Dam and north Queensland metallogenic provinces. Although most deposits of this type appear to be enriched in uranium (Hitzman and Valenta, 2005), this enrichment is generally sub-economic, with the highest uranium grades appear to be in deposits emplaced at very high levels in the volcanic pile formed during the A- or I-type magmatism, as at Olympic Dam.

Based on this model, which is discussed in more detail below, the characteristics of iron oxide copper-gold mineral systems in the Cloncurry district and for other areas (Williams et al., 2005), including the Olympic Dam province (Skirrow et al., 2009), the essential processes and components (Appendix A) that are important for uranium-bearing IOCG mineral systems are as follows. These components have been used as the basis for selecting mappable criteria in the analysis of potential for uranium-bearing iron oxide copper-gold systems in the study area, summarised below and in Table 6.

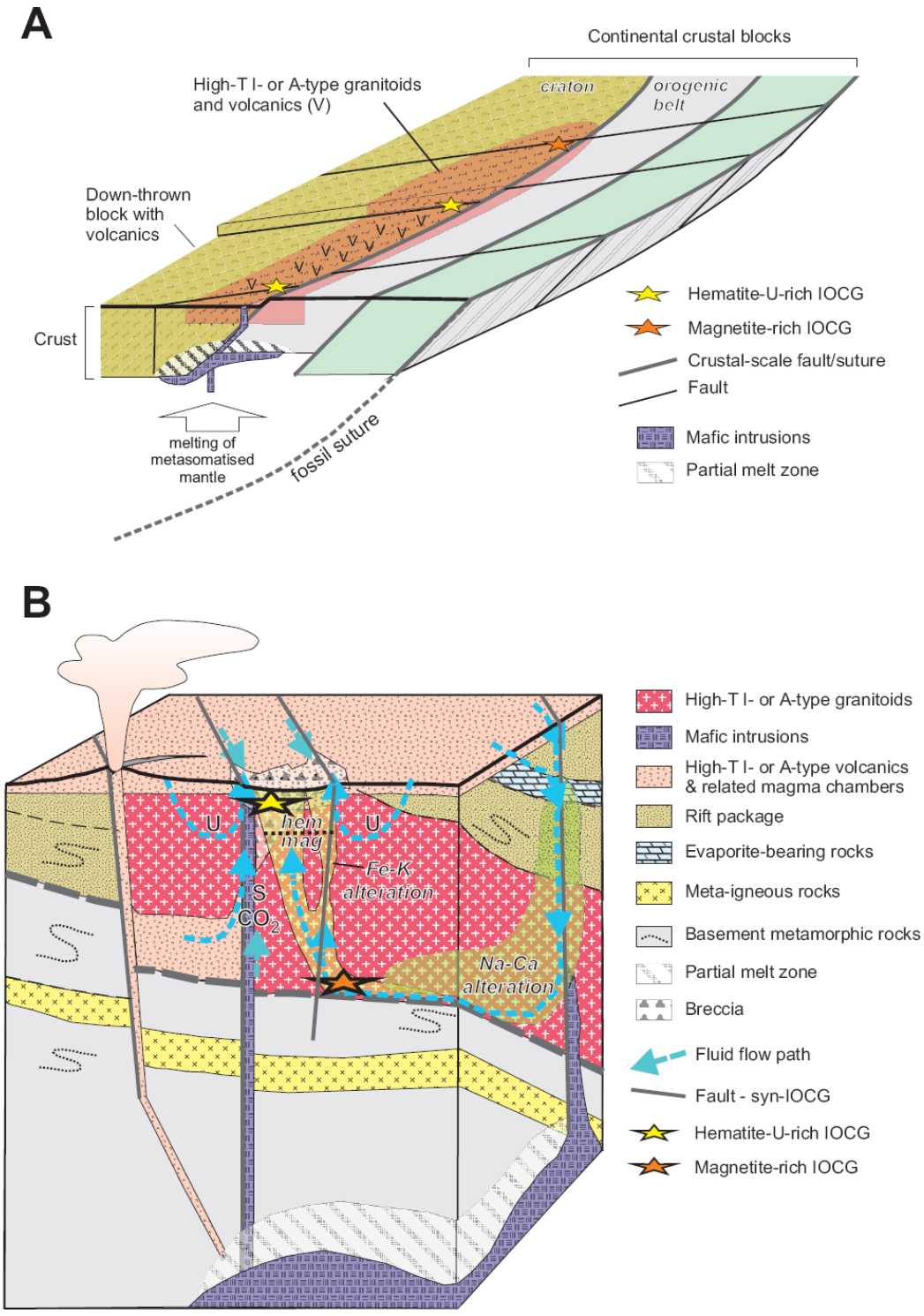

Figure 15: *Mineral system model for uranium-bearing iron oxide Cu-Au deposits. A: Schematic oblique view of crustal-scale section across idealised IOCGU province. B: Schematic oblique section of IOCGU deposit in (A), viewed from the right, showing district-scale features.*

Q1. What is the geodynamic and P-T history of the system?

The geodynamic evolution of major iron oxide copper-gold provinces, such as the Olympic Dam metallogenic province, resulted in voluminous U-rich (e.g. high-temperature I- and A-type) subaerial felsic volcanic and/or high-level felsic intrusive rocks, and allowed subsequent preservation of shallow crustal levels (e.g., iron oxide copper-gold timing immediately prior to cratonisation). Permissive settings include continental 'far-field back-arc' or intracontinental settings with evidence of a switch from compressive to extensional deformation, with crustal melting possibly driven by mantle lithosphere removal (convective, or delamination: Skirrow, 2009) or mantle plume.

Extension may lead to down-thrown blocks above mafic-underplated regions, where volcanic rocks are deposited and preserved. Note in Figure 15A the downthrown block with volcanics and preserved hematite-U-rich iron oxide copper-gold deposits. Exhumation of an active magnetite-forming hydrothermal regime allows telescoping of this alteration with oxidized surface-derived fluids in an environment favourable for fluid mixing. Exhumation may be favoured in some extensional settings where lithospheric mantle has been removed/eroded.

Based on these processes and system components, the following mappable criteria were considered in the mineral potential assessment (Table 6):

- Felsic igneous rocks derived from high-temperature crustal melting, including A-type, peralkaline, and high-temperature I-type magmas. In this study high melting temperatures have been determined from zircon saturation temperatures (Schofield, 2009), and are typical of some but not all peralkaline and A-type magmas. The Williams and Naraku batholiths are representative of high-temperature I-type magmatism in the Mt Isa region.
- High-K mafic igneous rocks, particularly as part of a bimodal suite, indicating melting of metasomatised lithospheric mantle.

The effects of syn-ore exhumation could be considered in the mineral potential assessment, but were not included in the current study due to limitations in available data. This exhumation would be indicated by (a) clastic sediments associated with exhumation during time of high-temperature magmatism and mineralisation (sedimentation will be peripheral to exhumed terranes); (b) similar 'cooling' ages of mid-crustal rocks and iron oxide copper-gold-related alteration and volcanics. Syn-mineralisation exhumation facilitates fluid mixing, a very effective depositional mechanism for ore metals. Alternatively, exhumed magnetite-sulfide iron oxide copper-gold alteration zones provide effective chemical depositional environments for reduction of uranium carried in oxidised fluids.

Q2. What is the structural and lithological architecture of the system?

The crustal-scale magma and fluid pathways are terrane boundary zones initiated during earlier orogenic belt formation, for example at a cratonic margin. Major iron oxide copper-gold systems may preferentially occur in hangingwall of boundary zones between crustal blocks, above zones of partial crustal melting and mafic underplating (Fig. 15A). Fluid flow is enhanced by juxtaposition of earlier rift basins with this high-temperature melt province. Pre-existing basinal structures and econd-order cross structures (e.g., conjugate fault sets) localise dilational deformation, brecciation (at high crustal levels), and fluid flow. The intersections of second-order with crustal-scale terrane boundaries are favoured locations for iron oxide copper-gold systems, as illustrated in Figures 15A and 15B.

Table 6: Mappable criteria used for potential assessment of uranium-rich iron oxide copper-gold deposits.

MINERAL SYSTEM QUESTION	CRITERION	SCORE	DATASET & REFERENCE	COMMENTS
1	*Terrane boundaries:* *10km into footwall,* *50km into hangingwall*	3	Henson et al. (2009); Kositcin et al. (2009)	Based on seismic, MT and potential field data; hangingwall zones of dipping boundaries are favoured.
1, 2	*A-type granitoids*	3	Solid geology (Liu, 2009); OZCHEM	Attribution of composition by Schofield (2009)
1, 2	*High temperature I-type granitoids*	3	Solid geology (Liu, 2009); OZCHEM	Attribution of composition by Schofield (2009), partly based on zircon saturation temperatures
1, 2	*Peralkaline igneous rocks*	2	Solid geology (Liu, 2009); OZCHEM	Attribution of composition by Schofield (2009)
1, 2	*Bimodal igneous suites*	2	Solid geology (Liu, 2009); OZCHEM	
1, 2, 6	*Felsic volcanic rocks*	3	Solid geology (Liu, 2009)	
3	*U-rich igneous rocks*	3 2	OZCHEM; Schofield (2009)	Distibuition of igneous suites with over 10 ppm U 10 km buffer
4	*Faults – F2 (Isan Orogeny)*	2	North Queensland GIS	
4	*Magnetite-bearing alteration*	3	Magnetic susceptibility and density inversions (Williams and Chopping, 2009)	3D data gridded with cell size 2x2x1km, then uppermost 1km extracted for use here as GIS layer.
4	*Hematite- and/or sulphide-bearing alteration and mineralisation*	5	Magnetic susceptibility and density inversions (Williams and Chopping, 2009)	3D data gridded with cell size 2x2x1km, then uppermost 1km extracted for use here as GIS layer.
5	*Uranium enrichment - evidence from radiomentric maps* Uranium enrichment (>10 ppm) within igneous rocks 10 km buffer around U-enriched igneous rocks	 3 2	Radiometric map of Australia (Minty, 2009)	Uranium values greater than and equal to 10 ppm were extracted from the filtered Uranium band and converted to a polygon shape file. A spatial query was used to select values for igneous rocks.

Based on these processes and system components, the following mappable criteria were considered in the mineral potential assessment (Table 6):

- Major crustal domain boundary zones such craton margin, with greatest potential in hangingwall above steps in Moho or above highly reflective seismic zones in mid-lower crust. Several crustal domain boundaries have been identified in the Mt Isa – Georgetown region from seismic, magnetotelluric, gravity and magnetic data (Korsch et al., 2009; Huston et al., 2009).
- Network of syn-orogenic major fault/shear zones, reactivated during high-temperature magmatic events. These structures may represent fluid flow pathways for IOCG-related fluids. The F_3 faults of the earlier phases of the Isan Orogeny appear to be one of the favourable fault sets for IOCG localisation, that were potentially reactivated during the D_4 later stages of the Isan Orogeny.
- Down-thrown blocks may preserve volcanics and IOCGU settings, and hence volcanic rocks, particularly those of high-temperature felsic composition, are a favourable criterion.

Q3. What are the fluids, their sources and/or reservoirs?

Multiple fluids are required to form U-rich IOCG deposits, including highly oxidized U-rich fluid (e.g., meteoric/ground waters), deep-sourced high-temperature brines (magmatic-hydrothermal and/or fluids reacted with metamorphic rocks), and possibly separate sulphur-bearing fluids. Figure 15B shows both deep-sourced and shallow hydrothermal fluids, the latter leaching uranium from granitoid or volcanic rocks. The sources of Cu, Au, S and CO_2 may be either coeval magmas (felsic and/or mafic) or the pre-existing metamorphic rocks, marked by Na-Ca regional alteration zones (Williams et al., 2005; Oliver et al., 2005).

Pre-existing basins tend to lack major reduced sections (Haynes, 2000) and commonly show evidence for the (former) presence of evaporite minerals; rift basin sequences may supply some of the Fe, Cl, and S to iron oxide copper-gold deposits. Exposure near/at the paleosurface of U-rich source rocks is favourable for sourcing highly oxidised surface-derived waters capable of transporting uranium. Topographic depressions (e.g., calderas, grabens, maar complexes, etc) are conducive to mixing of shallow-crustal and deep-sourced fluids.

Based on these processes and system components, the following mappable criteria were considered in the mineral potential assessment (Table 6):

- Uranium-rich igneous rocks, particularly volcanics, which represent potential source rocks for U-rich IOCG deposits. U-rich high-temperature crustal melts are especially favourable, which tend to occur late within the tectono-magmatic evolution of IOCG provinces. Igneous whole rock geochemistry and radiometric data may effectively map U-rich compositions.

Regional Na-Ca alteration zones may represent source regions for Fe, Cu, Au and other ore components (Oliver et al., 2004). Although this criterion has not been specifically included in the current assessment of uranium IOCG potential, some of the rock volumes identified in the inversion modelling of gravity and magnetic data (Williams and Chopping, 2009) may include areas of dense non-magnetic or weakly magnetic Na-Ca alteration. This alteration is characterised by the presence of albite, clinopyroxene (e.g., diopside) and/or amphibole (e.g., actinolite), and may contain minor magnetite, scapolite, and titanite. It should be noted that the inversion modelling does not discriminate between Na-Ca alteration and hematite ±sulfides.

Q4. What are the fluid flow drivers and pathways?

High to extreme paleogeothermal gradients are a probable driver of regional-scale uppermost crustal fluid flow in major iron oxide copper-gold systems; mafic/ultramafic intrusive magmatism may mark the locus of crustal-scale thermal anomalies, and may contribute ore metals and/or sulfur to

IOCG systems. Fluid pathways are active fault networks at regional scale, and primary and secondary permeability of (meta)sedimentary and (meta)volcanic rocks at deposit- to micro-scales.

Based on these processes and system components, the following mappable criteria were considered in the mineral potential assessment (Table 6):

- Inversion modelling of gravity and magnetic data, to map magnetite- and hematite-bearing hydrothermal alteration and iron oxide copper-gold mineralisation. District- to deposit-scale Fe-K alteration is closely associated with mid-crustal magnetite-rich iron oxide copper-gold deposits, and is characterised by K-feldspar and/or biotite with the Fe-oxide. This alteration marks deeper fluid flow pathways. Uranium mineralisation in iron oxide copper-gold deposits in the Olympic Dam iron oxide copper-gold-uranium province typically is associated with combinations of hematite, chlorite, sericite, carbonate, pyrite, chalcopyrite, bornite, chalcocite, barite and various REE and phosphate minerals. Hematitic alteration in these shallow styles of iron oxide copper-gold systems marks fluid flow pathways close to mineralisation, although some hematite alteration in the Cloncurry district may have formed at mid-crustal levels (e.g., Starra). Inversion modelling of regional gravity and magnetic data may map magnetite- and hematite-bearing iron oxide copper-gold alteration in 3D. However, it should be noted that the inversion modelling used in the mineral potential assessment is not able to discriminate between shallow-crustal low-temperature and deeper mid-crustal high-temperature hematite-rich alteration.
- Sodium-calcium regional alteration zones in deeper parts of some systems contain combinations of albite, amphibole, clinopyroxene, scapolite, titanite. Inversion modelling may map these manifestations of fluid flow pathways.

Exceptionally high geothermal gradients driving fluid flow may be evident in metamorphic mineral assemblages, and inferred from reconstruction of intrusion temperatures and depths. However, this criterion is not utilised in the current mineral potential assessment. A clearer understanding of metamorphic grade distribution through time, during the Isan Orogeny, and improved geochronology of iron oxide copper-gold mineralisation will be required if this criteria is to be used in the assessment.

Q5. What are the metal (and ligand) transport and depositional processes?

Based on iron-oxide coper-gold-uranium systems of the eastern Gawler Craton, a key Cu-Au-U depositional process was mixing of large volumes of oxidized groundwaters or basinal waters with deep-sourced Fe-rich brines (Haynes et al., 1995). Reduction of oxidized U-rich fluids requires reducing agents such as reduced deep-sourced fluids or Fe^{2+}-, reduced-S-bearing or reduced-C-bearing minerals in host rocks. Based on these processes and system components, the following mappable criteria were considered in the mineral potential assessment (Table 6):

- Hematite-rich zones may be lateral to, or above, magnetite-bearing zones; higher grade uranium mineralisation is generally associated with gold-rich and/or more oxidised parts of iron-oxide copper-gold-uranium deposits. Thus, inversion modelling of gravity and magnetic data may be used to map the spatial distribution of hematite- versus magnetite-bearing alteration. Hematite-bearing alteration is weighted more heavily in the assessment (Table 6) because of the known association of higher grade uranium with hematite in IOCG systems of the Gawler Craton.

Breccias of hydrothermal and/or phreatomagmatic origin are most favourable where associated with the mappable criteria above. However, at the scale of the assessment, most mapped breccia bodies in the Mt Isa and Georgetown regions will be insignificant, and hence we have not included this criterion.

Q6. What are the effects of post-depositional processes on metal accumulations?

Preservation of shallow-crustal settings of uranium-rich iron oxide copper-gold deposits requires either burial prior to late-stage exhumation, or minimal erosion, for example in areas cratonised during or immediately post-dating iron oxide copper-gold formation. Based on these process and components, the following mappable criteria were considered in the mineral potential assessment (Table 6):

- Felsic volcanic rocks of A-type or high-temperature I-type, possibly in down-thrown blocks, indicating preservation of near-surface crustal settings where uranium-bearing iron oxide copper-gold deposits are most likely to have formed.

The criterion of very low metamorphic grade could indicate preservation of uppermost crustal levels since time of uranium-rich iron oxide copper-gold system. However, the same caveat applies here as for Question 4, that is, the need for a better understanding of metamorphic grade through time.

3.4.4. Results of assessment analysis for uranium-rich iron oxide copper-gold systems

Based on the criteria and weighting listed in Table 6 the potential for iron oxide copper-gold systems is shown for North Queensland in Plate 5. The mineral potential map should be regarded as simply a regional guide towards areas requiring further investigation, rather than as a detailed deposit targeting map. Nevertheless, a number of regions are highlighted that we consider may have significant potential for iron oxide copper-gold deposit, of which a few are favourable for the hematite-rich style that can contain elevated uranium concentrations. These are outlined in on Plate 5, and discussed below.

A. Northern undercover extension of Ernest Henry – Cloncurry Mesoproterozoic iron oxide copper-gold belt. This area is highlighted by the presence of a major crustal boundary (evident in seismic, magneto-telluric, gravity and magnetic data), proximity to high-temperature igneous rocks of the Williams-Naraku suite, F_4 faults, and numerous areas identified in the inversion modelling with anomalous 'magnetite' 'and hematite/sulfide' contents. The area northwards of Ernest Henry also is favourable for preservation of shallower crustal levels than further south, based on the general pattern of northwards-decreasing metamorphic grade during the Isan Orogeny (not shown in Plate 5). If volcanic rocks equivalent in age to the Williams-Naraku suite were discovered, the potential of area A would be considerably enhanced. The depth of cover in area A will be a major factor in the 'explorability'.
B. Southern undercover extensions of Ernest Henry – Cloncurry Mesoproterozoic iron oxide copper-gold belt. Most of the same mineral system components are present in this area, and additionally the radiometric response for uranium is elevated. However, higher metamorphic grades than predicted in area A tend to downgrade the potential of this area for uranium-rich hematitic iron oxide copper-gold systems. Nevertheless, many areas are highlighted in Plate 5 for magnetite-rich variants of iron oxide copper-gold systems, that may contain anomalous quantities of uranium in addition to copper and gold. The depth of cover particularly in the south will be a major factor in the 'explorability' of area B.
C. Georgetown Paleo- to Mesoproterozoic belt. The major crustal suture evident in seismic data to the west of the Georgetown Province defines a second prospective iron oxide copper-gold belt, although fewer datasets are available than for the Mt Isa region to map iron oxide copper-gold potential (e.g., fault datasets). Two Cu-Au deposits with possible iron oxide copper-gold affinities, Einasleigh and Kaiser Bill (see above), occur to the south of Georgetown, close to the buffers adjacent to the crustal suture. The inversion modelling identified several large zones of anomalous 'magnetite' and 'hematite/sulfide' content in area C. Iron oxide copper-gold potential is higher where these zones are within buffer zones of favourable igneous rocks. The preservation of Proterozoic volcanic rocks such as the

Croydon Volcanics is a positive factor for the presence of hematite-rich IOCG systems. However, the oxidation-reduction state of the Proterozoic igneous and metasedimentary rocks in the Georgetown region requires better definition. If primary magmatic compositions were as reduced as indicated in previous studies (Budd et al., 2001), and/or the bulk of supracrustal sequences are reduced in this region, then the iron oxide copper-gold potential would be downgraded. This does not rule out potential for iron-sulfide rich copper-gold systems, however.

D. Paleozoic magmatic belt southwest of Cairns. Igneous rock chemistry, anomalous uranium contents, and preservation of volcanic rocks in this area are favourable factors for the presence of Paleozoic iron oxide-copper-gold systems. While most of the belt appears to lack anomalous 'hematite/sulfide' or 'magnetite' anomalous areas in the inversion modelling results, the southeastern extremity near Hinchinbrook contains several semi-coincident pairs of anomalies, and the depth of cover may be relatively shallow in some parts of this area. It is unclear whether the crustal structure in this area is conducive for iron oxide-copper-gold systems. If major northwest trending crustal domain boundaries were present in this belt the iron oxide-copper-gold potential would be considerably enhanced. However, other non-geological factors (population centres, infrastructure, environmental and agricultural characteristics, land ownership, etc) may influence the 'explorability' of this area. This area was also identified as having high potential for metasomatic uranium deposits.

3.5. MAGMATIC-RELATED URANIUM SYSTEMS (A SCHOFIELD AND D HUSTON)

According to Skirrow et al. (2009), magmatic- (and magmatic-hydrothermal-) related uranium systems comprise one of three end-member "families" of uranium mineral systems (Fig. 3). Magmatic-related uranium systems are those in which the formation of the deposit is directly controlled by igneous processes. This differentiates these systems from other deposit styles, such as uranium-bearing iron-oxide copper-gold, which though having a close temporal and spatial association with uranium-rich igneous rocks, involve non-magmatic processes and/or fluids in their formation and are classified as "hybrid"-style deposits.

Magmatic systems involve igneous processes of partial melting, fractional crystallisation and the evolution of magmatic-hydrothermal fluids as key ore-forming processes. As such, these can be subdivided on the basis of the relative importance of the magmatically-derived fluid into deposits formed by orthomagmatic processes, where hydrothermal fluids have subordinate importance, and magmatic-hydrothermal processes, whereby ore formation involves transport of metal by a hydrothermal fluid evolved from the magma. Both intrusive and extrusive igneous rocks may be involved in the formation of the mineral system, and mineralisation may be hosted within the igneous body, or may mineralise the surrounding country rock.

The Maureen and Ben Lomond deposits in north Queensland have been traditionally interpreted as volcanic-related deposits given their spatial association with volcanic rocks. However, following work of Wall (2006) and Mathison and Hurtig (2009), we interpret these deposits to be associated with the unconformity between Phanerozoic and Paleoproterozoic rocks, and these deposits are considered as unconformity-related deposits (section 3.2). As such, they will not be discussed here.

3.5.1. Orthomagmatic uranium systems

Although orthomagmatic deposits are not recognised in Australia, there are several globally significant examples, including the Rössing and Ross Adams deposits, which provide information about essential components for this deposit style. Although some evidence of late hydrothermal remobilisation is present in these systems, most of the uranium is thought to have been emplaced via magmatic processes, and hence we consider these deposits orthomagmatic in origin.

3.5.1.1. Rössing deposit, Namibia

The best known example of orthomagmatic uranium mineralisation is the giant Rössing deposit in Namibia, which is associated with pegmatitic alaskite (Cuney and Kyser, 2009). These alaskite bodies formed from partial melting within a migmatitic domain (Berning et al., 1976) and were emplaced late during deformation associated with the Pan-Africa Orogeny at ~510 Ma (Basson and Greenway, 2004). The Rössing body was emplaced as a mesh of alaskite dykes along the southern limb of a fold, near the contact between underlying, oxidised meta-red beds and an intermixed sequence of metapelite and marble. This sequence may correlate with the Zambian Copper Belt, which has an age of between 880 and 815 Ma (Selley et al., 2005). The underlying sediments are uranium-rich (Kinnaird and Nex, 2007).

Mineralised alaskite contains fluorine-rich biotite (to 1.8 wt.% F), which together with the presence of fluorite (Cuney and Kyser, 2009) suggests fluorine may play a major role, either as a solubility-enhancing agent or as a ligand for uranium transport. Cuney and Kyser (2009) interpreted the uranium-rich alaskites to have formed via low-degree partial melting of uranium-rich metasedimentary rocks, rather than derivation from an underlying granitoid body (Cuney and Kyser, 2009). Other Rossing-like deposits include Steward Lake in Canada and the Litsk district of the Kola Peninsula in Russia.

3.5.1.2. Ross Adams deposit, Alaska

The Ross Adams deposit, located in the Bokan Mountain granite complex of south-eastern Alaska, is an example of mineralisation associated with the extreme fractionation of a uranium-rich granitic body. The deposit occurs as a pipe-like body within a multi-phased felsic intrusive (Thompson, 1988). Other mineralisation styles include veins, or pods in shear zones. The host granite is post-orogenic (A-type) and is geochemically characterised by a peralkaline bulk rock composition, high zirconium, niobium, REE and fluorine (up to 3200 ppm), and is highly fractionated (Cuney and Kyser, 2009). In fresh samples, uranium content is approximately three times that of average granite, but is not exceptionally elevated at 12 ppm. Alteration zones occur in, and immediately adjacent to, the orebodies, and are characterised by pervasive albite, chlorite, calcite and hematite (Thompson, 1988). Fluid flow was concentrated in zones of weakness, such as faults and fractures (Cuney and Kyser, 2009). Stable isotope data indicate that this fluid was magmatic in origin (Thompson, 1988).

Mineralisation at Bokan Mountain occurred via extreme fractional crystallisation of a peralkaline felsic melt. Th/U ratios are close to that typical of fractionation trends. The peralkalinity and high F of the melt favour extremely high U solubilities (Peiffert et al., 1996). This allows U to concentrate in the melt with ongoing fractionation. Mineralisation is associated with the presence of magmatic-derived fluids. The localisation of this mineralisation may be related to cooling and the development of local reducing conditions in zones of competency contrasts, such as lithological boundaries or fractures (Thompson, 1998). Other deposits similar to Ross Adams include the Ilimaussaq deposit in Greenland and the Pacos de Caldas peralkaline complex in Brazil (Cuney and Kyser, 2009).

3.5.1.3. Mineral system models for orthomagmatic uranium systems

Favourable parental magmas for orthomagmatic uranium systems similar to the Ross Adams deposit may be either peralkaline melts, derived from partial melting of the mantle, or high temperature I- or A-type melts, sourced from partial melting of continental crust. These are generated under anorogenic of extensional tectonic regimes. At this stage, the uranium content of the magma will be determined by the initial concentration in the source. As the melt ascends through the crust, uranium is concentrated by the removal of more compatible elements during fractional crystallisation. If this is done in the presence of agents which enhance the solubility of uranium in silicate melts (fluorine, chlorine, peralkalinity), then uranium will remain incompatible and may be concentrated to high levels.

As the magma ascends to high crustal levels, a magmatic fluid phase may separate from the silicate melt. This can carry with it some uranium, as in the case of magmatic-hydrothermal systems, and produce mineralisation in the surrounding country rock (see 3.5.2 below). Low grade magmatic uranium mineralisation, represented by uranium bound up in accessory mineral phases, may be upgraded and concentrated within the igneous body if the exsolved magmatic fluid interacts with it sufficiently, and high concentrations of uranium may be deposited in fractures or cavities. This form of interaction with magmatic-derived fluids is seen in numerous examples of orthomagmatic mineralisation worldwide. This mineral systems model is presented in Figure 16.

Unlike other orthomagmatic systems, such as the Ross Adams deposit, geochemical data from Rössing and surrounding uraniferous alaskite occurrences display no evidence of uranium enrichment with fractional crystallisation (Nex et al., 2001, Kinnaird and Nex, 2007). Thus, factors concerning uranium solubility and magmatic evolution, which are so crucial for other orthomagmatic systems, are insignificant in the prospectivity for these deposits. With this in mind, the proposed model for Rössing-style mineralisation is one of anatectic partial melting of uranium-rich source rocks. At Rössing, this took place within a zone of intense deformation. Therefore migmatitic terranes are favourable for the generation of Rössing-style mineralisation. The melts produced will be of 'alaskitic' affinity (ie., K-feldspar-rich leucogranites), and will occur as dykes or sheeted granites. The depositional mechanism is uncertain, and may related to redox considerations (eg., Kinnaird and Nex, 2007), or due to interaction with carbonate-bearing units (Cuney, 1980). Localised interaction between magmatic fluids and the alaskite bodies in joints and fractures may lead to localised higher grade mineralisation.

3.5.1.4. Mappable criteria for orthomagmatic uranium systems

Although the Rössing and Ross Adams deposits are both (largely) orthomagmatic deposits and share some similarities, there are important differences with respect to their origin and tectonic setting. The Rössing deposit is inferred to have been formed by near-eutectic partial melting within a high grade metamorphic terrane, with crystallisation and mineralisation within the same metamorphic terrane. In contrast, the Ross Adams deposit formed by the extreme fractionation of a peralkaline melt, which formed in a post-tectonic (anorogenic) environment. As the site of melting, which may have been either the deep crust or mantle, is significantly separated from the site of crystallisation, these deposits can be hosted by much lower grade metamorphic terranes. Hence, although these deposits share some characteristics and, by implication, essential components and mappable criteria, in some important characteristics these systems will differ. The datasets compiled for this investigation do not readily lend themselves to the identification of Rössing-style mineralisation. Rather, we have focused on determining those igneous rocks most likely to produce orthomagmatic mineralisation (similar to Ross Adams), and which have the highest probability of having undergone hydrothermal upgrading of the resource. We consider the following criteria to be most important:

Q1. What is the geodynamic and P-T history of the system?
Magmas which form orthomagmatic uranium systems are typically generated in anorogenic or extensional tectonic settings. The source of the melts may be within the crust or, in the case of peralkaline magmas, in the upper mantle. High temperature melting is often significant, and this may be reflected in an anticlockwise P-T-t trajectory. Although difficult to test for, melting of a uranium-enriched source region is also significant.

Based on this discussion, the following criteria were considered in the potential assessment:

- Distribution of crustal melts, as approximated by felsic compositions
- Distribution of A-type and peralkaline igneous rocks
- Evidence of high temperature melting
- The location of uranium-rich igneous rocks may provide evidence of melting of a uranium-rich source region.

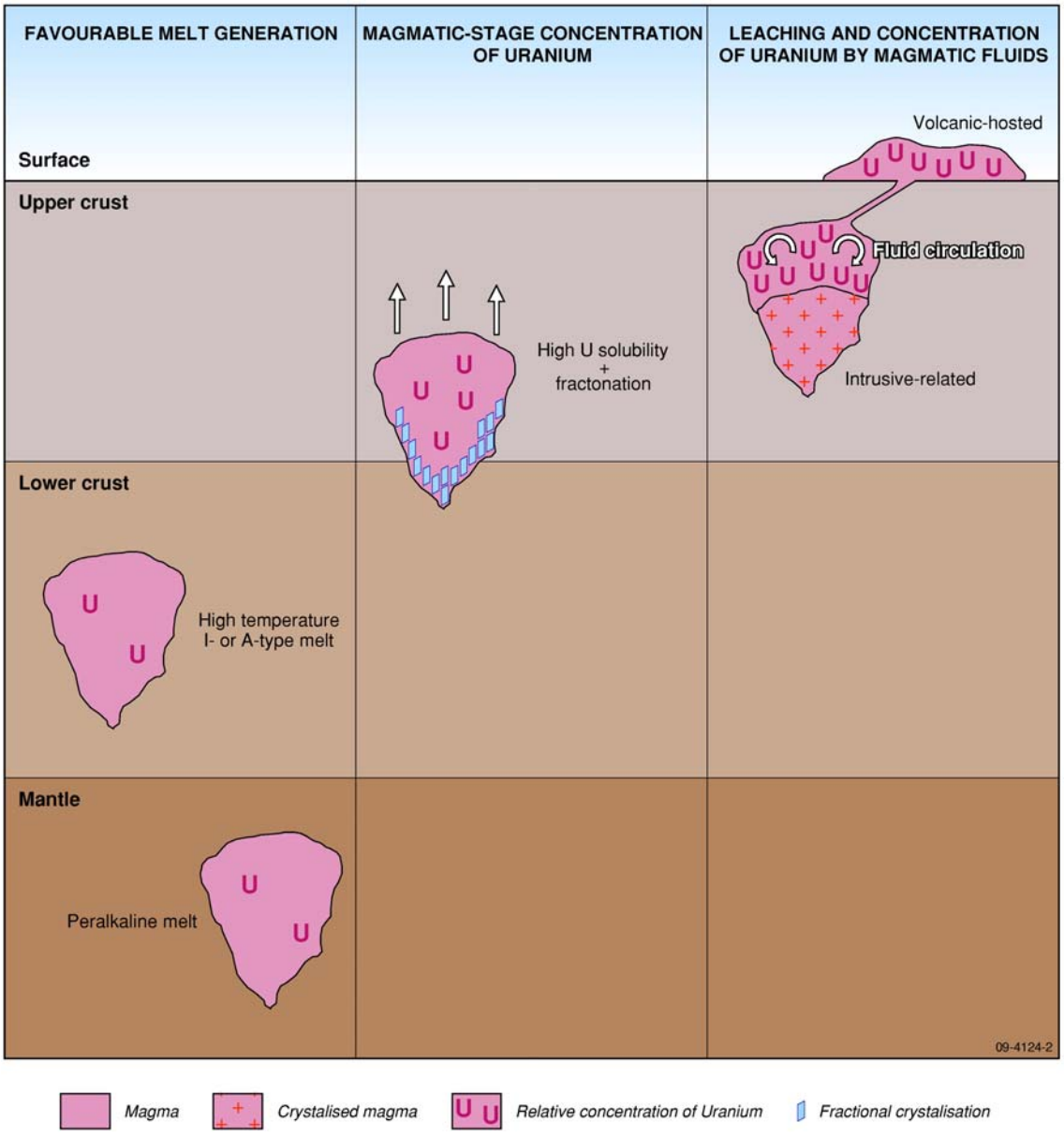

Figure 16: *Mineral system models for orthomagmatic uranium deposits.*

Q2. What is the structural and lithological architecture of the system?

Architecturally, orthomagmatic uranium systems as discussed here are confined to within the mineralising igneous body. Internal veining and fracturing may facilitate localised enrichment of ore grade, although these are difficult to map without detailed field investigations. The most apical parts of intrusions are commonly associated with the highest ore grade, although this is more a function of being the most fractionated component of the magma. No criteria corresponding to this question were used.

Q3. What are the fluids, their sources and/or reservoirs?

In orthomagmatic uranium systems, the igneous body itself is the source of any mineralising fluids, generally exsolved magmatic fluids. Unlike other uranium systems where fluid reservoirs and compositions are highly important, fluids in orthomagmatic systems have a secondary role. Rather, factors leading to the crystallisation of a uranium-rich melt are of greater importance, and provide

the fundamental metal source for these systems. Most notably, high degrees of fractional crystallisation in the presence of agents which enhance the solubility of uranium in silicate melts (peralkaline composition, high fluorine, and high chlorine) are important. Late-stage magmatic fluids may have a role in generating localised high grade zones within the igneous body, for example in fractures and cavities. In this case, the uranium must be available to leaching by the fluids and not locked up within refractory mineral phases.

Based on this discussion, the following criteria were considered in the potential assessment:

- High-level intrusives, which may have exsolved a late-stage magmatic fluid
- Igneous units where uranium is available to hydrothermal upgrading (eg. volcanics with a glassy matrix)
- Geochemical indicators suggesting a high degree of fractional crystallisation
- Geochemical indicators of high uranium solubility (peralkaline bulk rock composition, high fluorine, high chlorine)

Q4. What are the fluid flow drivers and pathways?

Fluid flow occurs as a result of the exsolution of magmatic fluids, typically occurring at high crustal levels. Granitoid emplacement may also establish hydrothermal convection cells within the upper crust. Such fluid flow, although not strictly considered within the orthomagmatic mineral system presented here, may assist in the generation of upgraded mineralised zones within the igneous body.

Based on this discussion, the following criteria were considered in the potential assessment:

- High-level intrusives, which may have exsolved a late-stage magmatic fluid

Q5. What are the metal (and ligand) transport and depositional processes?

Most uranium in igneous rocks is hosted by accessory mineral phases which incorporate uranium into their structures. Thus, uranium hosted in primary mineralogy is a product of the crystallisation of the magma. A notable example of this is the Kvanefjeld deposit in Greenland (Cuney and Kyser, 2009). If uranium is liberated from the primary mineralogy, it may be redeposited at a higher grade. Depositional mechanisms of uranium at magmatic temperatures are poorly constrained however, and may be either physical or chemical.

Based on this discussion, the following criteria were considered in the potential assessment:

- Low Th/U ratios indicate zones of uranium enrichment

Q6. What are the effects of post-depositional processes on metal accumulations?

Post-depositional history is not significant in orthomagmatic systems, although preservation of mineralisation is aided if the igneous body is not exposed to infiltrating fluids, particularly those which are highly oxidised. No criteria corresponding to this question were used.

These components are presented in more detail in Appendix A. Based on these components and available datasets, a series of mappable criteria were identified and are summarised in Table 7. These criteria have been used as the basis for uranium potential analysis. Table 7 also indicates the weightings used in the analysis, and the results of which are presented below.

Table 7: Mappable criteria used for potential assessment of orthomagmatic uranium deposits.

MINERAL SYSTEM QUESTION	CRITERIA	SCORE	DATASET & REFERENCE	COMMENTS
1	*Felsic igneous rocks* Felsic compositions Intermediate to felsic compositions Mafic to felsic compositions	 3 2 1	Solid geology (Liu, 2009)	Compositional classification is taken from geological unit descriptions
1	*U-rich igneous rocks* Solid geology polygon with average uranium content >10 ppm	 2	OZCHEM	
1	*High temperature melting* 5 km buffer around very high temperature melting 5 km buffer around high temperature melting	 3 2	OZCHEM	Temperatures are based on calculated zircon saturation temperature. Very high temperatures are >900^{o}C, high temperatures are >850^{o}C
1	*A-type composition* Solid geology with an A-type composition Solid geology polygon with intersecting A-type geochemical data point	 2 1	Solid geology (Liu, 2009); OZCHEM	Solid geology units identified as A-types as described in Champion and Heinemann (1994) were supplemented by solid geology polygons which host geochemical data points described as A-type
3	*Fractionated igneous rocks* 5 km buffer around highly fractionated igneous rocks 5 km buffer around fractionated igneous rocks	 3 2	OZCHEM	Degree of fractionation is approximated by Rb/Sr ratios. Highly fractionated is defined by Rb/Sr>10, fractionated is defined by Rb/Sr>1
3	*High uranium solubility* 5 km buffer around very high fluorine content (>3000 ppm) 5 km buffer around high fluorine content (>1000 ppm) 5 km buffer around very high chlorine content (>1000 ppm) 5 km buffer around high chlorine content (>500 ppm)	 3 2 2 1	OZCHEM	High solubilities allow uranium to become highly concentrated with progressive magmatic evolution
3	*Peralkaline composition* Solid geology described with peralkaline mineralogy Solid geology polygon with peralkaline geochemistry	 3 2	Solid geology (Liu, 2009); OZCHEM	Solid geology polygons described as having peralkaline mineralogy (e.g., riebeckite, aegerine) have been combined with other solid geology polygons containing geochemical data points with calculated Na+K/Al > 1

3, 4	*High-level emplacement* Solid geology with high-level descriptors	1	Solid geology (Liu, 2009)	These have been identified by descriptions indicating high levels of emplacement (e.g., miarolitic cavities)
3, 4	*High availability to leaching* Very high potential for leaching High potential for leaching	3 2	Solid geology (Liu, 2009)	High potential for uranium to be leached and concentrated. 'Very high' leachability is denoted by a "glassy" descriptor, while 'high' leachability is denoted by ignimbrites
5	*Evidence of U enrichment* 5 km buffer around geochemical samples with Th/U < 2	2	OZCHEM	Gives evidence of uranium concentration beyond typical magmatic levels.

3.5.1.5. Results of assessment analysis for orthomagmatic uranium systems

Several regions of high prospectivity for orthomagmatic uranium mineralisation occur within the study area (Plate 6). There are numerous, relatively isolated, occurrences of prospective regions throughout the study area (see Plate 6 for locations). The following lists areas with clusters of igneous rocks with high prospectivity:

A. Paleozoic volcanics west of Cairns. The Paleozoic volcanic rocks approximately 70-80 km west of Cairns, especially the Late Carboniferous to Early Permian Featherbed Volcanic Group and the Late Carboniferous Glen Gordon Volcanics of the Koolmoon Volcanic Group exhibit high prospectivity.
B. Paleozoic intrusives and volcanics scattered around the Georgetown Region. Intrusive and extrusive igneous rocks in the Georgetown Region are also highlighted in the prospectivity analysis. Notably, the Newcastle Range Volcanic Group, which is associated with several small uranium deposits (McKay and Miezitis, 2001) has been identified as prospective in the analysis.
C. The Mount Isa Inlier. In the Mount Isa region, potential for orthomagmatic uranium mineralisation is associated with uranium-rich Proterozoic intrusives (Plate 6). Moderate to highly prospective granitoids occur in the northern Sybella Suite in the Western Fold Belt and the Williams Supersuite in the Eastern Fold Belt. The most prospective unit in the Mount Isa region is the Wonga Granite, which is also linked to magmatic-hydrothermal mineralisation at Mary Kathleen (see below).

3.5.2. Magmatic-hydrothermal uranium systems

Magmatic-hydrothermal uranium resources comprise a tiny proportion of Australia's total known resource. Our interpretation of the geochronological and geological data (see below) suggest that the Mary Kathleen deposit (Fig. 2), with global resources of ~10 kt U_3O_8 (Table 1) is the only significant example of this system in Australia. In addition to the Mary Kathleen deposit, which is located in the Mary Kathleen belt in the Mount Isa Province, a number of prospects in the Etheridge Province are either hosted by, or closely related to Proterozoic granites. These prospects include the Oasis prospect in the Mywyn Granite and, more controversially, the Mount Hogan gold deposit, which contained significant uranium (Denaro et al., 1997).

3.5.2.1. Mary Kathleen deposit

McKay and Miezitis (2001) classified the Mary Kathleen U-REE deposit, which was discovered in 1954, as metamorphic-related. However, reconsideration of geochronological data, as discussed below, suggest that initial mineralisation was temporally, spatially and probably genetically associated with ~1740 Ma Wonga Suite Granites, hence we classify this deposit as magmatic-hydrothermal, although significant post-depositional remobilisation occurred. Total production at Mary Kathleen was just under 9 kt U_3O_8, with a small remnant resource (Table 1). There are numerous smaller uranium occurrences nearby (Brooks, 1975), including several small prospects.

3.5.2.1.1. Geological setting of the Mary Kathleen deposit

The Mary Kathleen deposit is located in the Eastern Fold Belt of the Mount Isa Inlier (Fig. 2), and is hosted in metasediments of the ~1780-1760 Ma Corella Formation. The Corella Formation consists of calc-silicate rocks, scapolitic metasediments, and slates (Brooks, 1975), which were deposited in a mixed clastic-carbonate shoreline and near-shore environment (Hawkins, 1975). The ores are associated with garnet-pyroxene skarn that has replaced carbonate and conglomeratic facies of the Corella Formation (Oliver et al., 1999). These skarns are spatially associated with the ~1740 Ma (Page, 1983) Burstall Granite and associated dykes. The steeply-dipping, D_3 Mary Kathleen Shear Zone wraps and truncates the ore-hosting skarn to the west (Oliver et al., 1999).

3.5.2.1.2. Uranium mineralisation at Mary Kathleen

Intrusion of the Corella Formation by the Burstall Granite resulted in the development of a large (~1.5 × 4 km) body of skarn along its western margin of the granite (Oliver et al., 1999). This skarn body consists of two types: banded garnet-pyroxene skarn and massive garnet skarn. It is cut by felsic dykes that are also affected by endoskarn assemblages. The deposit itself is associated with smaller bodies of skarn to the west of this large body (~3 km west of the Wonga Granite) within the tight, doubly plunging Mary Kathleen Syncline. Here the skarn assemblage has replaced calcareous cobble-pebble conglomerate, gabbro and banded calcareous sedimentary rocks (Oliver et al., 1999). The western limb of the syncline is sheared out by the Mary Kathleen Shear Zone.

The Mary Kathleen skarn body was overprinted by a set of steeply-dipping, anastomosing network of ore shoots that are cut to the west by the Mary Kathleen shear (Maas et al., 1987). The ore shoots are characterised by a decussate mass of allanite and apatite with minor ferrohastingsite, quartz, epidote, sphene, hematite and stillwellite and with minor to trace sulphides including chalcopyrite, pyrite, pyrrhotite and galena (Maas et al., 1987). Uraninite is a minor mineral that Maas et al. (1987) interpreted as the first to precipitate. Minor gold also occurs with U-REE mineralisation (Oliver, 1995). Maas et al. (1987) reported post-ore veins characterised by a calcite-sulphide-garnet-pyroxene-prehnite assemblage. Oliver (1995) also reported phases of regional post-ore hydrothermal activity.

Isotopic and fluid inclusion data for the early skarn assemblage suggest deposition from high temperature (500-700°C), and highly saline fluids (Oliver, 1995), with oxygen isotope data consistent with involvement of a fluid equilibrated with igneous rocks. Similarly, the later allanite-apatite assemblage formed from highly saline, high temperature (500-600°C: Oliver, 1995) fluids.

3.5.2.1.3. The age and genesis of uranium mineralisation at Mary Kathleen

The timing and origin of the Mary Kathleen deposit is contentious, with two interpretations advocated: (1) early skarn formation and uranium introduction associated with emplacement of the Burstall Granite, followed by recrystallisation and remobilisation of uranium during D_3 (Maas et al.,

1987); and (2) early skarn formation associated with emplacement of the Burstall Granite, followed by uranium introduction during D_3 (eg. Oliver, 1995). Consensus exists that garnet±pyroxene skarn formed by replacement of the Corella Formation synchronous with emplacement of the Burstall Granite. Maas et al. (1987) reported Sm-Nd isochron age, based on mineral separates from the skarn assemblage, of 1766±80 Ma, which overlaps the ages (1740-1730 Ma) of the Burstall Granite and associated felsic dykes (Page, 1983).

Disagreement arises regarding the interpretation of significantly younger ages derived from dating of uraninite and associated minerals of the crosscutting allanite-apatite assemblage. U-Pb dating of uraninite from the apatite-allanite assemblage yielded a date of 1550±15 Ma (Page, 1983), which is consistent with regional D_3 deformation and peak metamorphism (Oliver, 1995; Oliver et al., 1999). This is slightly older than a 1472±40 Sm-Nd date on mineral separates from the apatite-allanite assemblage obtained by Maas et al. (1987), although this discrepancy is likely to be a result of post-mineralisation disruption of the Sm-Nd system. Hence, the ~1550 Ma age represents either the remobilisation/recrystallisation of uranium or the introduction of new uranium into the system during D_3.

Neodymium isotope data support the interpretation that the hydrothermal event that formed the allanite-apatite assemblage remobilised pre-existing low grade U-REE mineralisation introduced during early skarn formation, concentrating uranium and REEs and depositing them in suitable sites. Based on ε_{Nd} values, LREE (and presumably uranium) in the Mary Kathleen ores are best interpreted to have been sourced from pre-existing ~1730 Ma skarn assemblages, although a very old crustal source (with Nd model ages of ~2500 Ma) cannot be excluded.

We agree with the interpretation of Maas et al. (1987) that these isotopic data reflect formation of a U-REE-bearing protore through metasomatism of the host Corella Formation during emplacement of the Burstall Granite at ~1730 Ma. The younger ages are probably related to recrystallisation and some remobilisation of the protore during D_3 to form the present orebody. This model is consistent with Sm-Nd modelling, which suggest that the second phase skarn was most simply derived from the protore and did not involve the introduction of new rare earth elements (Maas et al., 1987).

3.5.2.2. Magmatic-related deposits in the Etheridge Province

The eastern part of the exposed Etheridge Province contains a number of shear-related mineral deposits hosted by Proterozoic granites, the most important being the Mount Hogan and Oasis deposits. In addition to similar geological settings, these deposits are also uranium-rich. Whereas the Oasis deposit is a uranium-only deposit, the Mount Hogan gold deposit contains significant uranium grades. Of these deposits, the Mount Hogan is best described. This deposit comprises thin (2-600 mm), en echelon quartz veins within sericite-chlorite altered biotite granite of the ~1558 Ma (N Kositcin, unpublished data) Mount Hogan Granite (Denaro et al., 1997). These altered zones, which are 6-30 m wide, dip shallowly (mostly 15-20 toward the metamorphic country rock). The orebody at Mount Hogan consists of a series of sinusoidal quartz-sulphide veins in flat dipping shears. Accessory to minor minerals in these veins include pyrite, arsenopyrite, galena, tetrahedrite and electrum.

Unlike other vein gold deposits in the Etheridge Province, the Mount Hogan deposit also contains accessory molybdenite, (purple) fluorite, pitchblende, phosphuranylite and uraninite, along with torbernite and metatorbernite in oxidised zones (O'Rourke and Bennell, 1977; Denaro et al., 1997). O'Rourke and Bennell (1977) indicated that the uranium is intimately associated with quartz veining and sericitic alteration of the granite, which was accompanied by the introduction of gold, base metal sulphide minerals and pyrite. The age of these deposits is problematic. Rubidium-strontium and potassium-argon dating of the alteration assemblage at Mount Hogan yielded an age of ~400 Ma

(Bain et al., 1984), though Denaro et al. (1997) preferred a late Paleozoic age, similar to the Maureen deposit (see below). However, these Paleozoic ages are both inconsistent with lead isotope analyses of galena presented by Carr and Sun (1997). These results, discussed by Kositcin et al. (2009), indicate CSIRO-AGSO model ages of 1530-1515 Ma, with a similar composition to the estimated initial ratios of Proterozoic granites in the Etheridge Province. These results are consistent with a Proterozoic age of mineralisation and possible derivation from Proterozoic granites and are difficult to reconcile with a Paleozoic age of mineralisation.

The Oasis deposit is located several kilometres to the west of the Lynd Mylonite Zone, which marks the eastern exposed margin of the Etheridge Province. The following description is based on the Mega Uranium website (www.megauranium.com), discussion with Mega Uranium geologists and observations from a site visit in August 2007 and analytical results on samples collected from that visit. The deposit is hosted by the north-trending, steeply dipping shear zone that cuts the ~1558 Ma (N Kositcin, unpublished data) Mywyn Granite. This granite consists of foliated, feldspar porphyritic biotite granite. The mineralised zone is a steeply dipping, tabular zone up to 15 m thick (mostly < 10 m) that has been traced 300 m along strike and up to 175 m in depth. Typical grades for this zone are between 0.12 and 0.17% U_3O_8. The uranium is hosted by quartz-biotite schist, with the main uranium mineral being uraninite that occurs within biotite. At surface, a strong, north-trending fabric is present that dips 60-70° to the west; shear sense indicators indicate reverse motion with west side up. This shear zone is flanked on both sides by a zone of albite and biotite alteration of the granite. Other than a maximum age defined by the age of the host granite, the age of the Oasis deposit is unconstrained.

3.5.2.3. Mineral system model for magmatic-hydrothermal uranium deposits

The description of the magmatic-hydrothermal uranium systems above has led to the development of a two-phased mineral systems model (Fig. 17). Phase one involves the emplacement of uranium-rich intrusive rocks juxtaposed against a geological unit containing an appreciable carbonate component. Skarn formation within the carbonate and the exsolution of uranium-bearing fluids from the igneous intrusive led to the development of an initial low-grade uranium resource (Fig. 17a). Contact metamorphism of the sediments surrounding the intrusion established strong rheological contrasts which become important in phase two.

Phase two of the magmatic-hydrothermal uranium mineral system presented here relates to the hydrothermal upgrading of the initial protore to form an economic deposit. During metamorphism, metamorphic fluids exploiting major syn-metamorphic structures interact with the older protore. Remobilisation of uranium occurs, with fluid flow focused around zones of strong rheology contrast, most prominently those developed during contact metamorphism in phase one. This leads to the concentration of uranium in certain zones, and is accompanied by albitic alteration (Fig. 17b).

3.5.2.4. Mappable criteria for magmatic-hydrothermal uranium systems

Based on the above observations of known magmatic-hydrothermal uranium systems, key prospectivity criteria for this family of deposits may be derived:

Q1. What is the geodynamic and P-T history of the system?
The geodynamic setting for the magmatic-hydrothermal uranium systems described here is fundamentally one of partial melting and the generation of uranium-rich felsic magmas. The favourable geodynamic conditions for the formation of such magmas are discussed above for orthomagmatic systems. In the case of the systems described here, post-intrusion regional metamorphism is a key component of the geodynamic history.

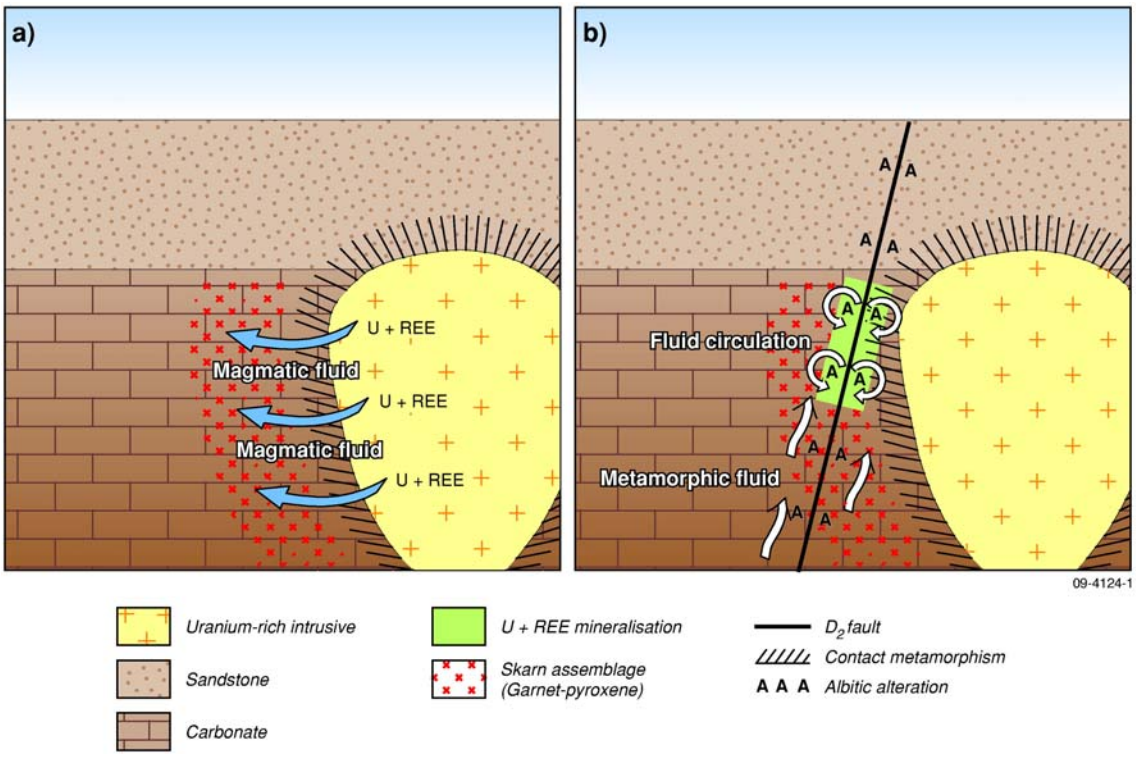

Figure 17: *Mineral system model for magmatic-hydrothermal uranium deposits.*

Based on this discussion, the following criteria were considered in the potential assessment:

- Emplacement of uranium-rich felsic igneous rocks
- Metamorphic-driven fluid flow, allowing for initial low grade U-REE mineralisation to be upgraded. In the Mary Kathleen area, this corresponds to D_3 high temperature-low pressure amphibolite grade metamorphism

Q2. What is the structural and lithological architecture of the system?

Granite intrusion immediately adjacent to a body of pre-intrusion carbonate-bearing sedimentary rocks is essential for the formation of the skarn-like Mary Kathleen deposit. Upgrading of the initial protore during D_3 metamorphism requires a major fluid flow pathway (i.e. faulting) within close proximity to the initial mineralisation.

Based on this discussion, the following criteria were considered in the potential assessment:

- The presence of pre-intrusion carbonate units to allow for skarn formation
- The presence of major structures to provide a fluid conduit during later phases of fluid flow

Q3. What are the fluids, their sources and/or reservoirs?

The initial fluid source for the Mary Kathleen deposit is the magmatic fluid exsolved from the crystallising Burstall Granite. Subsequent hydrothermal upgrading of the primary mineralisation sourced fluids derived from regional metamorphism. There is considerable debate over the ultimate source of uranium for the Mary Kathleen deposit. However, we consider the Burstall Granite to be the ultimate source of metal.

Based on this discussion, the following criteria were considered in the potential assessment:

- The distribution of intrusive igneous rocks which have the potential to have exsolved a magmatic fluid
- Emplacement of ~1740-1730 Ma granitoids, particularly the uranium-rich Wonga Suite, introducing uranium and REEs into the system. Other pre- D_3 uranium-rich granites also are considered to have potential

Q4. What are the fluid flow drivers and pathways?

Since the initial mineralising fluid is magmatic in origin, the fluid flow driver is the exsolution of a magmatic fluid. D_3 metamorphic fluids are driven by regional metamorphism in the Mount Isa region. Alteration resulting from either of these events is useful in prospectivity analysis. The key fluid flow pathways for the upgrading of the protore are D_3 faults. Fluid flow is also concentrated around zones of contrasting rheology, especially around the contact aureole of the mineralising granite.

Based on this discussion, the following criteria were considered in the potential assessment:

- The presence of major structures to provide a fluid conduit during later phases of fluid flow
- Distribution of Na-rich alteration assemblages, which may be approximated by depletion in K and detected with Th/K ratios derived from radiometric data
- Contact metamorphism related to early granite intrusion, setting up strong competency contrasts which may focus later fluid flow and remobilisation

Q5. What are the metal (and ligand) transport and depositional processes?

The depositional processes for the Mary Kathleen deposit are poorly constrained, but may be due to rheological contrasts or chemical factors (Hawkins, 1975; Oliver, 1995), either by pressure decrease or reduction, or both (Oliver et al., 1999). In contrast to other uranium systems such as sandstone-hosted deposits where the distribution of reductants is vital to prospectivity, depositional mechanisms in magmatic-hydrothermal systems are relatively minor in significance compared with other factors. No criteria corresponding to this question were used.

Q6. What are the effects of post-depositional processes on metal accumulations?

Post-depositional processes are of great significance for the magmatic-hydrothermal systems discussed here. Although we interpret to generation of the initial protore in association with granite emplacement to be the single most critical process in the formation of the Mary Kathleen deposit, later concentration of this initial mineralisation was essential to converting this into an economic deposit. These components, in combination with knowledge of magmatic-hydrothermal mineral systems in north Queensland such as the Mary Kathleen deposit, suggest the following mappable criteria:

- Metamorphic-driven fluid flow, allowing for initial low grade U-REE mineralisation to be upgraded. This may be mapped by the distribution of amphibolite grade metamorphism and D_3 faults

These components are presented in more detail in Appendix A. Based on these components and available datasets, a series of mappable criteria were identified and are summarised in Table 8. These criteria have been used as the basis for uranium potential analysis. Table 8 also indicates the weightings used in the analysis, and the results of which are presented below.

Table 8: Mappable criteria used for potential assessment of magmatic-hydrothermal uranium deposits.

MINERAL SYSTEM QUESTION	CRITERIA	SCORE	DATASET & REFERENCE	COMMENTS
1, 3	*Uranium source* 5 km buffer around Wonga-Burstall granitoids 5 km buffer around other U-rich granitoids	 3 2	Solid geology (Liu, 2009); OZCHEM	Wonga-Burstall granitoids were selected from the solid geology dataset. Other uranium sources were identified by selecting Paleoproterozoic felsic intrusives with an average uranium content calculated from the geochemical point data of >10 ppm
4	*Strong competency contrasts* 3 km buffer around U source rocks	 3	Solid geology (Liu, 2009);	Represented by contact aureoles of uranium source rocks. Contact metamorphism sets up competency contrasts which focus later fluid flow
2, 4	*Fluid flow pathways* 2 km buffer around D_3 faults 4 km buffer around D_3 faults 6 km buffer around D_3 faults	 3 2 1		D_3 faults acts a fluid flow pathways necessary for post-magmatic concentration of uranium
1, 6	*Metamorphic-driven fluid flow* Amphibolite facies metamorphic grade	 1		Metamorphic fluid flow in the Mary Kathleen area is associated with high temperature-low pressure amphibolite grade metamorphism
4	*Mineralisation-related alteration* Albitic alteration	 2	Radiometric Map of Australia (Minty et al., 2009)	Albitic alteration is represented by low Th/K ratios in radiometric data. These have been converted to shapefile format
2	*Skarn host rocks* Pre-granite carbonate units Pre-granite units including a carbonate component	 2 1	Solid geology (Liu, 2009)	These act as important host rocks for mineralisation

3.5.2.5. Results of assessment analysis for magmatic-hydrothermal uranium systems

Prospectivity analysis for magmatic-hydrothermal (Mary Kathleen-style) mineralisation successfully highlights the Mary Kathleen deposit (Plate 7). The potentially prospective regions identified are:

A. Along the strike length of the Wonga-Burstall Suite granitoids. The area immediately adjacent to the Wonga-Burstall Suite granitoids exhibits high prospectivity, as may be expected since the geological setting is very similar to that of Mary Kathleen.
B. Along the margins of the Sybella Suite. The area surrounding the uranium-rich Sybella Suite granitoids in the Western Fold Belt are identified as having high potential in the analysis.
C. The eastern margin of the Ewen Granite. The Paleoproterozoic Ewen Granite of the Kalkadoon Supersuite exhibits high potential along its eastern margin; although the lack of pre-intrusion carbonates limits prospectivity.
D. Along the western margin of the Kalkadoon Granodiorite. This area displays moderate prospectivity.

4. Geothermal systems (B Ayling and B Lewis)

A geothermal energy system comprises three key components: a heat source, a fluid to transport the heat, and sufficient permeability to enable the fluid to circulate through the rock. Of these three, a heat source is the only naturally-occurring requirement: fluids can be artificially injected into hot rocks, and permeability can be chemically or hydraulically created. Elsewhere in the world, conventional geothermal systems are associated with active volcanism. In these conventional geothermal systems, the three components of a geothermal energy system often naturally exist.

Geothermal energy systems in Australia are generally either Hot Rock (HR) systems (also known as Engineered Geothermal Systems) or Hot Sedimentary Aquifer (HSA) systems (Fig. 18). The heat sources for either geothermal system are basement rocks (typically felsic granites) or sediments that are enriched in the radioactive elements uranium (U), thorium (Th) and potassium (K). The decay of U, Th and K over time generates heat, and if these high-heat-producing rocks are buried beneath a sufficient thickness of insulating sediments, the heat is trapped and temperatures as high as 250°C can be found at less than 5 km depth. Only basement heat sources are considered in this geothermal assessment. The requirement for insulation (in the case of Hot Rock systems) and permeable stratigraphic formations (in the case of HSA resources) means that geothermal systems in Australia are more likely to be associated with sedimentary basins than areas of outcropping basement.

In areas where high-heat-producing basement rocks are not present, geothermal systems can still be found, because temperature in any location generally increases with crustal depth. In addition, hot fluid can migrate away from the area in which it was initially heated, forming HSA systems with no immediately obvious heat source. Geothermal systems remote from local sources of enhanced heat production are likely to be relatively low temperature systems.

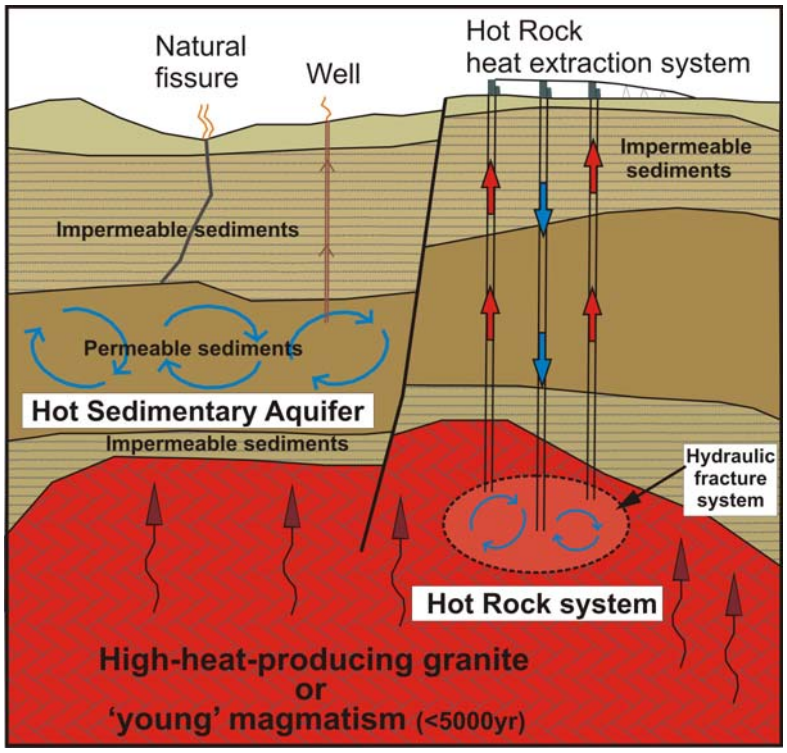

Figure 18: *Schematic diagram of styles of geothermal systems found in Australia*

The temperature of the geothermal resource dictates the potential end-uses for the heat. Higher-temperature resources (>200°C) are ideal for generating electricity. High temperature resources (e.g. 300°C) can have cycle conversion efficiencies up to 20% (Tester, 1982). In off-grid areas where the special case of fuel-limited economics comes into play, lower temperatures may be used to economically generate power, for example at Birdsville. While possible, electricity generation from lower temperature resources is thermodynamically less efficient with only ~6% of the thermal energy being converted into electrical energy. As an alternative to electricity generation, low temperature geothermal resources (<150°C) can be used to provide heat for industrial or domestic processes. For these lower temperature resources, direct use is a more thermodynamically-efficient use of the geothermal resource. Examples of potential applications where geothermal heat can be used directly are displayed in the Lindal diagram (Fig. 19).

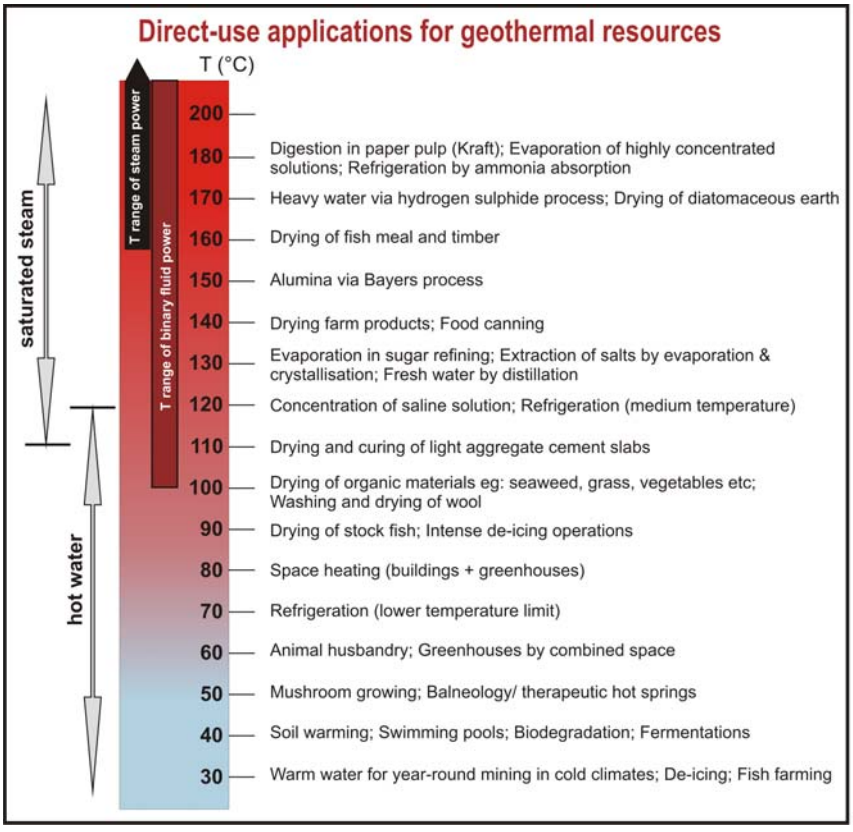

Figure 19: *The variety of applications for direct-use of geothermal heat, as a function the resource temperature (modified from Lindal, 1973).*

Although Australia is yet to generate electricity from its Hot Rock geothermal systems, a small binary power plant in Birdsville, SW Queensland, has been generating electricity from a low temperature (100°C) HSA system in the Great Artesian Basin. The plant has been operating since the early 1990's and is currently generating ~ 80 kW net.

A qualitative assessment of Hot Rock and Hot Sedimentary Aquifer geothermal potential in the north Queensland study area is presented below. It is a Geographic Information System (GIS)-based approach similar to that used elsewhere to identify potential regional-scale geothermal resources (e.g. Noorollahi *et al*., 2007).

4.1. HOT ROCK SYSTEMS

4.1.1. Hot Rock Geothermal Model & Datasets

Exploration for geothermal resources ultimately aims to locate commercially exploitable temperatures at economically-drillable depths. Ideally, this would be achieved by measuring temperature in deep drillholes distributed in a grid-like manner across Australia. However this is not economically feasible, and to supplement existing measured temperature data, other datasets such as shallow temperature gradient logs or heat flow measurements are used to predict temperature at depth. Hot Rock geothermal potential is also assessed on the basis of superposition of key features (e.g. a heat-generating body buried beneath thick thermally-insulating sediments).

The dominant mode of heat transport in Australia's Hot Rock systems is conduction. The steady state equation for conductive heat flow summarises the key parameters and is expressed as follows:

$$Q_0 = Q_d + \int A(z)\partial z$$

Where: Q_0 = surface heat flow, Q_d = heat flow at depth d, $\int A(z)\partial z$ = the integral of volumetric heat generation from the surface to d, A = heat production and z = depth.

The heat flow at depth d can be calculated from the following relationship:

$$Q_d = \lambda_d \cdot \left[\frac{\Delta T}{\Delta z}\right]_d$$

Where: λ_d = thermal conductivity at depth d and T = temperature

The key datasets for geothermal exploration are thus temperature, heat flow, thermal conductivity, and heat generation. The relationship between these variables is diagrammatically illustrated in Figure 20.

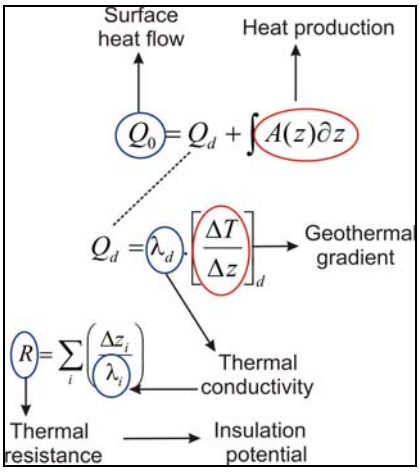

Figure 20: *Relationship between key physical parameters useful for geothermal resource exploration.*

In most instances, these datasets are incomplete and the predictive assessment of the Hot Rock potential in north Queensland uses a GIS-approach that involves several assumptions, approximations and interpolations of existing data. Currently, drilling technology is thought to limit the economic development of geothermal energy extraction systems to approximately 5 km depth,

and this is the depth to which the north Queensland geothermal resource assessments (Hot Rock and Hot Sedimentary Aquifer) are performed. The datasets used in this report are outlined below, and datasets used for the GIS-based approach for predicting Hot Rock geothermal prospectivity are compiled in Table 10.

4.1.1.1. Temperature and heat flow

The AUSTHERM07 database stores 5722 measurements of temperature and geothermal gradient that have been collected from drillholes around Australia (Chopra & Holgate, 2005). Using measured and estimated thermal gradients, surface temperature estimates, and depth to basement information, these data have been vertically extrapolated to 5 km depth and horizontally interpolated between the drillholes to produce a gridded map of crustal temperature at 5 km depth across the Australian continent. The temperature at 5 km raster covering the north Queensland study area is shown in Fig. 21. There are many areas where few temperature measurements have been made, and the interpolation is performed across vast areas. The 5 km temperature map is thus not reliable in all zones. The significant gaps in the database covering this study area are highlighted in Figure 21. In the north Queensland project area, there are 86 bottom-hole temperature (BHT) measurements incorporated in AUSTHERM07.

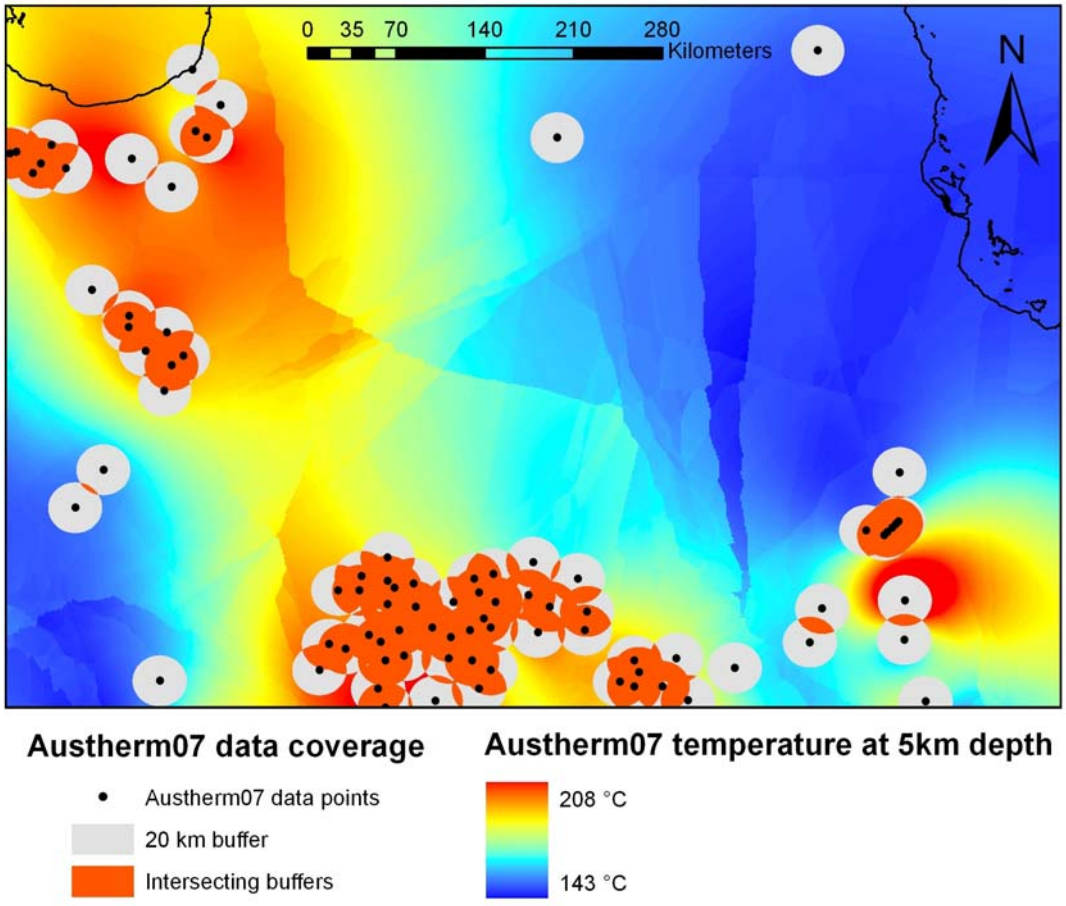

Figure 21: *Distribution of data points used to create the gridded Austherm07 raster in north Queensland, highlighting the concentrated data coverage in the sedimentary basin regions and sparse coverage over basement regions. The data contained in this product is derived from proprietary information owned by Earth Energy Pty Ltd ACN 078964735.*

When carefully assessed in conjunction with thermal conductivity, temperature data can be used to give an approximation of heat flow in the absence of adequate heat flow measurements. The heat

flow dataset was sourced from the global heat flow database (http://www.heatflow.und.edu). This dataset currently includes <200 points for Australia; only six of these are found in the north Queensland project area. Owing to insufficient data distribution, heat flow measurements were not used in the GIS predictive assessment.

4.1.1.2. Heat production/Heat generation

The radioactive decay of U, Th or K generates heat, thus lithologies that contain higher concentrations of these elements will be associated with increased heat production. Felsic intrusive rocks are more likely to be enriched in U, Th or K and are typically better candidates for heat generation than sediments, metamorphic or mafic igneous rocks.

In the north Queensland project area, the distribution of felsic intrusives drew extensively on published 1:100 000, 1:250 000 and smaller scale regional geological maps. Additional analysis and interpretation of closely spaced grids of regional aeromagnetic data from Geoscience Australia's aeromagnetic database, and Bouguer gravity and borehole data supplemented existing map data (Liu, 2009) and contributions from I.W. Withnall, L.J. Hutton (Geological Survey of Queensland), D. Champion, G. Gibson, and D. Huston (Geoscience Australia). Flat-lying Cenozoic and Mesozoic cover materials were removed across the map area; and Paleozoic sediments were also removed in the Mount Isa area in the west (north of the Diamantina Fault or NW of the Thomson Fold Belt).

Heat generation was calculated for felsic intrusives (predominantly granites; located from Liu (2009)) using geochemical data from the OZCHEM database. The granites were attributed with radiogenic heat production values by calculating the radiogenic heat production for each suitable OZCHEM data point within a given granite polygon. Three levels of radiogenic heat production assignation exist – polygons assigned with values based on real data (17% of the felsic polygons attributed this way), polygons attributed with values based on stratigraphic correlation with other granite polygons that do have OZCHEM values associated with them (42%), and polygons with no attributed value (39%; see Fig. 22 for spatial distribution of these polygons). Granite polygons that did not contain OZCHEM data points (but were represented elsewhere by other granite polygons with OZCHEM data points with the same unit were attributed with the same value as the 'parent' polygon. The data compiled in this study is an updated version of the Australian radiogenic granite and sedimentary basin geothermal hot rock potential map (Budd, 2007).

The radiogenic heat production was calculated for each geochemical sample point in the study area. Where multiple OZCHEM samples existed within a polygon, these were averaged to give one representative heat production value. The formula for the calculation is $A = 10^{-5} \rho(9.52_{cU} + 2.56_{cTh} + 3.48_{cK})$ where ρ = density in kg m^{-3} and c_U, c_{Th} and c_K are the concentration of uranium and thorium in parts per million and potassium in weight percent (Beardsmore and Cull, 2001). A density of 2.67 g cm^{-3} is assumed as representative for granites (Beardsmore and Cull, 2001).

4.1.1.3. Thermal conductivity and thermal resistance

The GIS prospectivity approach relies on using 2D datasets as inputs. Thermal conductivity varies in the vertical dimension, and any map illustrating thermal conductivity is only able to display thermal conductivity at a particular depth horizon. This provides no information about the net insulation potential because the thickness of sediments that have this thermal conductivity are not quantified. Thermal conductivity can be used to calculate thermal resistance, which provides an estimation of net insulation potential. Resistance for a defined thickness of sediments can be calculated using the following equation:

$$R = \sum_i \left(\frac{\Delta z_i}{\lambda_i} \right)$$

Where: R = thermal resistance (m²K/W), z = depth interval i in metres, and λ = thermal conductivity (W/mK)

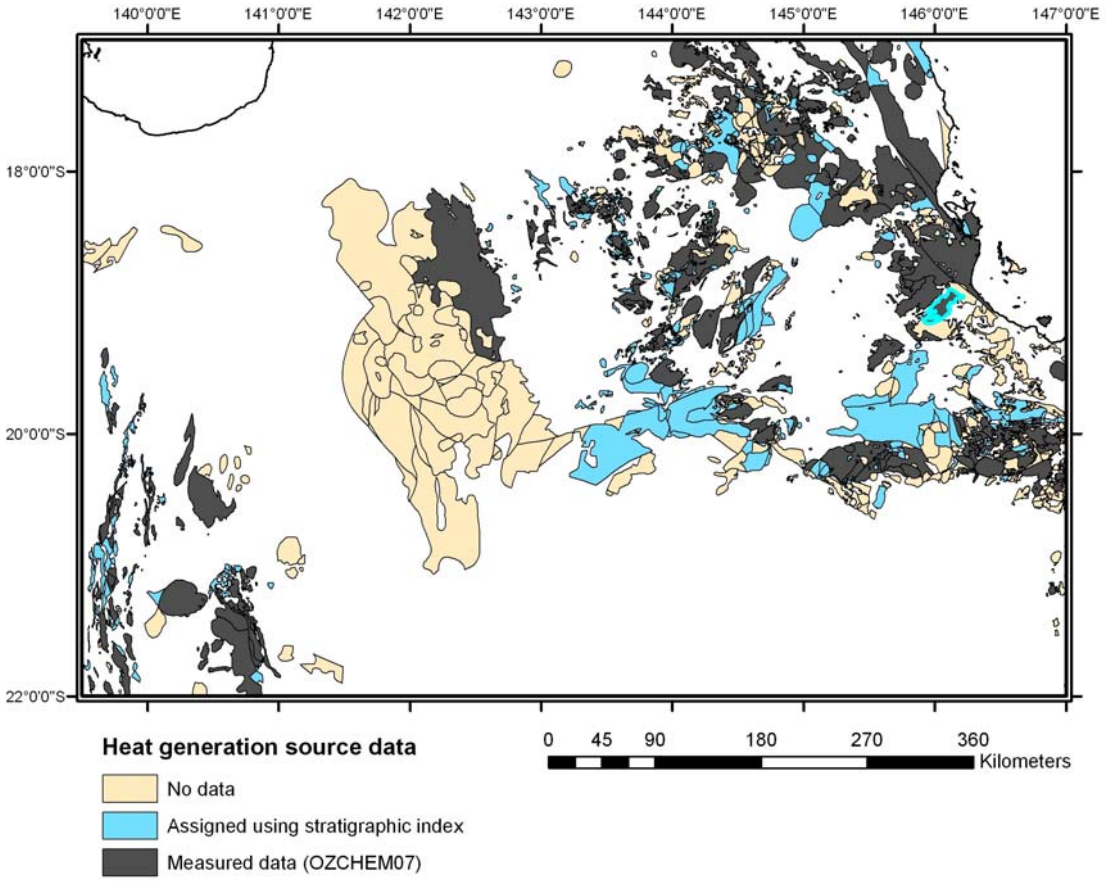

Figure 22: *Data sources for heat generation values assigned to felsic intrusive polygons in north Queensland.*

In this assessment, thermal resistance was calculated to 5 km depth, to be consistent with the AUSTHERM07 dataset and the understanding that the economic development of geothermal resources is presently limited to ~5 km depth or less.

To accurately map spatial variation in thermal resistance of a rock column, a 3D geological model that enables stratigraphic formations to be attributed with thermal conductivity and then integrated vertically in each cell is required. In the absence of a detailed 3D model and in-situ thermal conductivity measurements for much of the study area, thermal conductivity 'regions' were defined on the basis of sedimentary basin vs. basement areas. These are illustrated below in Figure 23.

For each region, the key litho-stratigraphic units were defined, and their proportional contribution to a 5km column of rock was estimated. Correspondingly, thermal conductivity was assigned to each of these units, using measured data where possible (e.g. Eromanga Basin units) or approximations on the basis of lithology where thermal conductivity relationships were assigned based on existing literature.

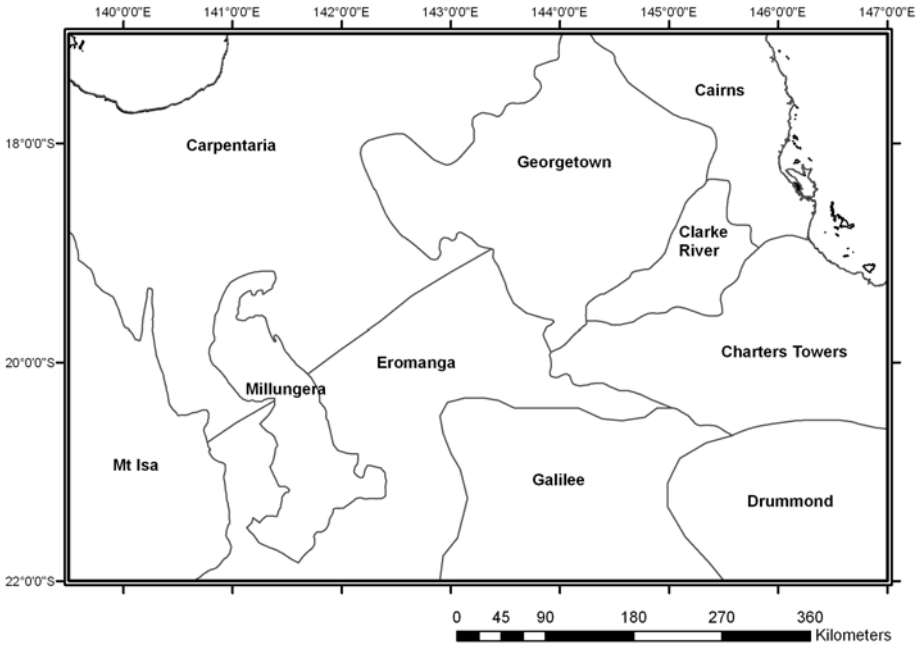

Figure 23: *Thermal conductivity regions in north Queensland, assigned on the basis of basement versus sedimentary basin contribution to a 5 km-thick lithologic column. Regions based on geological regions and sedimentary basin extents from Bain and Draper (1997).*

The average thermal conductivity values assigned to different lithologies are summarised in Table 9, along with data sources. The FrOGTech (2006) OZ SEEBASE™ depth to basement raster was instrumental in enabling the proportion contribution of basin sediments vs. basement for each 5 km-depth column to be defined. This dataset has been supplemented with new high resolution 3D mapping of the Eromanga Basin (van der Wielen et al., 2009) and Millungera basin (Kirkby et al., unpub. data).

4.1.1.4. Geographic Information System (GIS) methodology

Areas of Hot Rock and HSA geothermal potential in the North Queensland study area were determined by incorporating key geological, geochemical and thermal datasets into a GIS, classifying the individual datasets, and applying a weighed overlay approach. This process can be simply expressed by the following equation:

$$\left(\frac{a}{a_n}\cdot w_1\right)+\left(\frac{b}{b_n}\cdot w_2\right)+\left(\frac{c}{c_n}\cdot w_3\right)=Total\ geothermal\ potential\ value$$

Where:
a, b, c are classification values for individual datasets;
a_n, b_n, c_n are total number of classification categories for each dataset; and
w_1, w_2 and w_3 are the weighing factors for each dataset (must sum to 100%). Refer to Table 10 and 11.

Table 9: *Average thermal conductivity data applied to north Queensland lithologies*

Lithology	Mean thermal conductivity (W/mK)	Reference	Lithology	Mean thermal conductivity (W/mK)	Reference
Alluvium	1.62	12	Halite	5.58	1,11,15,18,19
Amphibolite	3.20	12	Limestone	2.69	1-15, 17-20, 22
Andesite	2.11	7,12,21	Marble	3.10	12
Argillite	3.65	12,22	Marl	2.44	1,2,3,11,13,15,19
Basalt	1.66	7,12-14,17,19,21	Mudstone	2.37	6,7,12,13,18,19
Chert	2.33	1,11,15	Quartz monzonite	2.87	12,22
Claystone	2.07	2,3,12-14,19,20	Quartzite	5.50	12,13,17,18,19,22
Coal	0.22	1,6,11,14,15	Rhyolite	2.44	7,12
Conglomerate	2.61	1,4,7,11,15	Sandstone	3.45	1-13, 15,16,18-20, 22
Dacite	2.30	7	Schist	2.74	12
Diorite	2.29	12	Serpentinite	2.30	12
Dolerite	2.11	7,21	Shale	1.69	1,4,5,8-13, 15,16,18,19
Dolomite	4.18	1,2,4,8-12,15,17-20	Siltstone	2.67	1-3, 6,7, 11,13,15,16,18
Dunite	1.54	21	Syenite	2.10	12
Gabbro	2.72	12,20,21	Trachyte	2.50	7
Gneiss	2.75	12	Tuff	1.34	12,14,21
Granite	3.15	4,12,17,19,20,21	Unconsolidated sediments	1.75	12
Granodiorite	2.79	4,7,12,22			

Data sources: 1 Majorwicz & Jessop (1981); 2 Hurtig & Schlosser (1979a); 3 Hurtig & Schlosser (1979b); 4 Clarke (1966); 5 Garland & Lennox (1962); 6 Funnell *et al*. (1996); 7 Norden & Forster (2006); 8 Blackwell & Steele (1989); 9 Carter *et al*.(1998); 10 Gallardo & Blackwell (1999); 11 Beach *et al*. (1987); 12 http://www.smu.edu/geothermal/georesou/alldata.csv; 13 Beardsmore (1996); 14 Raznjevic (1976); 15 Reiter & Jessop (1985); 16 Taylor et al. (1986); 17 Roy et al. (1981); 18 Reiter & Tovar (1982); 19 Barker (1996); 20 Galson *et al.* (1987); 21 Horai & Suzaki (1989); 22 Davis *et al*. (2007)

The above components, and the weighting applied to each within the GIS, are summarised in Table 10. The weighting assigned to each component dataset within the GIS framework was loosely based on the mathematical relationship between key parameters summarised in Figure 20. The order of priority assumes that of the elements required for a Hot Rock system, insulation is the most fundamental, hence resistance and sediment thickness together dominate the weighting. Resistance is considered to be a more sophisticated indicator of insulation potential than pure sediment thickness and is therefore weighted more heavily in the overall ranking.

As fluid presence is not a natural requirement for a Hot Rock system and this study is not considering the ease of exploitation of Hot Rock systems in the north Queensland area, fluid presence was not assessed in the final Hot Rock GIS framework. However, it is noted that the significant volumes of fluid present in the GAB would seem to bode well for adequate local available fluid supplies if an economically viable Hot Rock system is discovered.

Table 10: *Input datasets used for the Hot Rock geothermal potential GIS-assessment, including their individually-assigned classification and overall weighting. The classification values for each dataset were normalised prior to weighting and subsequent summation.*

Key indicator	Dataset name	Data source	Data type	Data range	Categories (classification)	Final weight
Insulation	Resistance	N/A	Raster	1557 - 2121 m²K/W	Contour categories: <1650 m²K/W **(1)**, 1650-1725 m²K/W **(2)**, 1725-1800 m²K/W **(3)**, 1800-1875 m²K/W **(4)**, 1875-1950 m²K/W **(5)**, 1950-2025 m²K/W **(6)**, >2025 m²K/W **(7)**	**30%**
	Sediment thickness	Frogtech (2006); van der Wielen et al. (2009); Kirkby et al. (unpub. data)	Raster	0 to >8000 m	Contour categories: 0-1000m **(1)**, 1000-2000m **(2)**, 2000-3000m **(3)**, 3000-4000m **(4)**, 4000-5000m **(5)**, >5000m **(6)**	**25%**
Temperature availability	Temperature at 5 km depth	AUSTHERM 07 (Earth Energy Pty Ltd)	Raster	143 - 208°C	Contour categories: 140-154°C **(1)**, 154-168°C **(2)**, 168-182°C **(3)**, 182-196°C **(4)**, 196-210°C **(5)**	**30%**
Temperature potential	Heat generation	Liu (2009); OZCHEM 07	Polygons	0 – 18 µW/m³	Heat generation categories: No data **(0)**, 0.01-1 µW/m³ **(1)**, 1-2µW/m³ **(2)**, 2-4µW/m³ **(3)**, 4-8µW/m³ **(4)**, >8µW/m³ **(5)**	**15%**
	Felsic intrusives	Liu (2009)	Polygons	N/A	Felsic polygon: Yes **(1)**, No **(0)**	

4.1.2. North Queensland Hot Rock Observations

4.1.2.1. Temperature and heat flow data

The key observation from the AUSTHERM07 data is that above average temperatures are associated with the Eromanga Basin, Galilee, Drummond and Carpentaria Basins. Predicted minimum temperatures at 5 km depth are up to 208°C in these areas (Fig. 24). The basement terranes of the Mt Isa region, and the eastern fold belts appear cooler with a minimum temperature prediction of 143°C. However this may also reflect the limited measurements available in these areas (cf. Fig. 21 for distribution of BHT data points). BHT measurements are typically made in petroleum wells, thus the data coverage is predominantly concentrated in sedimentary basins and scarce in basement terranes. Heat flow data for the north Queensland project area range between 72 mW/m² and 100 mW/m².

The Drummond Basin hot spot appears 70 km wide, however this is relatively unconstrained with only one temperature measurement. The hot spots in the Eromanga and Carpentaria are perhaps more reliable, owing to greater data coverage (cf. Fig. 21). However it is acknowledged that advection could impact upon this data, depending on the depth of drilling. In the Eromanga Basin, modelled temperatures reach a maximum of 190°C, which is comparable to the highest temperatures modelled in the Carpentaria Basin (a maximum of 180°C at 5km depth).

4.1.2.2. Heat sources: felsic intrusive distribution and heat generation

Heat sources in the north Queensland area are associated with high-heat-producing felsic rocks, where heat production values range from 0.06-18.32 μW/m³ and average 3.5 μW/m³. Approximately 10% of the study area is underlain by high-heat-producing (>8 μW/m³) or moderate-heat-producing (4-8 μW/m³) felsic intrusives. The heat production values and the spatial area covered by each heat production ranking category are summarised below in Table 11 and illustrated in Figure 25.

The highest heat production values (>8 μW/m³) are associated with felsic intrusives of the Mesoproterozoic Williams Supersuite in the Mt Isa region and the Late Carbonifereous O'Briens Creek Supersuite in the Cairns region. As 60% of these polygons are attributed using direct geochemical measurements, we can be confident that these felsic intrusives are indeed high-heat-producing. Moderately high-heat-producing felsic intrusives (4-8 μW/m³) are also concentrated in the Mt Isa and Cairns regions. The majority of these high-heat-producing basement rocks are exposed at the surface, however the spatially extensive (4751 km^2) Mesoproterozoic Esmeralda Granite is an exception. The Esmeralda Granite underlies the Carpentaria/Eromanga basins and has a heat production value of 4.71 μW/m³: an ideal situation for creating a Hot Rock geothermal system.

Many of the unnamed and unattributed felsic intrusive polygons underlying the Carpentaria and Eromanga regions could be important heat sources for Hot Rock and HSA resources, and additional geochemical data is needed to attribute these polygons with heat production data and better evaluate the potential for Hot Rock and HSA exploration in these areas.

4.1.2.3. Insulation potential: sediment thickness and resistance

Areas with greatest Hot Rock potential typically reflect burial of heat sources by insulating sediments (>2 km thick). In the north Queensland area, the areas with greatest sediment thickness correspond to the Drummond and Galilee basins, the Millungera basin and the north-western part of the Carpentaria basin (underlain by the Georgina Basin) (Fig. 26). The thickest sediments occur in the Drummond Basin, where sediment thickness reaches 10100 m. Thick sediments are also present in the Galilee region, where the Eromanga Basin overlies the Galilee Basin. For much of the Eromanga and Carpentaria region, sediments are less than 1000 m thick, and these areas may therefore have lower potential for Hot Rock geothermal resources unless excellent insulating lithologies (e.g. coal-bearing sediments) are present.

The depth to basement dataset was used to calculate thermal resistance to 5 km depth in the study area. The results of this approach are illustrated in Figure 27. The distinct differences between some regions are an artefact of the resistance calculation where average thermal conductivity values were estimated for each *region*. This in turn affects the final resistance calculation. Despite these offsets, it is apparent that the parts of the north Queensland project area with greatest thermal resistance correspond to sedimentary basins. This is consistent with the greater contribution of low thermal conductivity rocks (e.g. carbonaceous sediments and shale) to these areas vs. the contribution of crystalline and/or quartz-rich basement rocks (which have higher thermal conductivity).

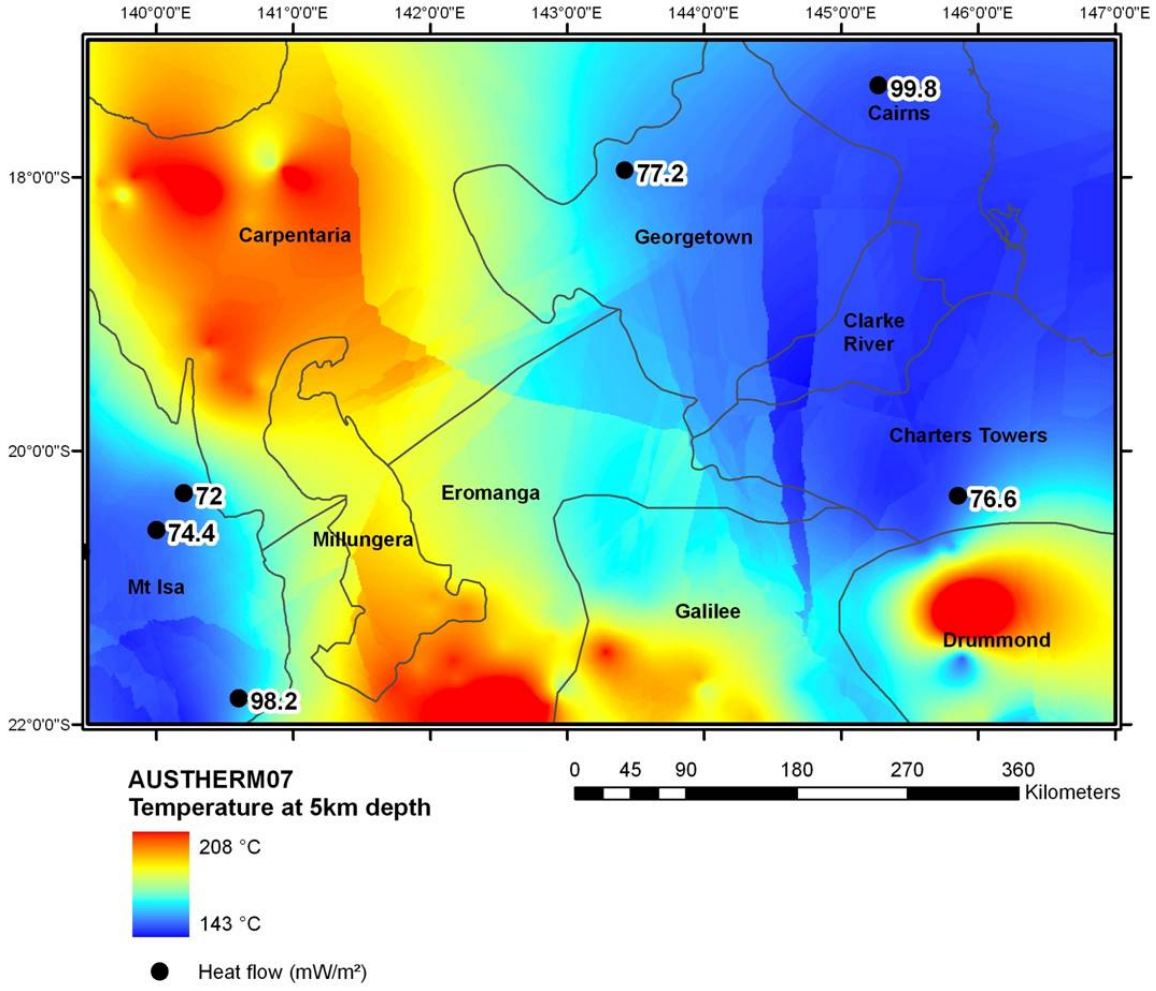

Figure 24: *AUSTHERM07 and heat flow in north Queensland. The data contained in this product is derived from proprietary information owned by Earth Energy Pty Ltd ACN 078964735.*

Table 11: *Heat production values as a function of spatial extent. Area % is calculated as the percentage of the total study area covered by a given heat production interval.*

Heat Production (µW/m³)	Area (m²)	Area %
0-1	43433	10.0
1-2	5339	1.2
2-4	9840	2.3
4-8	19700	4.6
>8	21025	4.9

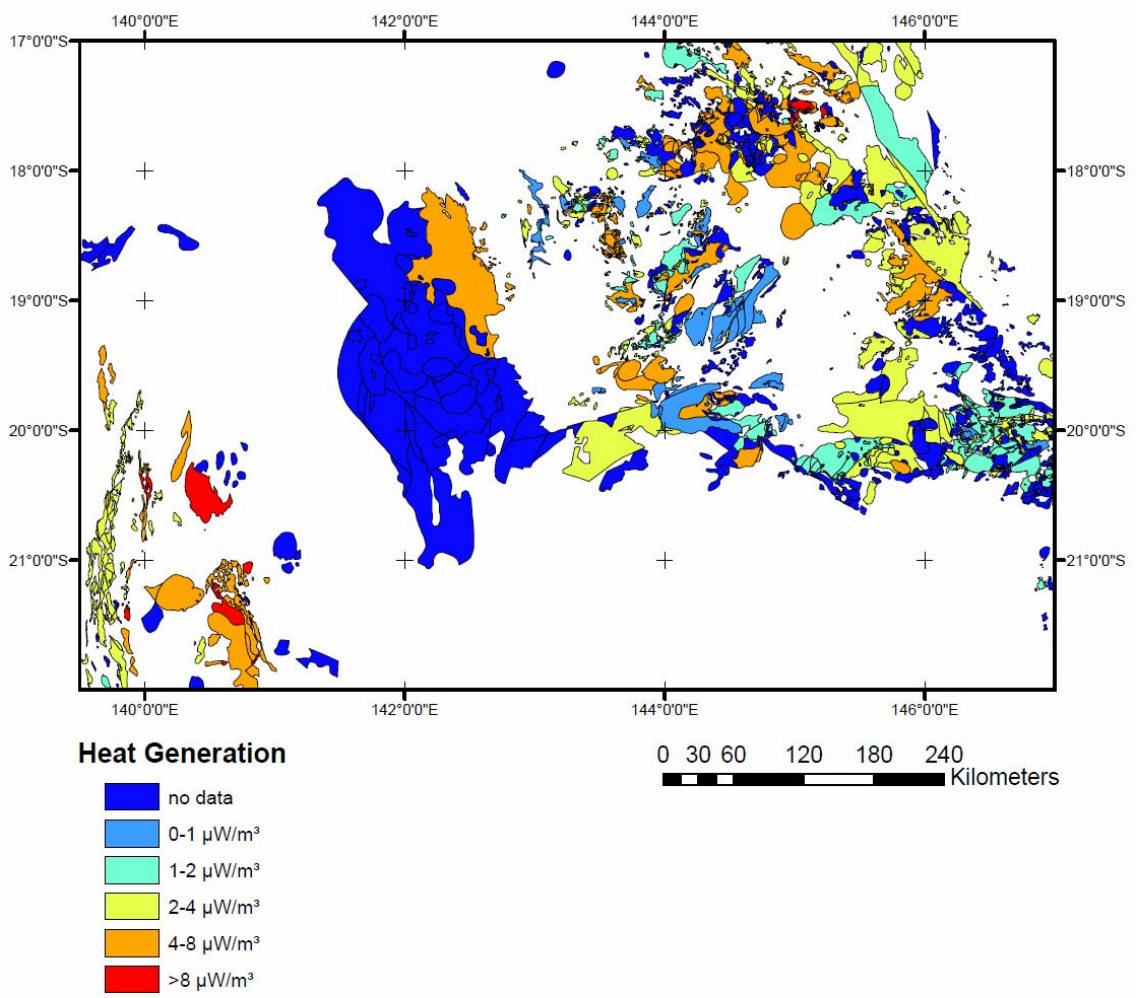

Figure 25: *Heat generation as calculated for felsic intrusives in the north Queensland.*

4.1.3. Hot Rock Potential Analysis: Results & Interpretation

The GIS weighted-overlay approach (Table 10) of evaluating geothermal potential indicates that the north Queensland study area appears to have significant potential for Hot Rock geothermal resources (Plate 8).

Significant areas of moderate - high Hot Rock potential are located in the Carpentaria, Eromanga, Millungera, Galilee and Drummond sedimentary basins. This result reflects the significant contribution of insulation potential to the overall ranking, which is based on the principle that Hot Rock heat sources require burial beneath a sufficient thickness of insulating sediments to generate above-average temperatures at relatively shallow depths. The basin sediments were assigned lower average thermal conductivity values relative to the basement regions, because the shale, coal and carbonaceous units common in these basins are characterised by low thermal conductivities.

More localised zones of highest Hot Rock potential occur where these insulating sediments reach maximum thickness in the Drummond and Galilee basins, the Millungera basin and the north-western part of the Carpentaria basin (underlain by the Georgina Basin). Localised zones of moderate Hot Rock potential occur in the basement-dominated regions, which directly reflect the location of felsic intrusives with high heat-generation values. In most cases, these felsic intrusives

are not buried beneath adequate thicknesses (>500 m) of insulating cover sequences, and thus it is unlikely that anomalously high temperatures will be found at shallow depths in these regions.

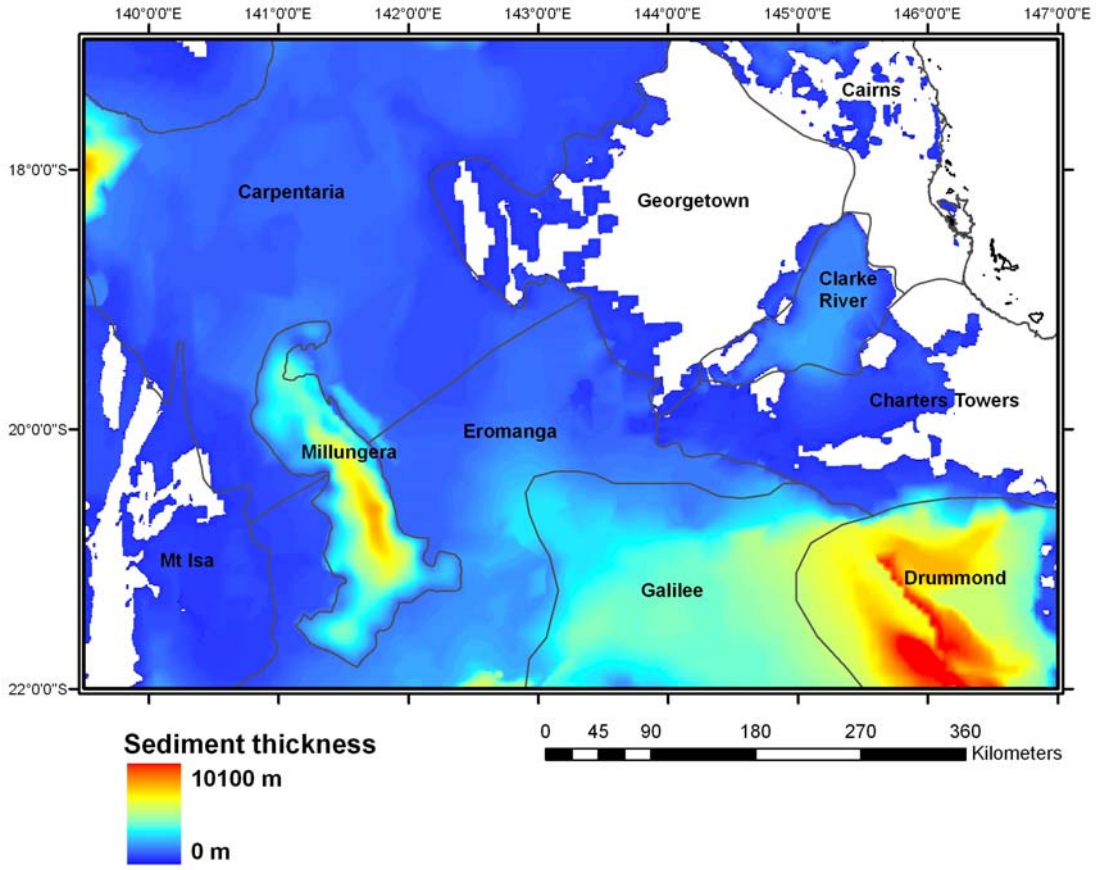

Figure 26: *Variation in sediment thickness across the north Queensland.*

In summary, the north Queensland study area appears quite promising for Hot Rock geothermal system exploration, particularly in the sedimentary basins where the vast insulation potential of the thick sedimentary pile suggest viable temperatures for geothermal use could be reached at relatively shallow levels. Areas of particular interest include those where felsic intrusives are overlain by sediments at the margins of the Eromanga and Carpentaria basins. Measured geochemical data from these intrusives is required before their heat generation potential can be assessed to enable a rigorous assessment of Hot Rock potential in these areas.

4.2. HOT SEDIMENTARY AQUIFER SYSTEMS

4.2.1. Hot Sedimentary Aquifer Model and Datasets

The key datasets for identifying HSA potential are similar to those used for Hot Rock assessment - temperature, heat flow and sediment thickness. Additional datasets indicate the presence of fluid in the rock, water temperatures, and sufficient volumes of porous, permeable sediments: these are discussed in the following section. Datasets used in the final HSA GIS analysis are shown in Table 12. As for the Hot Rock assessment, classification values developed for each dataset were normalised prior to weighting (refer to Section 4.1.1.4).

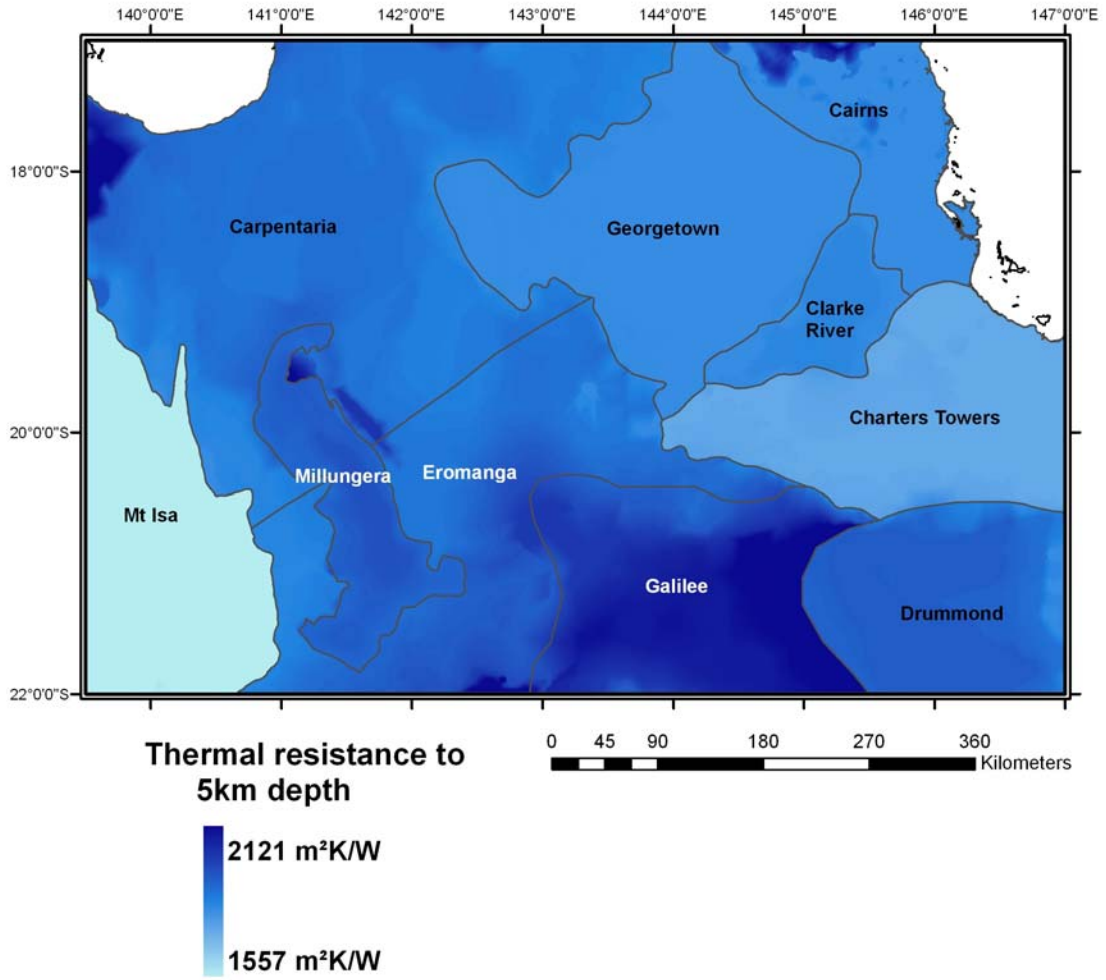

Figure 27: *Thermal resistance across the north Queensland project area, calculated to 5 km depth by integrating thermal conductivity with depth*

4.2.1.1. Fluid presence

The spatial distribution of surface expressions of the Great Artesian Basin (GAB) was assessed using the dataset: 'Springs of Queensland' (Fensham and Fairfax, 2006). These were not used as part of the final ranking, but included to demonstrate the pervasiveness of GAB-derived fluid in the study area. Only springs listed as actively discharging were included in this study.

The GABLOG borehole database compiles information on wireline logged wells penetrating the GAB across Queensland, New South Wales, South Australia, and the Northern Territory. Tucker and Ivkovic (1997) and later Welsh (2000), Radke et al., (2000), and Habermehl (2001) have reported extensively on the initial database and the application of this data to understanding the physical properties of the GAB. These data points are displayed here to indicate the presence of fluid at depth, they have not been included in the final ranking...

4.2.1.2. GAB aquifer thickness data

The digital versions of the GAB aquifer thickness rasters were provided by Wendy Welsh (CSIRO). They form the basis of the GABFLOW steady state groundwater flow model (Welsh, 2000). Nine principal hydrogeologic units were delineated based on stratigraphic information from well logs.

Approximately 34,000 unit thickness measurements were used to generate the thickness rasters – specific information on this process can be found in Welsh (2000).

The purpose of this analysis is to give an indication of the lateral distribution of vertical variation in aquifer and aquitard thickness. The total thickness of both aquifer and aquitard stratigraphic units was calculated for each 5 km x 5 km cell in the study area. To achieve this, five aquifer layers (WINT, CADN, ADOR, HUTT, and CLEM) representing the major aquifers in the GAB were summed generating a new 'total aquifer thickness' raster for the study area. The ALLA, WEST, BIRK, and MOOL aquitard layers were summed to provide the equivalent 'total aquitard thickness' raster. The sum of these two rasters gives a total sediment thickness raster for the GAB (excluding the Cainozoic cover or underlying basins). Note that the total sediment thickness that results from this calculation is quite distinct from the depth-to-basement raster.

4.2.1.3. Water temperature

Downhole water temperature measurements in the Cadna-Owie - Hooray Aquifer are sourced from the GABLOG borehole database (Tucker and Ivkovic, 1997 etc.). This database compiles information on wire-line logged wells penetrating the GAB across Queensland, New South Wales, South Australia, and the Northern Territory. These points have been interpolated in ArcGIS to generate a gridded dataset. The gridded data was then contoured using 10°C intervals to generate ranking seven polygons as defined in Table 12.

4.2.2. North Queensland Hot Sedimentary Aquifer Observations

4.2.2.1. The Great Artesian Basin

The Great Artesian Basin is a hydrogeological basin that includes the geological units present in the Eromanga, Surat and Carpentaria Basins and the upper sedimentary sequences of the underlying Galilee and Bowen Basins. The GAB underlies approximately 20% of the Australian continent, and represents one of the largest groundwater resources the world. It is a confined aquifer system, with laterally continuous aquifers and aquitards extending across the basin. In the north Queensland project area, the maximum depth to GAB aquifers is approximately 2000 m and these are present in the Eromanga, Carpentaria and Galilee Basins (Fig. 28). The Eromanga and Carpentaria Basins are separated by a ridge of basement rocks (the Euroka Arch), and the Galilee Basin underlies the Eromanga Basin. HSA geothermal resources in the north Queensland project area are most likely to be associated with the GAB, as fluid and formation permeability exist in the basin. Deeper sedimentary sequences are present in the north Queensland project area, but as porosity and permeability decrease with increasing depth, the potential for naturally-exploitable HSA resources decreases. The following discussion centres on existing knowledge of the GAB in the project area with respect to HSA potential.

4.2.2.2. GAB water temperatures

Water temperature measurements collected from the Cadna-Owie aquifer in the GAB range between 22°C and 89°C (Fig. 29). At present there are 174 downhole water temperature measurements collected in wells ranging from 50 – 1208 m deep. Eighty percent of wells are drilled to 500 m or less and only one well is drilled to greater than 1000 m. The highest temperatures are located along the axis of the GAB, while temperatures along the eastern margin of the basin are all less than 40°C. This trend reflects the depth distribution of aquifer units in the GAB. Typically, higher water temperatures are measured in deeper areas in the GAB (Fig. 29). However in the vicinity of the Euroka Arch, this trend is not observed. The moderate temperatures at relatively shallow levels in the GAB may instead reflect advection of hot groundwater from deeper depths in the GAB.

Table 12: *Input datasets used for the Hot Sedimentary Aquifer geothermal potential GIS- assessment, including their individually-assigned classification and overall weighting.*

Key indicator	Dataset name	Data source	Data type	Data range	Buffer	Categories (classification)	Final weight
Sediment availability	Sediment thickness	Frogtech (2006); van der Wielen et al. (2009); Kirkby et al. (unpub data)	Raster	0 to >8000 m	No	Contour categories: 0-1000m **(1)**, 1000-2000m **(2)**, 2000-3000m **(3)**, 3000-4000m **(4)**, 4000-5000m **(5)**, >5000m **(6)**	**25%**
Water Availability	GAB aquifer thickness	Welsh (2000)	Raster	0 - ~700m	No	Contour categories: 0-100m **(1),** 100-200m **(2)**, 200-300m **(3)**, 300-400m **(4)**, 400-500m **(5)**, 500-600m **(6)**, 600-700m **(7)**, >700m **(8)**	**35%**
Temperature availability	GAB water temperature	GABLOG database, Tucker and Ivkovic (1997)	Points - Raster	22 - 89°C	No	Categories: < 40°C **(1)**, 40-50°C **(2)**, 50-60°C **(3)**, 60-70°C **(4)**, 70-80°C **(5)**, 80-90°C **(6)**	**15%**
	Temperature at 5 km depth	AUSTHERM 07 (Earth Energy Pty Ltd)	Raster	143 - 208°C	No	Contour categories: 140-154°C **(1)**, 154-168°C **(2)**, 168-182°C **(3)**, 182-196°C **(4)**, 196-210°C **(5)**	**15%**
Temperature potential	Heat generation of felsic bodies	Liu (2009); OZCHEM 07	Polygons	0 - 18	No	Heat generation categories: 0.01.-1 µW/m³ **(1)**, 1-2µW/m³ **(2)**, 2-4µW/m³ **(3)**, -8µW/m³ **(4)**, >8µW/m³ **(5)**	**10%**
	Felsic intrusives	Liu (2009)	Polygons	N/A	No	Felsic polygon: Yes **(1)**, No **(0)**	

In addition, the pattern of temperature anomalies predicted by AUSTHERM 07 (Fig. 30) corresponds remarkably well with areas of high groundwater temperature. This implies that GAB groundwater is largely in thermal equilibrium with the rocks through which it flows, and that AUSTHERM 07 could be a useful dataset in prospecting for HSA type geothermal systems in the north Queensland project area.

Figure 31 suggests a linear correlation between groundwater temperature and well depth, but it is far from perfect (R^2 = 0.75). One possible explanation for these results could be local anomalies in groundwater temperature/depth relationships beyond a standard geothermal gradient with depth relationship (such as advection).

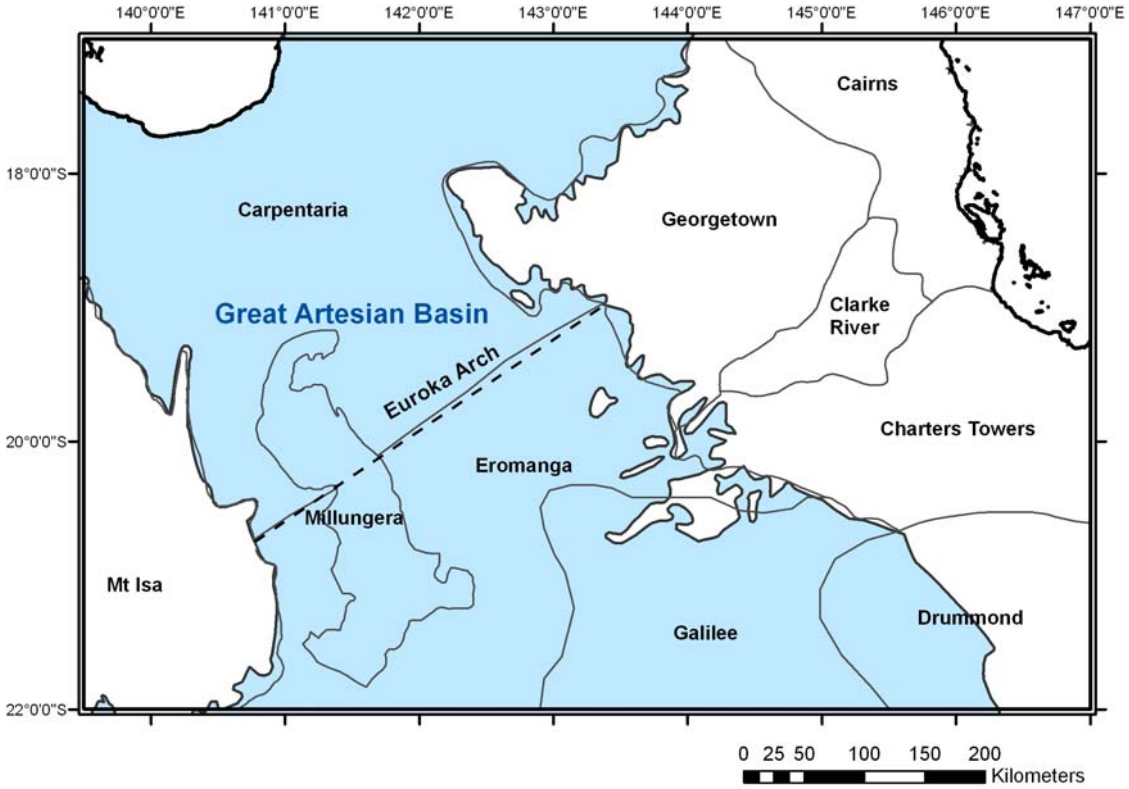

Figure 28: *Distribution of the hydrogeological province "the Great Artesian Basin" in the north Queensland project area, and its relationship to the regions used in the Hot Rock geothermal assessment.*

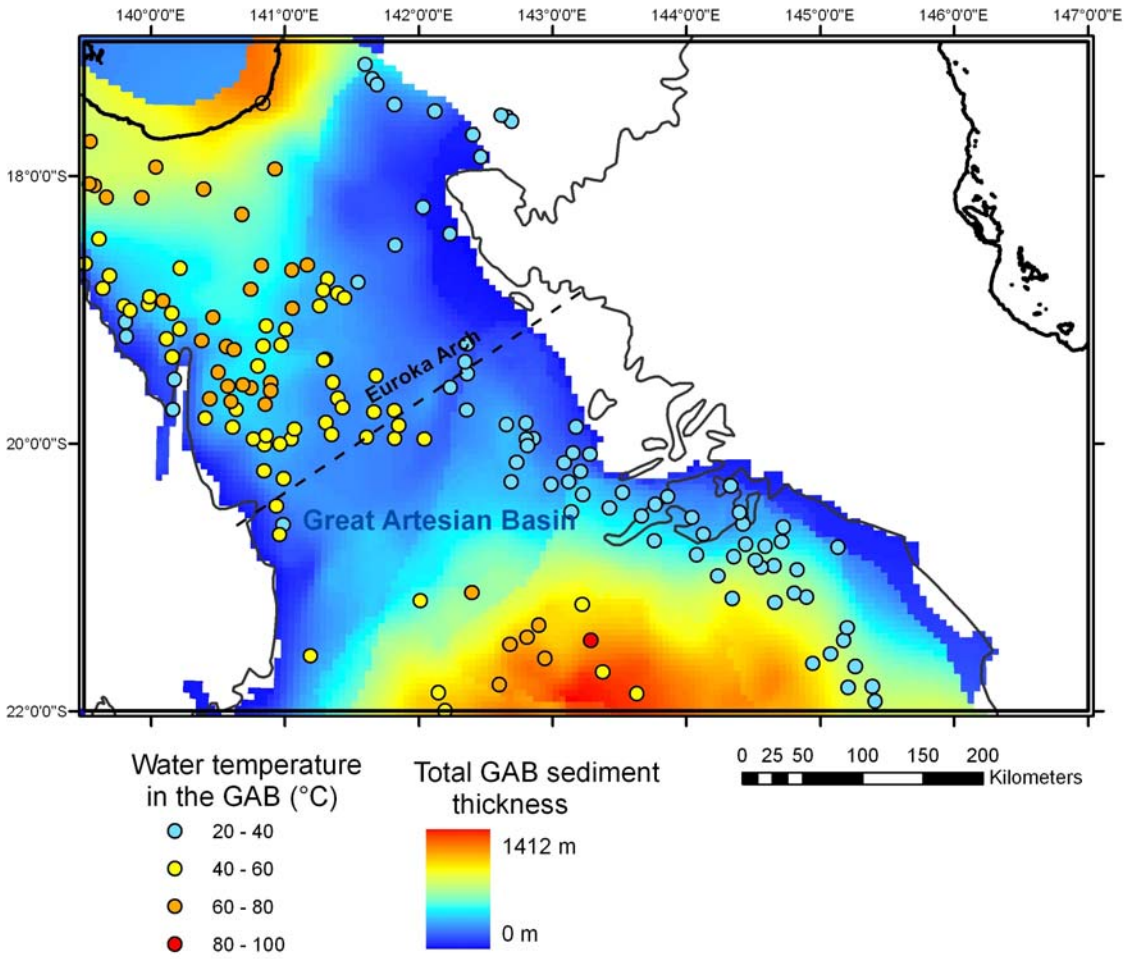

Figure 29: *Total thickness of sediments in the GAB, and location of groundwater temperature measurements.*

4.2.2.3. GAB aquifer distribution

The GABFLOW aquifer rasters were used to assess distribution and thickness of GAB aquifers in the north Queensland project area. The total aquifer dataset (Fig. 32) is the result of merging five GABFLOW modelled aquifers and thus the figure quoted as the 'total aquifer thickness' potentially represents five GAB aquifers. As such, a limitation of this dataset is that it only gives an overall representation of the available aquifers, not a breakdown of how thick each individual aquifer is. For more detail on individual aquifers as modelled in the GABFLOW study, see Welsh (2000). It is also noted that while the hydrogeological units used here are approximately correlative with stratigraphic units on a regional basis, many stratigraphic units have irregular inclusions of aquifer/aquitard material on a local scale. Thus both the total aquifer and total aquitard datasets presented here are indicative only.

Aquifers are thickest in the central Eromanga Basin and underlying the Galilee Basin, between 0-3000 m depth (Fig. 32). Aquifers are also present in the Carpentaria Basin and underlying Georgina Basin area adjacent to the Gulf of Carpentaria coast. These occur in very shallow level sediments in the 0 - 1000 m depth range. The limited aquifer thickness over the Euroka Arch emphasises the hydrogeological division of the northern and southern parts of the GAB. The aquifer thickness distribution statistics for the study area are summarised in Table 13.

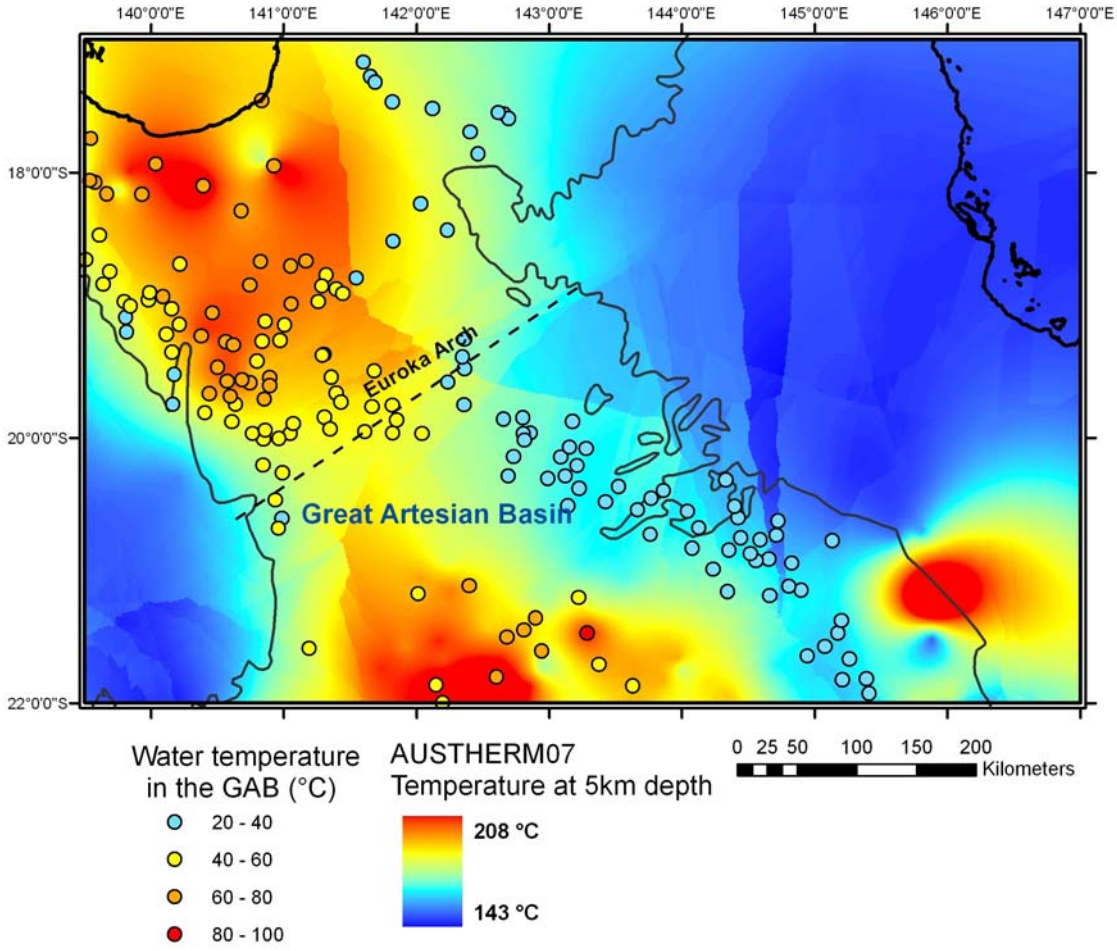

Figure 30: *Relationship between AUSTHERM07 temperature at 5km depth, and groundwater temperature measurements collected in the GAB at less than 2km depth. The data contained in this product is partly derived from proprietary information owned by Earth Energy Pty Ltd ACN 078964735*

In conjunction with the total aquifer thickness dataset generation, the total aquitard dataset was generated to give an indication of seal/confinement potential. In the study area, total aquitard thickness ranges from 0-900 m in thickness with maximums occurring in the Galilee region and in the Carpentaria Basin adjacent to the Gulf of Carpentaria coast (Fig. 33). Aquitard units are more spatially extensive than aquifers, extending further towards the western margin of the GAB. The aquitard sediments also extend in a narrow band up to 200 m thick over the Euroka Arch.

4.2.2.4. Known groundwater occurrence: surface springs and groundwater wells

In the study area, there are 303 actively discharging springs. Over 80% of these springs occur as surficial expressions of the GAB near the margins of the basin and near faults and basement highs (the Euroka Arch). The other 20% of springs occur in basement blocks with minimal sedimentary cover. Many of these springs occur in the Einasleigh Uplands region of the Georgetown Block and in the Charters Towers region (Fig. 34).

The GABLOG database contains 1234 wells that intersect aquifers in the study area. These wells delineate the lateral extent of the GAB as modelled in the Welsh (2000) GABFLOW study. A cluster of 1960s wells northwest of Croydon are the exception in that they lie beyond the extent of the GAB. However, the cluster does fall on a subtle sedimentary high visible in the sediment thickness dataset.

This area was beyond the spatial extent of the GABFLOW model as poor data quality to the north east of the Gilbert River was excluded from the model (Welsh, 2000). Figure 35 displays the distribution of the GABLOG wells.

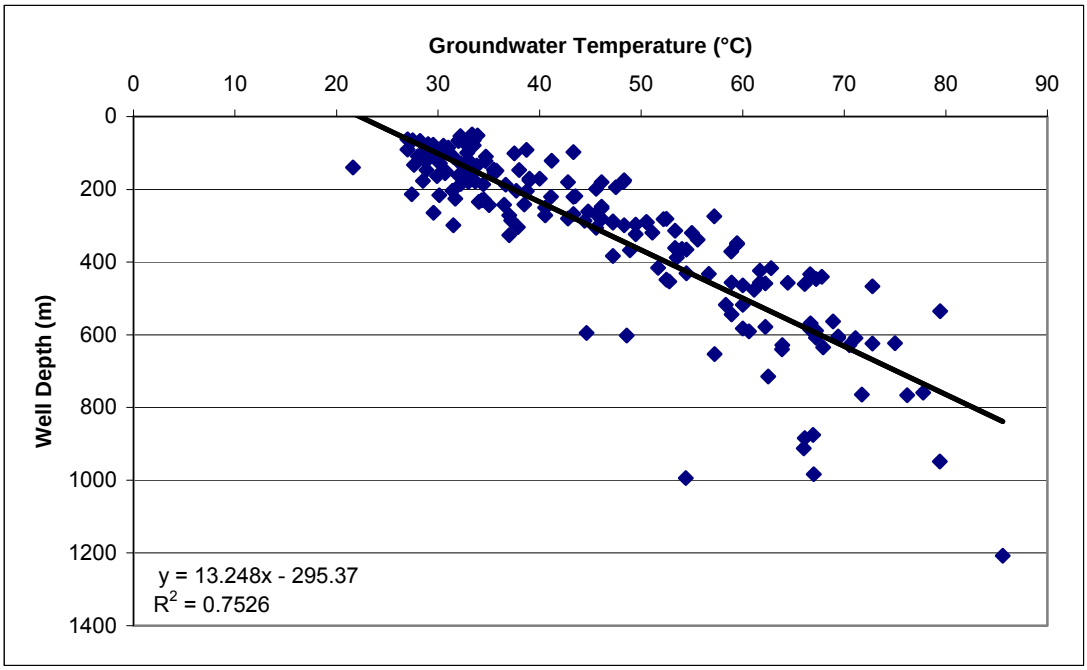

Figure 31: *Well depth (m) vs. measured groundwater temperature (°C) in the north Queensland energy assessment study area.*

Table 13: *Breakdown of total aquifer thickness by depth and area covered in the north Queensland energy assessment study area. Area % is calculated as the percentage of the total study area covered by a given aquifer thickness interval.*

Aquifer Thickness Interval (m)	Area (m^2)	Area %
0-100	92320	21.4
100-200	53820	12.5
200-300	28570	6.6
300-400	18734	4.3
400-500	9798	2.3
500-600	6635	1.5
600-700	4247	1.0
700-800	651	0.2%

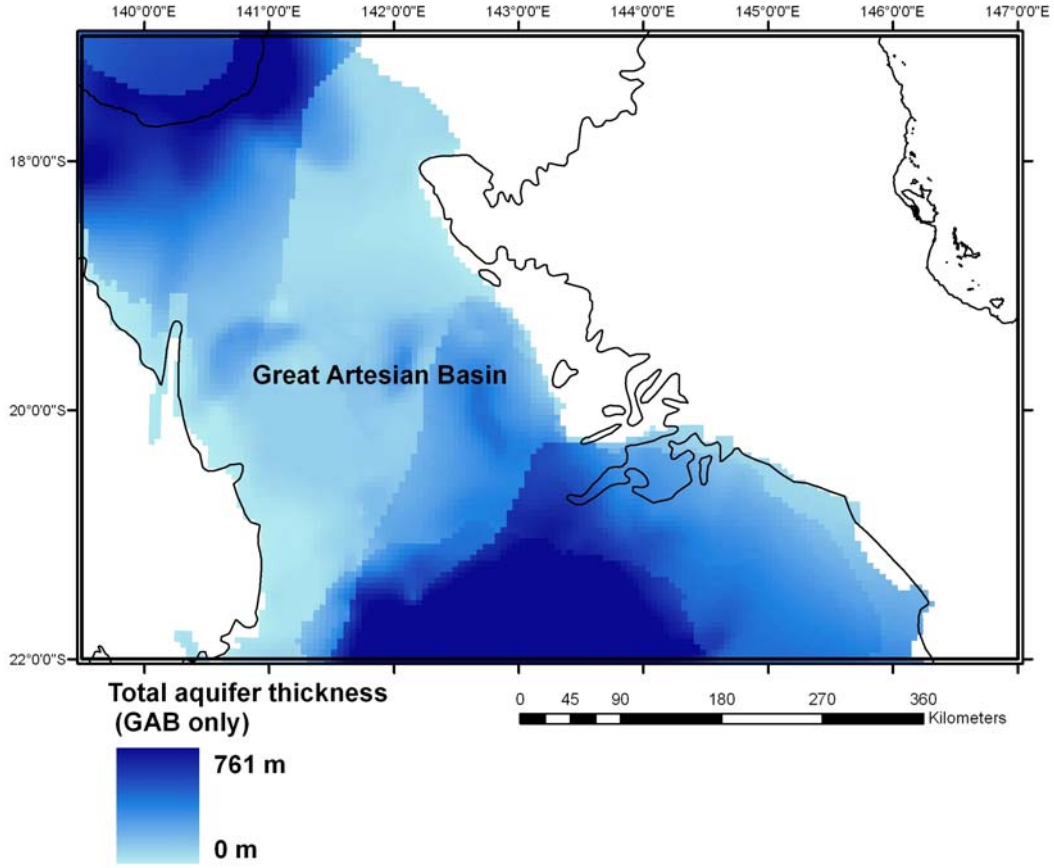

Figure 32: *Aquifer thickness in the north Queensland Energy Assessment study area. The thickest aquifer units occur in the central Eromanga Basin and under the Galilee Basin in the south, and in the Carpentaria Basin/underlying Georgina Basin area.*

4.2.2.5. Potential for HSA resources beneath the GAB

As sediments are a key requirement for HSA geothermal systems, sediment thickness gives an indication of the areas that may be prospective for HSA geothermal resources. While much of the focus of this study is on sediments within the GAB, sediments beneath the GAB may also host HSA systems. Maximum sediment thicknesses occur in three main sediment centres (cf. Fig. 26): the thickest sediments are found in the Drummond Basin region (>10 000 m), while in the Carpentaria/Georgina Basin area, sediments reach 6450 m in thickness and sediments in the Millungera Basin are modelled to reach ~6500 m (Kirkby et al., unpub. data). The areas occupied by each classification category of sediment thickness are compiled in Table 14.

4.2.3. HSA Potential Analysis: Results & Interpretation for north Queensland

The final HSA GIS ranking image highlights areas of greatest and least potential for HSA exploration (Plate 9). The GIS assessment was clipped to the sediment thickness dataset, as by definition, HSA resources are located only in sediments. Areas of known HSA potential correspond to the GAB as discussed in Section 4.2.2, and this pattern is apparent in the GIS assessment of HSA potential. It worth noting that while the greatest known and predicted temperatures are located in some of the deepest areas of the GAB, the highest water temperatures do not necessarily occur in the deepest reaches of the basin – groundwater convection and advection disturb the simplistic increasing groundwater temperature with depth relationship, causing seemingly anomalous

groundwater temperature distributions. This constant movement of fluid also makes it difficult to assume all water in the basin has reached equilibrium with the surrounding rock, thus it may be unrealistic to expect water temperatures to reach the high temperatures predicted/measured for the surrounding rock (e.g. AUSTHERM07).

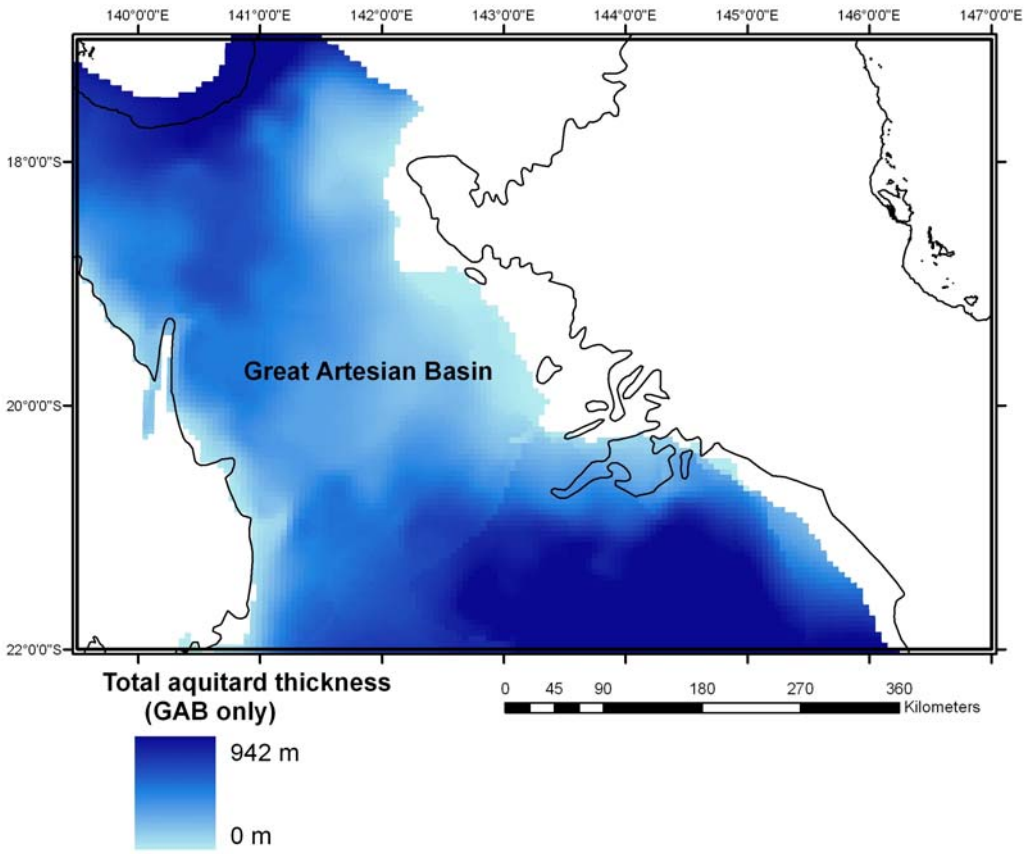

Figure 33: *Distribution of aquitards in the north Queensland Energy Assessment study area. Non-hydraulically conductive sediments are more widespread than the aquifers illustrated in Figure 32.*

Areas of highest potential correspond to greatest aquifer thickness, greatest sediment thickness, highest predicted temperature at depth (AUSTHERM07), and in localised areas, known high water temperatures. These include a small region under the Eromanga Basin on the extreme southern edge of the study area and a small area in the northern Carpentaria Basin/Georgina Basin overlap area (Plate 9). Other areas of highest potential also occur near these two anomalies in the vicinity of high temperature water wells.

While the areas with greatest potential are of limited spatial extent, the high potential area spanning the Galilee and Eromanga region border is more widespread. This anomaly occurs where maximum values for aquifer thickness, predicted temperature at depth (AUSTHERM07) and moderate values for sediment thickness occur. There are wells in this area that produce hot fluid in the 66 – 85 °C range. Moderate HSA potential polygons cover a significant portion of the study area, encompassing most of the Galilee, Drummond, and Millungera basins and smaller areas in the northern Carpentaria Basin near the coast, and in the Georgina/Carpentaria Basin overlap region.

This study has also delineated areas of very low HSA potential. HSA potential cannot exist where there are no sediments, and in the absence of other contributing factors (especially a heat source) only low potential can exist where sediments are very thin. The eastern regions (Georgetown, Charters Towers, Cairns, and Clarke River blocks) and Mt Isa in the west are basement dominated

blocks with very thin sediment cover –these regions all show low overall HSA potential. Of these areas, Clarke River exhibits the most potential with sediments up to 1500 m thick and some felsic intrusives nearby. Charters Towers and Mt Isa show localised potential in the vicinity of high-heat-producing felsic intrusives, but the overlying sedimentary cover is very thin (<500 m).

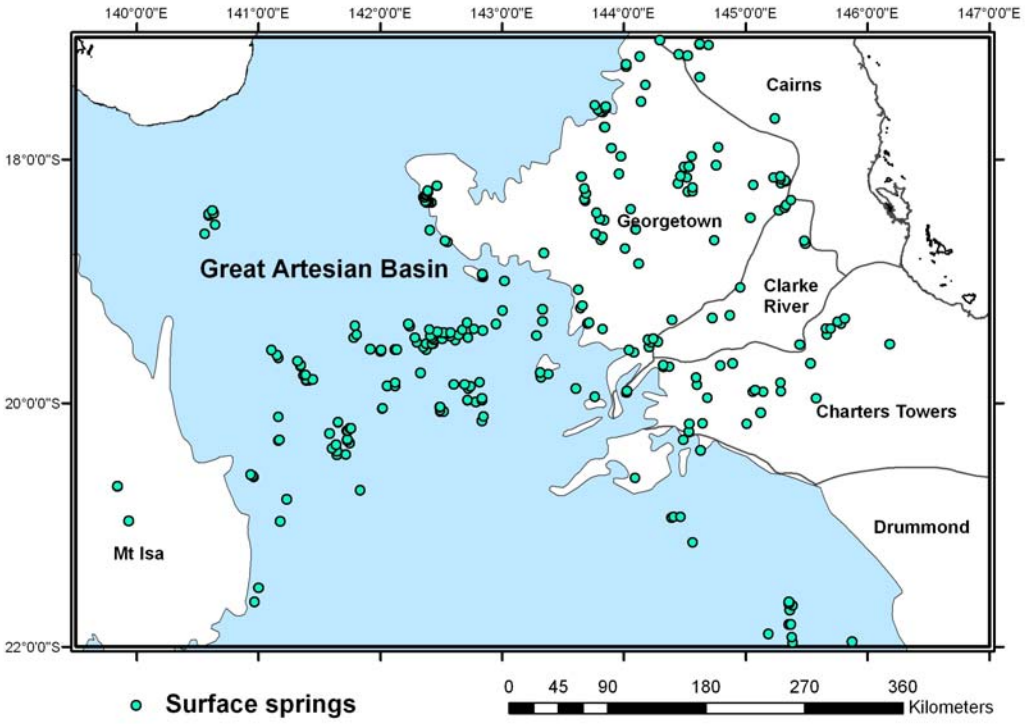

Figure 34*: Discharging surface springs in the north Queensland project area*

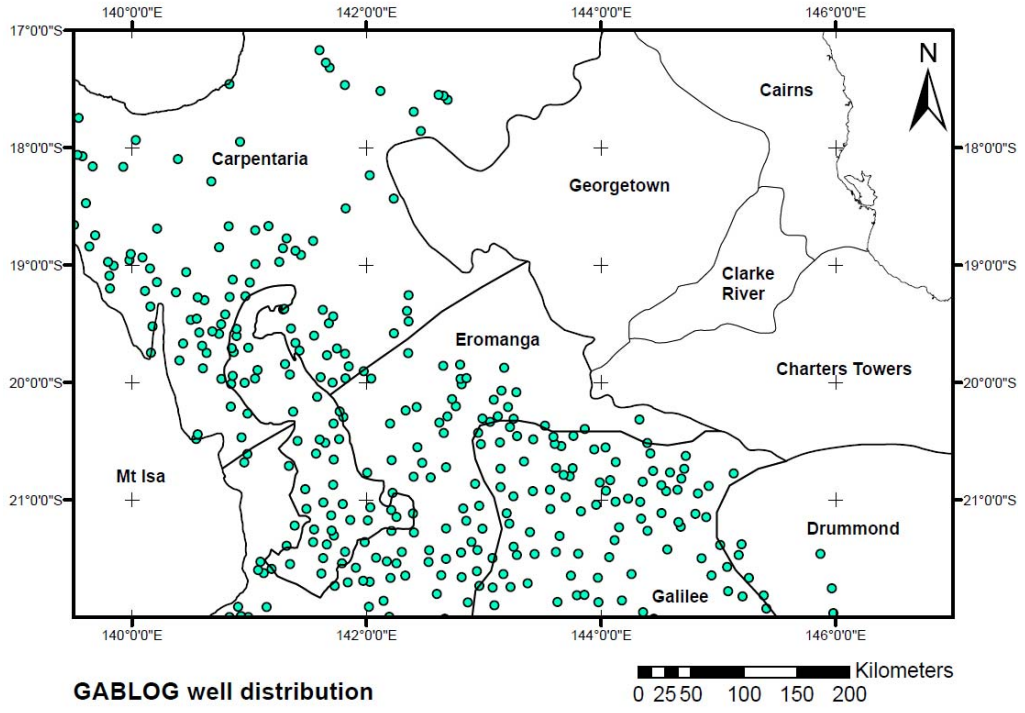

Figure 35*: Known groundwater occurrence – distribution of GABLOG wells*

Table 14: *Breakdown of sediment thickness by area in the north Queensland Energy Assessment study area. Area % is calculated as area in m^2 in given depth interval as a percentage of study area covered by sediments.*

Depth Interval (m)	Area (m^2)	Area %
0-1000	20299	64%
1000-2000	42993	13%
2000-3000	23632	7%
3000-4000	22723	7%
4000-5000	11433	4%
5000-6000	15850	5%

5. Synthesis and conclusions

The uranium and geothermal energy potential of north Queensland has been assessed using a geosystems approach. Four types of uranium mineral systems are known to have produced significant uranium-bearing deposits in north Queensland: (1) unconformity-related deposits (Westmoreland, Maureen and Ben Lomond), (2) metasomatic deposits (Mount Isa uranium field), (3) uranium-bearing iron oxide copper-gold deposits, and (4) magmatic-hydrothermal deposits (Mary Kathleeen). In addition, sandstone-hosted uranium mineral systems may have produced uranium accumulations in the Mesozoic to Cenozoic Eromanga and Carpentaria basins based on analogies with the Frome Embayment in South Australia. Based on the characteristics of known deposits and the geology of north Queensland, a modified pmd*CRC five-questions approach to mineral system analysis was used to identify areas considered to have potential for uranium mineralisation.

Although there are no known sandstone-hosted deposits in north Queensland, anomalous uranium values have been recorded associated with the organic-rich Toolebuc Formation, confirming the potential of the Eromanga-Carpentaria basin system for these types of deposits. Potential in this basin system was assessed based on (1) the distribution of uranium-rich source rocks in the hinterlands to the basin system from radiometric data, (2) evidence of uranium deposition in the basin system from radiometric and down-hole gamma logging data, (3) pH and redox gradients within the basin as determined from water chemistry, (4) the distribution of organic-rich units, and (5) the distribution of paleochannels. Using these criteria, three areas were identified as having significant potential for sandstone-hosted deposits (Plates 1 and 2): (A) an area east of Cloncurry, (B) an area 90 km north of Hughenden, and (C) an area around the township of Richmond.

~1640 Ma uranium deposits in the Westmoreland district and late Paleozoic deposits at Maureen and Ben Lomond are interpreted as unconformity-related deposits. In north Queensland, this style of deposit appears to be mostly localised in siliciclastic sedimentary rocks and associated mafic intrusions and felsic volcanic rocks above unconformities with older rocks. A synthesis of known deposits and mineral system characteristics, combined with the availability of data sets, led to the following characteristics being used by potential analysis: (1) distribution of unconformities, (2) distribution of fluid sources and potential depositional sites, (3) uranium source regions in basement to the basins as determined from radiometric data, (4) the distribution of potential fluid conduits, (5) evidence of fluid flow, as indicated by zones of demagnetisation in aeromagnetic data and by zones of sericite and kaolinite alteration identified from Aster data, (6) distribution of mafic potential depositional sites from national-scale geologic maps, and (7) evidence of uranium deposition from radiometric data. Using these criteria, the following areas were identified as having significant potential for unconformity-related uranium deposits (Plate 3): (A) the Westmoreland region, (B) the Leichhardt River Fault Trough, (C) the Esmeralda Supersuite, (D) the Paleozoic magmatic belt southwest of Cairns including the Georgetown region, (E) the Eastern Charters Towers Region, and (F) the Western Charters Towers Region.

~1540 Ma uranium deposits in the Mount Isa uranium field, including the Valhalla deposit, are interpreted to be metasomatic deposits related to inversion of the Leichhardt River Fault Trough. A synthesis of known deposits and mineral system characteristics, in combination with the availability of data sets led to the following characteristics being used for potential analysis: (1) metamorphic grade and gradients in metamorphic grade, (2) distribution of inferred fluid sources, (3) distribution of uranium source rocks using radiometric data and whole rock geochemical data, (4) fluid pathways as identified by basin-margin faults, syn-ore faults and regional calcite-albite-hematite alteration

assemblages, (5) distribution of mafic potential depositional sites from national-scale geologic maps, (6) distribution of vanadium deposits, which indicate redox gradients, and (7) uranium deposition as indicated from radiometric data. Based on these criteria, the following areas were identified as having high potential for metasomatic uranium deposits (Plate 4): (A) the Mount Isa uranium field, (B) the extension of Mount Isa uranium field to the south, (C) the eastern margin of Leichhardt River Fault Trough, (D) the Mary Kathleen area, (E) aureoles associated with Naruku Suite Plutons, (F) the Westmoreland area, (G) a 50 km wide by 200 km long, northwest trending belt southwest of Cairns, and (H) the Croydon area, particularly in association with the Esmerelda Suite.

The ~1520 Ma iron-oxide copper-gold deposits in the Cloncurry district contain significant, though sub-economic, concentrations of uranium. Synthesis of the characteristics of these deposits, including an assessment of limited uranium assay data, suggests that uranium is not directly associated with copper and gold in these systems. Rather, the highest uranium grades occur outside of mineralised zones defined by copper and gold, and there are a number of uranium-dominant prospects (e.g. U2 and Amethyst Castle). This suggests that although there may be a broad spatial association of uranium with copper and gold in these systems, in detail uranium may be separated from copper and gold. Based on this analysis, existing understandings of uranium-rich iron-oxide copper-gold systems in the Olympic Dam metallogenic province, and the availability of data sets, the following characteristics were used for potential analysis: (1) extent of major terrane boundaries as determined from seismic, magnetotelluric, gravity and aeromagnetic data, (2) distribution of A-type and high temperature I-type granites, (3) distribution of peralkaline and bimodal magmatic suites, (4) extent of felsic volcanic rocks, (5) distribution of U-rich igneous rocks as determined from whole-rock geochemical data, (6) distribution of F_2 faults, (7) distribution of magnetite and hematite-sulphide alteration assemblages as determined from inversion of gravity and aeromagnetic data, and (8) uranium deposition as indicated from radiometric data. Based on these criteria the following areas were identified as having high potential for uranium-rich iron-oxide copper-gold deposits: (A) undercover extension of the Cloncurry iron oxide copper-gold district to the north, (B) undercover extension of the Cloncurry iron-oxide copper-gold district to the south, (C) an northwest trending belt to the south of Georgetown, and (D) a 50 km wide by 200 km long, northwest trending belt southwest of Cairns.

Although orthomagmatic uranium deposits are not known in Australia, north Queensland is considered to have many of the geologic features associated with both the Rössing and Ross Adams types of deposits. Based on descriptions of these deposits, in particular the Ross Adams deposits, the following characteristics, mostly based on whole-rock geochemical data were considered for mineral potential analysis: (1) the distribution of felsic igneous rocks, with emphasis on uranium-rich suites, high-temperatures suites and A-type suites, (2) evidence of magmatic fractionation, (3) fluorine-rich melts, (4) peralkaline melt composition, (5) emplacement of magmas at high crustal level from geological data, (6) availability of uranium for leaching from geological data, and (7) evidence of uranium enrichment within individual granite bodies. Based on these criteria the following areas were identified as have high potential for orthomagmatic uranium deposits: (A) Paleozoic volcanic rocks west of Cairns, (B) Paleozoic intrusives and volcanics scattered around the Georgetown Region, and (C) The Mount Isa Inlier.

Based on analysis of available data, the Mary Kathleen deposit is interpreted as a skarn deposit associated with the ~1730 Ma Burstall Granite that was remobilised during later fluid flow associated with deformation at ~1550 Ma. Based on this interpretation, and on dataset availability, the following characteristics were used for potential analysis: (1) distribution of Wonga-Burstall Suite-aged and other U-rich granite suites, which are interpreted as the primary source of uranium, (2) distribution of inferred contact aureoles around these granites, (3) distribution of F_3 faults, (4) distribution of amphibolite facies metamorphism, (5) distribution of albitic alteration assemblages as determined by Th/K ratios determined from radiometric data, and (6) distribution of carbonate rocks

predating granite emplacement. Based on these criteria, the following areas were identified as having potential for magmatic-hydrothermal uranium deposits: (A) along the strike length of Wonga-Burstall Suite granites, (B) along the margins of the Sybella Suite, (C) the eastern margin of the Ewen Granite, and (D) along the western margin of the Kalkadoon Granodiorite.

Uranium potential analysis has identified areas of known mineral occurrences as well as areas or potential without known uranium occurrences. Some of the new areas are extensions of known districts under cover or along geological elements thought to control mineralisation. In several cases potential analysis using different mineral system models identified similar areas. Examples of this include the Westmoreland area, which was identified using both the unconformity-related and metasomatic models, the Mary Kathleen area and eastern margin of the Sybella Granite were identified by the magmatic-related, the unconformity-related and metasomatic models, and the northwest trending belt to the southwest of Cairns was identified using the iron-oxide copper-gold-uranium, orthomagmatic and the metasomatic models. These areas, along with extensions of known uranium districts are considered to have highest likelihood of hosting additional or new uranium resources.

A systems approach has also been applied to assess geothermal potential of north Queensland. Although no geothermal systems have yet been commercially developed in north Queensland, theoretical considerations and analogies with known systems in South Australia and elsewhere were used to identify essential elements for geothermal systems. Two types of geothermal systems were considered in the analysis: Hot Rock and Hot Sedimentary Aquifer. For Hot Rock systems, the following characteristics were used to assess geothermal potential: (1) predicted temperature at 5 km depth, from the AUSTHERM07 dataset, (2) estimated heat generation potential derived from whole-rock geochemistry and then extended undercover using solid geology maps and geophysical data, (3) estimated thermal resistance based on inferred lithological characteristics of basins and the thermal conductivity of different rock types, and (4) estimated thickness of sedimentary basins based on OZSEEBASE and other datasets. From this analysis, the highest Hot Rock geothermal potential was identified in the: (A) Millungera Basin, (B) the top northwest section of the Carpentaria Basin, near Burketown, (C) the north-central Drummond Basin, and (D) the Galilee Basin.

With the exception of thermal resistance of sedimentary basins, all datasets used in the analysis of Hot Rock systems were also used for Hot Sedimentary Aquifer systems. As potential for this analysis was concentrated on the Great Artesian Basin (i.e. the combined Eromanga and Carpentaria basins), this analysis used the following datasets in addition to those used in the Hot Rock potential analysis: (1) the thickness of aquifers in the Great Artesian Basin, and (2) water temperature within Great Artesian Basin aquifers. Based on this analysis, the greatest Hot Sedimentary Aquifer geothermal potential was identified in the: (A) Eromanga Basin, (B) the northern part of the Carpentaria Basin, near Burketown and Normanton, (C) the north-central Drummond Basin, and (D) the Galilee Basin.

Like some of the uranium systems, the GIS-based approach to identifying areas with Hot Rock and Hot Sedimentary Aquifer potential has delineated similar geographic areas that appear to have high potential for these types of geothermal resources. The highest potential is in the very northwest part of the Carpentaria Basin, near Burketown, with high potential also associated with the Millungera, Drummond and Galilee basins.

Acknowledgements. This record benefited from reviews by Andy Barnicoat, Richard Blewett, Anthony Budd and Laurie Hutton.

References

Ahmad, M. and Wygralak, A.S. 1990. Murphy Inlier and environs; regional geology and mineralisation. In: Hughes, F.E. (ed.) Geology of the mineral deposits of Australia and Papua New Guinea. Monograph Series - Australasian Institute of Mining and Metallurgy 14, 819-826.

Bain, J.H.C. 1977. Uranium mineralisation associated with late Palaeozoic acid magmatism in northeast Queensland. Bureau of Mineral Resources Journal of Geology and Geophysics 1, 137-147.

Bain, J.H.C. and Draper, J.J. (eds) 1997. North Queensland Geology. Bulletin of the Australian Geological Survey Organisation 240, and Queensland Department of Mines and Energy Geology 9, 600pp.

Bain, J.H.C., Withnall, I.W. and Black, L.P. 1984. Some aspects of the geology and geochronology of gold mineralization in the Georgetown region, Queensland, Australia. Geological Society of Australia Abstracts 12, 44.

Bain, J.H.C., Heinrich, C.A. and Henderson, G.A.M. 1992. Stratigraphy, structure and metasomatism of the Haslington Group, East Moondarra area, Mount Isa: a deformed and mineralised Proterozoic multi-stage rift-sag sequence. In: Stewart, A.J. and Blake, D.H. (eds) Detailed Studies of the Mount Isa Inlier. AGSO Bulletin 243, 125-136.

Barker, C. 1996. Thermal modelling of petroleum generation: theory and applications. Amsterdam: Elsevier Science B.V.

Barnicoat, A. 2008. The Mineral Systems approach of the pmd*CRC. Geoscience Australia Record 2008/09, 1-6.

Basson, I.J. and Greenway, G., 2004. The Rössing uranium deposit: a product of late-kinematic localization of uriniferous granites in the Central Zone of the Damara Orogen, Namibia. Journal of African Earth Sciences 38, 413-435.

Bastrakov, E.N., Skirrow, R.G. and Davidson, G.J. 2007. Fluids in sub-economic Fe-oxide Cu-Au systems of the Olympic Cu-Au-(U) province. Economic Geology 102, 1415-1440.

Beach, R.D.W., Jones, R.W. and Majorowicz, J.A. 1987. Heat flow and heat generation estimates for the Churchill Basement of the Western Canadian Basin in Alberta, Canada. Geothermics 16, 1-16.

Beardsmore, G.R. 1996. The thermal history of the Browse Basin and its implications for petroleum exploration. PhD dissertation, Monash University, Victoria, Australia.

Beardsmore, G.R. and Cull, J.P. 2001. Crustal heat flow: a guide to measurement and modelling. Cambridge University Press, 324p.

Beardsmore, T.J., Newbery, S.P. and Laing, W.P. 1988. The Maronan Supergroup: an inferred early volcano-sedimentary rift sequence in the Mount Isa Inlier, and its implications for ensialic rifting in the Middle Proterozoic of northwest Queensland. Precambrian Research 40/41, 487-507.

Berning, J., Cooke, R., Hiemstra, S.A. and Hoffman, U. 1976. The Rössing uranium deposit, south west Africa. Economic Geology 71, 351-368.

Betts, P.G. and Giles, D. 2006. The 1800-1100 Ma tectonic evolution of Australia. Precambrian Research 144, 92-125.

Bierlein, F.P. Black, L.P. Hergt, J. and Mark, G. 2008. Evolution of pre-1.8 Ga basement rocks in the western Mt Isa Inlier, northeastern Australia; insights from SHRIMP U/Pb dating and in situ Lu-Hf analysis of zircons. Precambrian Research 163, 159-173.

Black, L.P. and McCulloch, M.T. 1990. Isotopic evidence for the dependence of recurrent felsic magmatism on new crust formation; an example from the Georgetown region of northeastern Australia. Geochimica et Cosmochimica Acta 54, 183-196.

Black, L.P., Gregory, P., Withnall, I.W. and Bain, J.H.C. 1998. U–Pb zircon age for the Etheridge Group, Georgetown region, north Queensland: implications for relationship with the Broken Hill and Mt Isa sequences. Australian Journal of Earth Sciences 45, 925-935.

Black, L.P., Withnall, I.W., Gregory, P., Oversby, B.S. and Bain, J.H.C. 2005. U-Pb zircon ages from leucogneiss in the Etheridge Group and their significance for the early history of the Georgetown region, north Queensland. Australian Journal of Earth Sciences 52, 385-401.

Blackwell, D.D. and Steele, J.L. 1989. Thermal conductivity of sedimentary rocks: measurement and significance. In: Neaser, N.D. and McCulloh, T.H. (eds.) Thermal history of sedimentary basins: methods and case histories. New York: Springer-Verlag.

Brooks, J.H. 1975. Uranium in the Mount Isa/Cloncurry District. Australasian Institute of Mining and Metallurgy Monograph Series 5, 396-397.

Budd, A.R., Wyborn, L.A.I. and Bastrakova, I.V. 2001. The metallogenic potential of Australian Proterozoic granites. Geoscience Australia Record 2001/12

Budd, A.R. 2007. Australian radiogenic granite and sedimentary basin geothermal hot rock potential map (preliminary edition), 1:5 000 000 scale. Geoscience Australia, Canberra.

Carr, G.R. and Sun, S.-S. 1997. Lead isotope ratios of magmatic and hydrothermal activity. In: Bain, J.H.C. and Draper, J.J. (eds) North Queensland Geology. Australian Geological Survey Organisation Bulletin 240 and Queensland Department of Mines and Energy Geology 9, 442-447.

Carter, L.S., Kelly, S.A., Blackwell, D.D. and Naeser, N.D., 1998. Heat flow and thermal history of the Anadarko Basin, Oklahoma. American Association of Petroleum Geologists Bulletin 82, 291–316

Chopping, R., Henson, P., Meixner, T., Roy, I.G. and Milligan, P. 2009. Use of potential field data sets to support the North Queensland seismic interpretations. Australian Institute of Geoscientists Bulletin 49, 143-148.

Chopra, P.N. and Holgate, F. 2005. A GIS analysis of temperature in the Australian crust, Proceedings of the World Geothermal Congress, Anatalya, Turkey, 1-7.

Clarke, J.S.P. 1966. Handbook of physical constants. Geological Society of America Monograph 97.

Connors, K.A. and Page, R.W. 1995. Relationships between magmatism, metamorphism and deformation in the western Mount Isa Inlier, Australia. Precambrian Research 71, 131-153.

Cotton, T.B., Scardigno, M.F. and Hibburt, J.E., Eds. 2006. The petroleum geology of South Australia. Vol. 2: Eromanga Basin. 2nd edn. South Australia. Department of Primary Industries and Resources. Petroleum Geology of South Australia Series.

Cuney, M., 1980. Preliminary results on the petrology and fluid inclusions of the Rössing uraniferous alaskites. Transactions of the Geological Society of South Africa, 83, 39-45.

Cuney, M. and Kyser, K. (eds) 2009. Recent and not-so-recent developments in uranium deposits and implications for exploration. Mineralogical Association of Canada Short Course Notes 39.

Cuney, M., Brouand, M., Cathelineau, M., Derome, D., Frieberger, R., Hecht, L., Kister, P., Lobaev, V., Lorilleux, G., Peiffert, C., and Bastoul, A.M., 2003. What parameters control the high-grade – large tonnage of the Proterozoic unconformity related uranium deposits? Proceedings of Uranium Geochemistry 2003, Nancy, France, April 2003, 123-126.

Czarnota, K., Blewett, R.S., Goscombe, B. and Brennan, T. 2008. Scale 2: district analysis – how to identify the location of major mineral camps (60 km × 60 km are selection). Project Y4 final report – parts I and II January 2005 - July 2008. Concepts to targets: a scale-integrated mineral systems study of the Eastern Yilgarn Craton. Unpublished pmd*CRC report, 41-87.

Davis, M.G., Chapman, D.S., Van Wagoner, T.M. and Armstrong, P.A. 2007. Thermal conductivity anisotropy of metasedimentary and igneous rocks, Journal of Geophysical Research 112, B05216.

Denaro, T.J. Withnall, I.W. Bain, J.H.C. and Mackenzie, D.E. 1997. Mineral resource assessment, Georgetown-Croydon area. Queensland Minerals and Energy Review Series 1997, 228pp.

Derome, D., Cathelineau, M., Cuney, M., Fabre, C. and Lhomme, T. 2005. Mixing of sodic and calcic brines and uranium deposition at McArthur River, Saskatchewan, Canada: a Raman and laser-induced breakdown spectroscopic study of fluid inclusions. Economic Geology 100, 1529-1545.

Dickson, B.L. and Ramsden, A.R.; 1986. Significance of the Toolebuc gamma ray anomaly in the search for and evaluation of oil shale in the Eromanga Basin. Australian Journal of Earth Sciences 33,429-441.

Eggers, A.J. 1999. The Valhalla Uranium Project Northwest Queensland, an update. Australian Uranium Summit, extended abstracts, March 29–30 1999, Rydges Plaza Hotel, Darwin, Northern Territory, Australia, 22.

Evins, P.M. Wilde, A.R. Foster, D.R.W. McKnight, S.W. and Blenkinsop, T.G. 2007. Significance of monazite EPMA ages from the Quamby Conglomerate, Queensland. Australian Journal of Earth Sciences 54, 19-26.

Fensham, R.J. and Fairfax, R.J. 2006. 'Springs of Queensland 2006'. Queensland Herbarium, Environmental Protection Agency (https://www.epa.qld.gov.au/nature_conservation/habitats/wetlands/springs/).

Fortowski, D.B. and McCracken, S.J.A. 1998. Australian Resources, Mount Isa, Queensland, Australia. Australasian Institute of Mining and Metallurgy Monograph 22, 775-782.

Foster, D.R.W. and Rubenach, M.J. 2006. Isograd patterns and regional low-pressure, high-temperature metamorphism of pelitic, mafic and calc-silicate rocks along an east–west section through the Mt Isa Inlier. Australian Journal of Earth Sciences 53, 167-186.

FrOGTech, Pty. Ltd. 2006. OZ SEEBASE™ Proterozoic Basins Study. Unpublished report to Geoscience Australia.

Funnell, R., Chapman, D., Allis, R. and Armstrong, P. 1996. Thermal state of the Taranaki Basin, New Zealand. Journal of Geophysical Research 101, 25197-25215.

Gallardo, J. and Blackwell, D.D. 1999. Thermal structure of the Anadarko Basin. American Association of Petroleum Geologists Bulletin, 83, 333-361.

Galson, D.A., Wilson, N.P., Scharli, U. and Rybach. L. 1987. A comparison of the divided-bar and QTM methods of measuring thermal conductivity. Geothermics 16, 215-226.

Garland, G.D. and Lennox, D.H. 1962. Heat flow in Western Canada. Geophysical Journal 6, 245-262.

Garrett, S.J.M. 1992. The geology and geochemistry of the Mount Elliott copper-gold deposit, northwest Queensland. Unpublished MSc thesis, University of Tasmania.

Gibson, G.M., Rubenach, M.J., Neumann, N.L., Southgate, P.N. and Hutton, L.J. 2008. Syn- and post-extensional tectonic activity in the Paleoproterozoic sequences of Broken Hill and Mount Isa and its bearing on reconstructions of Rodinia. Precambrian Research 166, 350-369.

Giles, D. and Nutman, A.P. 2002. SHRIMP U-Pb monazite dating of a ca 1600–1580 Ma amphibolite facies metamorphism in the southeastern Mt Isa Block, Australia. Australian Journal of Earth Sciences 49, 455-465.

Glikson, M., Chappell, B.W., Freeman, R.S. and Webber, E., 1985. Trace elements in oil shales, their source and organic association with particular reference to Australian deposits, Chemical Geology 53, 155-174.

Gravestock, D.I., More, P.S. and Pitt, G.M. 1986. Contributions to the geology and hydrocarbon potential of the Eromanga Basin. Geological Society of Australia Special Publication 12, 184 pp

Gregory, M.J., Wilde, A.R. and Jones, P.A. 2005. Uranium deposits of the Mount Isa region and their relationship to deformation, metamorphism, and copper deposition. Economic Geology 100, 537-546

Gurnis, M., Müller, R.D. and Moresi, L. 1998. Cretaceous vertical motion of Australia and the Australian-Antarctic discordance. Science 279, 1499-1504.

Habermehl, M.A. 2001. Wire-line logged waterbores in the Great Artesian Basin. Digital data of logs and waterbore data acquired by AGSO. Bureau of Rural Sciences, Canberra.

Hand, M. and Rubatto, D. 2002. The scale of the thermal problem in the Mount Isa Inlier. Geological Society of Australia Abstracts 67, 173.

Hannan, K.W., Golding, S.D., Herbert, H.K., and Krouse, H.R. 1993. Contrasting alteration assemblages in metabasites from Mount Isa, Queensland; implications for copper ore genesis. Economic Geology 88, 1135-1175.

Hawkins, B. W. 1975. Mary Kathleen uranium deposit. Australasian Institute of Mining and Metallurgy Monograph 5, 398-401.

Haynes, D.W. 2000. Iron oxide copper (-gold) deposits: their position in the ore deposit spectrum and modes of origin. In: Porter, T.M. (ed.) Hydrothermal iron oxide copper-gold and related deposits: A global perspective. PGC Publishing, Adelaide, 71-90.

Haynes, D.W., Cross, K.C., Bills, R.T. and Reed, M.H. 1995. Olympic Dam ore genesis: a fluid mixing model. Economic Geology 90, 281-307.

Heinrich, C.A., Bain, J.H.C., Mernagh, T.P., Wyborn, L.I., Andrew, A.S. and Waring, C.L. 1995. Fluid and mass transfer during basalt alteration and copper mineralization at Mount Isa, Australia. Economic Geology 90, 705-730.

Henderson, R.A. and Withnall, I.W. 2009. Phanerozoic geology of north Queensland. Australian Institute of Geoscientists Bulletin 49, 135-136.

Henson, P., Blewett, R., Chopping, R., Champion, D., Korsch, R., Huston, D., Nicoll, M., Brennan, T., Roy, I., Hutton, L. and Withnall, I., 2009. 3D Geological map of North Queensland. Australian Institute of Geoscientists Bulletin 49, 175-180.

Hitzman, M.W. and Valenta, R.K. 2005. Uranium in iron oxide-copper-gold (IOCG) systems. Economic Geology 100, 1657-1661.

Hoeve, J., Sibbald, T. I. I., Ramakers, P. and Lewry, J. F., 1980. Athabasca Basin unconformity-type uranium: a special type of sandstone-type deposits? In: Furguson, J. and Goleby, A.B. (eds) Uranium in the Pine Creek Geosyncline. International Atomic Energy Agency, Vienna 575-594.

Holcombe, R.J., Pearson, P.J. and Oliver, N.H.S. 1991. Geometry of a Middle Proterozoic extension decollement in northern Australia. Tectonophysics 191, 255-274.

Horai, K. and Susaki, J., 1989. The effect of pressure on the thermal conductivity of silicate rocks up to 12 kbar. Physics of the Earth and Plantary Interiors 55, 292-305.

Hurtig, N., 2008. Maureen, a Palaeozoic unconformity-related U-Mo-F deposit, Queensland, Australia. Unpublished M.Sc. thesis, ETH Zurich.

Hurtig, E. and Schlosser, P. 1979a. Geothermal studies in the GDR and relations to the geological structure. In: Adam, A. (ed) Geoelectric and geothermal studies. KAPG Geophysical Monograph . Budapest, Akademiai Kiado, 384-394.

Hurtig, E. & Schlosser, P. 1979b. Vertical changes of heat flow in boreholes in the north German sedimentary basin. In: Adam, A. (ed) Geoelectric and geothermal studies. KAPG Geophysical Monograph . Budapest, Akademiai Kiado, 395-401.

Huston, D.L., Blewett, R.S., Champion, D.C., Henson, P.A., Korsch, R.J., Roy, I.G., Hutton, L.J. and Withnall, I.W. 2009. Links between geodynamic evolution and energy and mineral potential in North Queensland. Australian Institute of Geoscientists Bulletin 49, 185-190.

Hutton, L.J. and Sweet, I.P. 1982. Geological evolution, tectonic style and economic potential of the Lawn Hill Platform cover, northwest Queensland. Journal of Australian Geology and Geophysics 7, 125-134.

Hutton, L. J., Draper, J.J., Rienks, I.P., Withnall, I.W. and Knutson, J. 1997. Charters Towers region. In: Bain, J.H.C. and Draper, J.J. (eds) North Queensland Geology. Australian Geological

Survey Organisation Bulletin 240 and Queensland Department of Mines and Energy Geology 9, 165-224.

Hutton, L.J., Gibson, G.M., Kosrch, R.J., Withnall, I.W., Henson, P.A., Costelloe, R.D., Holzschuh, J., Huston, D.L., Jones, L.E.A., Maher, J.L., Nakamura, A., Nicoll, M.G., Roy, I., Saygin, E., Murphy, F.B. and Jupp, B. 2009. Geological interpretation of the 2006 Mt Isa seismic survey. Australian Institute of Geoscientists Bulletin 49, 137-141.

IAEA 2009. World distribution of uranium deposits (UDEPO) with uranium deposit classification. International Atomic Energy Agency Technical Document 1629, 117 p.

Jackson, M.J., Scott, D.L. and Rawlings, D.J. 2000. Stratigraphic framework for the Leichhardt and Calvert Superbasins: review and correlations of the pre-1700 Ma successions between Mt Isa and McArthur River. Australian Journal of Earth Sciences 47, 381-404.

Jaireth, S., Mckay, A., Lambert, I. 2008. Association of large sandstone uranium deposits with hydrocarbons. AusGeo News 89:8-12

Johnson, J.D., and Wall, V.J. 1984. Why unconformity-related U deposits are unconformity related. Geological Society of Australia Abstracts 12, 285-287.

Jones, D.G. 2006. Technical report for Mega Uranium Ltd. On the Georgetown Project (Maureen Deposit), North Queensland, Australia. Unpublished Technical Report for Mega Uranium Ltd., 47 p.

Joplin, G.A. 1963. Chemical analyses of Australian rocks. Pt I: Igneous and metamorphic rocks. Bureau of Mineral Resources, Australia. Bulletin 65 p1-446.

Kinnaird, J.A. and Nex, P.A.M. 2007. A review of geological controls on uranium mineralisation in sheeted leucogranites within the Damara Orogen, Namibia. Transactions of the Institute of Mining and Metallurgy, Applied Earth Science B116, 68-85

Korsch, R.J., Withnall, I.W., Hutton, L.J., Henson, P.A., Blewett, R.S., Huston, D.L., Champion, D.C., Meixner, A.J., Nicoll, M.G. and Nakamura, A. 2009. Geological interpretation of the deep seismic reflection line 07GA-IG1: the Cloncurry to Croydon transect. Australian Institute of Geoscientists Bulletin 49, 153-158.

Kositcin, N., Champion, D.C. and Huston, D.L. 2009. Geodynamic Synthesis of the North Queensland Region and Implications for Metallogeny. Geoscience Australia Record 2009/30, 196 pp.

Kyser, T. K. 2007. Fluids, basin analysis, and mineral deposits. Geofluids 7, 238-257.

Lacy, W.C. 1974.view of Upper Palaeozoic metallogensis in the northern part of the Tasman Orogenic Zone. In: Denmead, A.K., Tweedale, G.W. and Wilson, A.F. (eds) The Tasmana Geosyncline -- a symposium. Geological Society of Australia, Queensland Division, 221-243.

Lally, J.H., and Bajwah, Z.U., 2006. Uranium deposits of the northern Territory, Northern Territory Geological Survey Report 20, 87 p.

Leaman, D.E. 1991. Surface gravity and magnetic responses of mineralization, Mt. Isa, Northwest Queensland, Australia. Geophysics 56, 542-549.

Lees, T. and Buckle, P. 2009. Base metal deposits in the Einasleigh area. Australian Institute of Geoscientists Bulletin 49, 75-78.

Lilley, F.E.M., Wang, L.J., Chamalaun, F.H., Ferguson, I.J. 2001. The Carpentaria Electrical Conductivity Anomaly, Queensland, as a major structure in the Australian Plate. GSAA Monograph 1, 1-16.

Lindal, B. 1973. Industrial and other applications of geothermal energy. Geothermal Energy: Review of Research and Development, LC No. 72-97138. Paris, UNESCO, 135-148

Liu, S.F. 2009. Basement Geology of Northern Queensland (First Edition), 1:1 000 000 scale, Geoscience Australia, Canberra.

Lyons, P. and Goleby, B.R. (compilers) 2005. The 2003 Gawler Craton seismic survey; notes from the seismic workshop. Geoscience Australia Record 2005/19, 81pp.

Maas, R., McCulloch, M. T., Campbell, I. H. and Page, R. W. 1987. Sm–Nd isotope systematics in uranium rare-earth element mineralisation in the Mary Kathleen mine. Economic Geology 82, 1805-1826.

Magoon, L.B. and Dow, W.G., (eds) 1994. The petroleum system – from source to trap. American Association of Petroleum Geologists Memoir 60, 655 p.

Majorowicz, J.A. and Jessop, A.M. 1981. Regional heat flow patterns in the western Canadian sedimentary basin. Tectonophysics 74, 209-238.

Mark, G., Oliver, N.H.S. and Carew, M.J. 2006. Insights into the genesis and diversity of epigenetic Cu-Au mineralisation in the Cloncurry district, Mt Isa Inlier, northwest Queensland. In: Betts, P.G. and Goleby, B.R. (eds) Mt Isa tectonics. Australian Journal of Earth Sciences 53, 109-124.

Mathison, I. and Hurtig, H.C. 2009. The Maureen U-Mo-F deposit. Australian Institute of Geoscientists Bulletin 49, 85-88.

McKay A., 2008, Uranium. In: Geoscience Australia 2008: Australia's Identified Mineral Resources 2008. Geoscience Australia, Canberra, pp 70-77

McKay, A.D. and Miezitis, Y. 2001. Australia's uranium resources, geology and development of deposits. AGSO – Geoscience Australia, Mineral Resource Report 1, 200pp.

McLaren, S., Sandiford, M., Hand, M., Neumann, N., Wyborn, L., Bastrakova, I. 2003 The hot southern continent: heat flow and heat production in Australian Proterozoic terranes IN: Hillis, R.R. and Muller, R.D. (eds.) "Evolution and Dynamics of the Australian Plate" Geological Society of Australia Special Publication and Geological Society of America Special Paper 22 : 372 p157-167

Mernagh, T.P., Heinrich, C.A., Leckie, J.F., Carville, D.P., Gilbert, D.J., Valenta, R.K. and Wyborn, L.A.I., 1994. Chemistry of low temperature hydrothermal gold, platinum, and palladium (±uranium) mineralisation at Coronation Hill, Northern Territory, Australia. Economic Geology 89, 1053-1073.

Mernagh, T.P., Wyborn, L.A.I., and Jagodzinski, E.A. 1998. Unconformity-related U±Au±platinum-group-element deposits. Australian Geological Survey Organisation Journal of Australian Geology and Geophysics 17, 197-205.

Miller, G.W., and Mortimer, G.W. 1974. Report of Investigations of the Maureen U-F-Mo Prospect, Georgetown, N. Qld. Getty Mining. GSQ Company Report 5201, 34 p.

Minty, B.R.S., Franklin, R., Milligan, P.R., Richardson, L.M., and Wilford, J., 2009. Riadiometric Map of Australia (First Edition), scale 1:5,000,000, Geoscience Australia, Canberra.

Murphy, F.C., Gessner, K., Bierlein F., and Hutton, L. 2008. Q1: What is the geodynamic setting? Project I1 final report April 2005 - July 2008. Mineral system analysis of the Mt Isa-McArthur region, northern Australia. Unpublished pmd*CRC report, 23-35.

Neumann, N.L. 2007. Time-Space evolution of the Mount Isa Inlier and southern McArthur Basin. In: Neumann, N.L. and Fraser, G.L. (eds) Geochronological synthesis and time-space plots for Proterozoic Australia. Geoscience Australia Record 2007/06, 52-73.

Neumann, N.L., Southgate, P.N., Gibson, G.M. and McIntyre, A. 2006. New SHRIMP geochronology for the Western Fold Belt of the Mount Isa inlier: developing a 1800–1650 Ma event framework. Australian Journal of Earth Sciences 53, 1023-1039.

Neumann, N.L., Southgate, P.N. and Gibson, G.M., 2009. Defining unconformities in Proterozoic sedimentary basins using detrital geochronology and basin analysis – an example from the Mount Isa Inlier, Australia. Precambrian Research 168, 149-166.

Nex, P.A.M., Kinnaird, H.A. and Oliver, G.J.H., 2001. Petrology, geochemistry and uranium mineralisation of post-collisional magmatism around Goanikontes, southern Central Zone, Damaran Orogen, Namibia. Journal of African Earth Sciences 33, 481-502.

Noorollahi, Y., Itoi, R., Fujii, H. and Tanaka, T. 2007. GIS Model for Geothermal Resources Exploration in Akita and Iwate Prefecture, northern Japan., Computer and Geosciences 33, 1008-1021.

Norden, B. and Forster, A. 2006. Thermal conductivity and radiogenic heat production of sedimentary and magmatic rocks in the Northeast German Basin. American Association of Petroleum Geologists Bulletin 90, 939-962.

OECD Nuclear Energy Agency, 2008: Uranium 2007 - Resources, Production and Demand. Organisation for Economic Cooperation and Development Publishing, Paris. 420pp.

Oliver, N.H.S. 1995. Hydrothermal history of the Mary Kathleen Fold Belt, Mt Isa Block, Queensland. Australian Journal of Earth Sciences 42, 267-280.

Oliver, N.H.S., Pearson, P.J., Holcombe, R.J., and Ord, A. 1999. Mary Kathleen metamorphic-hydrothermal uranium-rare-earth element deposit; ore genesis and numerical model of coupled deformation and fluid flow. Australian Journal of Earth Sciences 46, 467-484.

Oliver, N. H. S., Cleverley, J. S., Mark, G., Pollard, P. J., Fu, B., Marshall, L. J., Rubenach, M. J., Williams, P. J. and Baker, T. 2004. The role of sodic alteration in the genesis of iron oxide – copper – gold deposits, eastern Mt Isa Block, Australia. Economic Geology 99, 1145-1176.

O'Rourke, P.J. and Bennell, M.R. 1977. The Mount Hogan gold, silver and uranium prospect, north Queensland. Queensland Government Mining Journal 78, 424-433.

Ozimic, S. 1981. Stratigraphic drilling in the Cretaceous Toolebuc Formation in southern and Eastern Eromanga Basin, a contribution to BMR/CSIRO NERRDC project 78/2616. BMR Record 1981/012.

Page, R.W. 1983. Timing of superimposed volcanism in the Proterozoic Mount Isa Inlier, Australia. Precambrian Research 21, 223-245.

Page, R.W. and Sun, S-S. 1998. Aspects of geochronology and crustal evolution in the Eastern Fold Belt, Mt Isa Inlier. Australian Journal of Earth Sciences 45, 343-361.

Page, R.W., Jackson, M.J. and Krassay, A.A. 2000. Constraining sequence stratigraphy in north Australian basins: SHRIMP U– Pb zircon geochronology between Mt Isa and McArthur River. Australian Journal of Earth Sciences 47, 431-460.

Peiffert, C., Nguyen-Trung, C. and Cuney, M., 1996. Uranium in granitic magmas: Part 2. Experimental determination of uranium solubility and fluid-melt partition coefficients in the uranium oxide-haplogranite-H2O-NaX (X = Cl, F) system at 770^{o}C, 2 kbar. Geochimica et Cosmochimica Acta 60, 1515-1529.

Perkins, C., Heinrich, C.A. and Wyborn, L.A.I. 1999. $^{40}Ar/^{39}Ar$ Geochronology of copper mineralization and regional alteration, Mount Isa, Australia. Economic Geology 94, 23-36.

Polito, P.A., Kyser, T.K., Rheinberger, G., and Southgate, P.N. 2005. A paragenetic and isotopic study of the Proterozoic Westmoreland uranium deposits, southern McArthur basin, northern Territory, Australia. Economic Geology 100, 1243-1260.

Polito, P.A. Kyser, T.K and Stanley, C. 2009. The Proterozoic, albitite-hosted, Valhalla uranium deposit, Queensland, Australia: A description of the alteration assemblage associated with uranium mineralisation in diamond drill hole V39. Mineralium Deposita 44, 11-40.

Pollard, P.J., Mark, G., Mitchell, L.C. 1998 Geochemistry of Post-1540Ma Granites in the Cloncurry District, Northwest Queensland Economic Geology 93 (8) p1330-1344.

Radke B. 2009. Hydrocarbon and geothermal prospectivity of sedimentary basins in central Australia; Warburton, Cooper, Perdirka, Galilee, Simpson and Eromanga basins. Geoscience Australia Record 2009/25.

Radke, B.M., Ferguson, J., Cresswell, R.G., Ransley, T.R. and Habermehl, M.A. 2000. Hydrochemistry and implied hydrodynamics of the Cadna-owie – Hooray Aquifer, Great Artesian Basin, Australia. Bureau of Rural Sciences, Canberra

Ramsden, A.R., Dickson, B.L. and Meakins, R.L. 1982. Origin and significance of the Toolebuc gamma-ray anomaly in parts of the Eromanga Basin. Australian Journal of Earth Sciences 29, 285-296

Raznjevic, K. 1976. Handbook of Thermodynamic Tables and Charts. :Hemisphere Publishing Corporation, Washington DC

Reiter, M.A. and Jessop, A.M. 1985. Estimates of terrestrial heat flow in offshore Eastern Canada. Canadian Journal of Earth Sciences 22, 1503-1517.

Reiter, M.A. and Tovar, R.J.C. 1982. Estimates of terrestrial heat flow in Northern Chihuahua, Mexico, Geological Society of America Bulletin 93, 613-624.

Riley, K.W. and Saxby, J.D. 1982. Association of organic matter and vanadium in oil shale from the Toolebuc Formation of the Eromanga Basin, Australia. Chemical Geology 37, 265-275.

Roy, R.F., Beck, A.E., and Touloukian, Y.S. 1981. Thermophysical properties of rocks. In: Touloukian, Y.S., Judd, W.R. and Roy, R.F. (eds) Physical Properties of Rocks and Minerals. New York, McGraw-Hill, 409-502.

Rubenach, M. 2008. Tectonothermal and metasomatic evolution of the Mount Isa Inlier. Project I1 final report April 2005 - July 2008. Mineral system analysis of the Mt Isa-McArthur region, northern Australia. Unpublished pmd*CRC report, Appendix 2, 58 p.

Ruzicka, V., 1993. Unconformity-associated uranium deposits. Geological Association of Canada Special Paper 40, 125-149.

Ryan, A. 1998. Ernest Henry copper-gold deposit. Australasian Institute of Mining and Metallurgy Monograph 22, 759-767.

Schofield, A. 2009. Uranium content of igneous rocks of Australia 1:5000000 maps– Explanatory notes and discussion. Geoscience Australia Record 2009/17, 20pp.

Scrimgeour, I.R., Kinny, P.D., Close, D.F. and Edgoose, C.J. 2005. High-T granulites and polymetamorphism in the southern Arunta region, central Australia; evidence for a 1.64 Ga accretional event. Precambrian Research 142, 1-27.

Selley, D., Broughton, D., Scott, R., Hitzman, M., Bull, S., Large, R., McGoldrick, P., Croaker, M., Pollingotn, N. and Barra, F. 2005. A new look at the geology of the Zambian copperbelt. Economic Geology 100th Anniversary Volume, 965-1000.

Skirrow, R.G., Bastrakov, E.N., Barovich, K, Fraser, G.L, Creaser, R.A., Fanning, C.M., Raymond, O.L., and Davidson, G.J., 2007, Timing of iron oxide Cu-Au-(U) hydrothermal activity and Nd isotopic constraints on metal sources in the Gawler Craton, South Australia: Economic Geology, v. 102, p. 1441-1470.

Skirrow, R.G. 2009 'Hematite-group' IOCG±U ore systems: Tectonic settings, hydrothermal characteristics, and Cu-Au and U mineralizing processes. In: Corriveau, L. and Mumin, H. (eds) Exploring for Iron Oxide Copper-Gold Deposits: Canada and Global Analogues. Shortcourse Notes, GAC-MAC-SEG-SGA 2008, Quebec City, 29-30th May 2008. Geological Association of Canada, in press.

Skirrow, R.G., Jaireth, S., Huston, D.L., Bastrakov, E.N., Schofield, A., van der Wielen, S.E. and Barnicoat, A.C. 2009. Uranium mineral systems: Processes, exploration criteria and a new deposit framework. Geoscience Australia Record 2009/20, 57 p.

Southern Methodist University (SMU) geothermal database – http://www.smu.edu/geothermal/georesou/alldata.csv

Southgate, P.N., Bradshaw, B.E., Domagala, J., Jackson, M.J., Idnurm, M., Krassay, A.A., Page, R.W., Sami, T.T., Scott, D.L., Lindsay, J.F., McConachie, B.A. and Tarlowski, C. 2000. Chronostratigraphic basin framework for Palaeoproterozoic rocks (1730-1575 Ma) in northern Australia and implications for mineralisation. Australian Journal of Earth Sciences 47, 461-485.

Taylor, A.E., Judge, A., and Allen, V. 1986. Terrestrial heat flow from Project Cesar, Alpha Ridge, Arctic Ocean. Journal of Geodynamics 6, 137-76.

Tester, J.W. 1982. Energy Conversion and Economic Issues for Geothermal Energy. Handbook of Geothermal Energy. Gulf Publishing Co., Houston, Texas, 471–586.

Thompson, T.B., 1988. Geology and uranium-thorium mineral deposits of the Bokan Mountain Granite Complex, southeastern Alaska. Ore Geology Reviews 3, 193-210.

Tucker, A. and Ivkovic, K. 1997. GABLOG: The Great Artesian Basin wire-line logged database. Australian Geological Survey Organisation Record 1997/19, 43p

van der Wielen S., Kirkby A, Britt A., Schofield A, Skirrow R., Bastrakov, E., Cross A., Nicoll M, Mernagh T, Barnicoat A., 2009: Large-Scale Exploration Targeting for Uranium Mineral Systems within the Eromanga Basin. In Williams P.J., et. al. (editors) "Smart Science for Exploration and Mining" Proceedings of the Tenth Biennial SGA Meeting, Townsville, 2009 Volume 2 p607-609.

Vigar, A. and Jones, D.G. 2005. Ben Lomond uranium-molybdenum deposit Queensland Australia. Unpublished Technical Report for Mega Uranium Ltd., 37 p.

Wall, V.J., 2006. Unconformity-related uranium systems: Downunder and over the top. Geological Society of Australia Abstracts 82, 4 p.

Walshe, J.L., Cooke, D.R. and Neumayr, P. 2005. Five questions for fun and profit: A mineral systems perspective on metalloginic epochs, province and magmatic hydrothermal Cu and Au deposits. In: Mao, J. & Bierlein, F.P. (eds) Mineral Deposit Research: Meeting the Global Challenge. Springer, Berlin, 477-480.

Welsh, W.D. 2000. GABFLOW: A steady state groundwater flow model of the Great Artesian Basin. Bureau of Rural Sciences, Department of Agriculture, Fisheries and Forestry, Kingston, Australia.

Williams, P.J., Barton, M.D., Johnson, D.A., Fontboté, L., de Haller, A., Mark, G., Oliver, N.H.S., Marschik, R. 2005. Iron oxide copper-gold deposits; geology, space-time distribution, and possible modes of origin. Economic Geology 100th Anniversary Volume5, 371-405.

Withnall, I.W. 1985. Geochemistry and tectonic significance of Proterozoic mafic rocks from the Georgetown Inlier, north Queensland. BMR Journal of Australian Geology and Geophysics 9, 339-351.

Withnall, I.W., Mackenzie, D.E., Denaro, T.J., Bain, J.H.C., Oversby, B.S., Knutson, J., Donchak, P.J.T., Champion, D.C., Wellman, P., Cruikshank, B.I., Sun, S.S. and Pain, C.F. 1997. Georgetown Region. In: Bain, J.H.C. and Draper, J.J. (eds) North Queensland Geology. Australian Geological Survey Organisation Bulletin 240 and Queensland Department of Mines and Energy Geology 9, 19-69.

Withnall, I.W., Neumann, N.L. and Lambeck, A. 2009. Palaeoproterozoic to Mesoproterozoic geology of North Queensland. Australian Institute of Geoscientists Bulletin 49, 129-134.

Whitaker, A.J., Champion, D.C., Sweet, I.P., Kilgour, P., Connolly, D.P., 2007, Surface geology of Australia 1:1,000,000 scale, Queensland - 2nd edition [Digital Dataset] Canberra: The Commonwealth of Australia, Geoscience Australia.

Wyborn, L.A.I. 1987. The petrology and geochemistry of alteration assemblages in the Eastern Creek Volcanics, as a guide to copper and uranium mobility associated with regional metamorphism and deformation, Mount Isa, Queensland. Geological Society Special Publication 33, 425-434.

Wyborn, L. 1998. Younger ca 1500 Ma granites of the Williams and Naraku Batholiths, Cloncurry district, eastern Mt Isa Inlier: geochemistry, origin, metallogenic significance and exploration indicators Australian Journal of Earth Sciences 45(3) p397-411

Wyborn, L.A.I., Heirich, C.A. and Jaques, A.L. 1994, Australian Proterozoic mineral systesm: essential components and mappable criteria. Austalasian Institute of Mining an Metallurgy Publications Series, 5/94, 109-115.

Yang, K., Scott, K., Quigley, M., Huntington, J., Mason, P. and Hewson, R. 2000. Field and airborne mineral mapping in the Mt. Isa Valley, Queensland. CSIRO Restricted Report 752R, 41 pp.

Appendix A -- Tables summarising characteristics of uranium mineral systems

Sandstone-hosted uranium ± vanadium

Question[#]	Ingredients	Reasons	Importance	Mappable/measurable features	Outstanding questions	Scale
1, 2	Intracratonic, continental or intermontane basin	Preferred basin type (see below)	Essential	Basement of continental crust; paleogeography	Nomenclature of basin types?	Continental
1	Deposition of host sandstone in continental fluvial and/or mixed fluvial-marine environment	Generate rocks of high permeability	Essential	Sedimentary facies assemblages and distribution; sequence stratigraphy		Terrane (basin)
1	Age of basin and mineralisation younger than atmosphere inversion at ~2.4 Ga; mostly younger than late Devonian	Younger than 2.4 Ga for oxidising atmospheric conditions; younger than Devonian to ensure presence reactive organic reductant	Essential	Ages of host basin and mineralisation	Are paleoclimates important in producing suitable ore fluids?	Continental
1-5	Evidence of uranium (and related) mineral system activity	Evidence that mineralising process has taken place	Desirable	Distribution of mineral occurrences (U, Cu, V, Co, Pb-Zn, etc)	What is relationship between U and other mineral systems?	Continental to terrane (basin)
2	Topographic gradient (preferably 5-10°) at time of mineralisation, for instance: • Primary depositional dip • Tilting of sequence due to reactivation of basin margin faults • Change in continental stress fields (e.g. compression or extension) • Basinal subsidence • Doming	Topography of basin providing hydraulic head and fluid flow towards an outflow zone	Essential	Geometry of basin, at time of mineralisation, as determined from field mapping, sedimentary facies, structural measurements, depth-to-basement (Euler deconvolution and/or drill hole data), seismic, gravity, MT and AEM data. Structural/movement history, including neotectonics		District (camp)
2, 4	Embayments of basin into basement	Focus of ore fluids into district??	Desirable	Geometry of basin	What is importance: fault control; proximity to granite; facies variations?	District (camp)
3	Low temperature (<50°C), highly oxidised (initially air-saturated) fluid	Fluids most suitable for high U solubilities	Essential	Fluid inclusion data; other methods of estimating temperature, modern hydrochemistry (?), diagenetic history, alteration assemblages[1]	Are there any other fluid types that could transport U in this setting? Is silica content of fluids important?	District (camp) and deposit
3	Source of highly oxidised fluids • Recharge zone in hydrologic upland area • Other sources	Chemistry allowing high U solubility	Essential	O-H isotopes; alteration assemblages[1] (e.g. hematite-stable); upland areas at time of mineralisation for hydrologic recharge	Are paleoclimates important in producing suitable fluids? Are there other ways to get highly oxidised fluids?	District (camp)
3, 4	Preservation of redox state of fluids during migration controlled by fluid flow rates sufficient to move the redox roll front	Chemistry maintaining high U solubility	Essential	Alteration assemblages[1], hydrology of fluid flow at time ofmineralisation	Are evaporites important in maintaining redox state of fluids?	District (camp)
3	Leachable U-enriched source, fitting one or more of the following: • U-rich felsic rocks rimming and/or underlying the basin. • Lithic fragments of felsic rocks (including volcanic ash) in the sandstone aquifer. • Leachable detrital U-rich minerals (zircon, monazite, allanite, apatite etc) in sandstone • Felsic volcanics in and/or close proximity to the sandstone aquifer • Uranium occurrences in hinterland	Uranium source	Leachable U: essential; U enrichement: highly desirable	U enrichment indicated by γ-ray spectrometric data and geochemical analyses of potential sources	Which are more important U sources: basement rocks or sediments eroded from basement rocks? If basement U is important source, how do fluids from basement get into sandstone aquifer? Can you make a U deposit from a garden variety source?	Terrane (basin)
3	Leaching of potential U sources	Uranium source	Desirable	U depletion zones as indicated by γ-ray spectrometric data, wire-line logs and geochemical analyses; oxidised paleoweathering profiles		District (camp) and terrane (basin)
4, 2	Hydrologically connected, highly permeable, unlithified, immature (feldspathic-arkosic) sandstone (less commonly pebble conglomerate or eolian siltstone/sandstone) as aquifer and ore host	Fluid pathway and redox buffer at time of mineralisation	Essential	Lithostratigraphy, sequence stratigraphy, permeability and diagenetic and cement history of potential host		District (camp)
4	Lateral and vertical variations in permeability focussing fluid flow in aquifer	Fluid conduit	Essential	Litho- and sequence stratigraphy; facies distribution; structural mapping; mapping of shales/siltstone and other impermeable rocks	How important are silcretes as aquicludes? How important are aquicludes, paleochannels, etc in determining size and grade of deposits?	District (camp)
4, 5	Regional gradation from oxidized (upstream) to reduced conditions (downstream) in host sandstone	Redox boundary in plumbing/trap system	Essential	Mineral occurrences and regional mapping of alteration assemblages[1] and geochemistry[2] in host sandstone; mapping of hydrochemical gradients[3] in groundwater from regional aquifers		Terrane (basin) to deposit
5	Presence of reductants, including: • Solid carbonaceous material (e.g. woody material, coal, humic/humate components • Hydrocarbons and/or H_2S (derived from reservoir or coal seams) that are focussed into deposition site along pathways including local structures and permeable facies • Inorganic reductants (e.g., Fe^{2+}-rich rocks, sulphides (particularly pyrite) and/or H_2S)	Reduction of uranium-carrying fluids and deposition of uranium	Essential	EM contrasts/conductors; drill hole logs from water and exploration drill holes; sedimentary facies analysis; structural mapping (including distribution and history of movement of second and third order structures, potential field data); hydrocarbon shows; alteration facies along permeable pathways; C-O and S isotopes of ore-related minerals		District (camp)
5	Uranium deposition caused by water-rock interaction and fluid mixing from • Reduction (the major factor) • pH changes • changes in silica saturation • changes in vanadium saturation	Chemical trap for uranium (and vanadium)	Essential	Mineral occurrences. Zoning about ore as follows: Oxidized (brown/red) sandstone with total oxidation of pre-existing sulphide minerals→ Se enrichment → U ores±silcrete → Mo and sulphide mineral enrichment/replacement of Fe-bearing silicates and silicates → reduced (green/gray) sandstone± silcrete. Groundwater zonation from upstream to downstream as follows: high (oxidized) Eh → ore → low (reduced) Eh. Redox and related reactions may also be reflected in δD, $\delta^{13}C$, $\delta^{18}O$, $\delta^{34}S$ and U-series disequilibria variations in rock and in groundwater.	What is the relation between silcrete, silica saturation, coffinite and ore depositional processes?	District (camp) and deposit
6	Insulation of ores from reaction with oxidised groundwater flows	Preservation of ore deposit	Essential	Regional redox and chemical gradients in aquifers; post-mineralisation tectonic and climate history		Terrane (basin), District (camp) and deposit

[#]Questions are as follows:
(1) What are the geodynamic and P-T histories (including timing of mineralisation) of the system?
(2) What is the structural and lithological architecture of the system?
(3) What and where are fluid reservoirs and metal sources for the mineral system?
(4) What are the fluid flow drivers and pathways?
(5) What are the metal (and ligand) transport and depositional processes?
(6) What are the effects of post-depositional processes on metal accumulations?

[1]Alteration assemblages can be mapped using rock colour, PIMA, whole rock geochemistry, isotope geochemistry, geophysical properties (aeromagnetics, radiometrics and gravity) at hand sample and regional scales) on outcrop and drill material, and using potential field inversion and hydrochemistry (including isotopes).
[2]Alteration geochemistry can be mapped using mineralogy, redox (e.g., $FeO/(FeO+Fe_2O_3)$, and S, C, Fe, Mo, V, etc. abundances.
[3]Particularly pH, Eh, carbon (CO_2 and CH_4) and sulphur (SO_4 and H_2S) contents, salinity, and stable and radiogenic isotopes.

Unconformity-related uranium

Question[#]	Ingredients / process	Reasons	Importance	Mappable/measurable features	Outstanding questions	Scale
1, 2	Intracratonic, epicontinental or foreland basin unconformably overlying U-rich basement rocks (e.g.. granite-gneissic domes and/or inliers and/or felsic (meta)sediments)	Preferred basin type (see below)	Essential	Unconformity between reduced basement and overlying oxidising aquifer/basin; paleogeography	Are foreland basins important?	Continental
1	External changes in plate stress	Initiate fluid flow	Highly desirable	Major changes to apparent polar wander paths	What other mechanisms initiated fluid flow (e.g. convection, compaction)? How do we map these effects?	Continental
1	Clock-wise P-T-t path to metamorphism of the basement rocks	Unknown	Unknown	Determination of metamorphic P-T-t paths in basement	Is this important (or a furphy)? If so, why?	Continental to terrane (basin)
1-5	Evidence of uranium (and related) mineral system activity	Evidence that mineralising process has taken place	Desirable	Distribution of mineral occurrences (U, Cu, V, Co, Pb-Zn, etc)	What is relationship between U and other mineral systems?	Continental to terrane (basin)
2, 4	Major disconformity (generally unconformity) between basement and overlying basin	Juxtaposes oxidised & reduced rocks	Essential	Spatial distributions and ages of major unconformities from solid geology maps and geophysical data sets (e.g. gravity, aeromagnetics and land seismic)	Can low-angle thrusts or detachments serve same purpose as unconformity? Is unconformity a fluid pathway? Can unconformity U deposits form if discontinuity has been folded?	Terrane (basin)
2, 4	Oxidised Fe^{2+}-poor highly permeable sandstones that overlie the unconformity	Possible source & conduit for (buffered) oxidised, U-bearing fluids	Essential	Distribution of oxidised sandstone; sedimentary facies assemblages and distribution; sequence stratigraphy; diagenetic and cement history; redox variations; permeability	What is diagenetic history of basal sandstone of basin? Effect of diagenesis on permeability? How "clean"?	Terrane (basin) and district (camp)
2	Periodic reactivation of basement faults during and after basin development,	Control of (sub)-basin accommodation, palaeo-relief, architecture and later fluid flow	Essential	Relative and absolute timing of fault movement relative to units in basin and basement; changes in unit thickness	Role of extension vs compression? Are all deposits in reverse faults?	Terrane (basin) to district (camp)
2	Close association of deposits with gravity highs and/or ridges	Unknown; possible basement highs or major structures?	Unknown	Variations in the gravity field; deep seismic	What are sources of gravity anomalies?	Terrane (basin)
2	Onlapping relationship between basin and basement	Unknown	Unknown	Sequence strat	Is role of onlap the juxtaposition of sandstone on basement?	Basin
3	Leachable U-enriched source, fitting one or more of the following: • U-rich felsic rocks rimming and/or underlying the basin. • Lithic fragments of felsic rocks (including volcanic ash) in aquifer. • Leachable detrital U-rich minerals (zircon, monazite, allanite, apatite etc) in sandstone • Felsic volcanics within and/or close stratigraphic proximity to the aquifer	Uranium source	Leachable U: essential; U enrichment: highly desirable	U enrichment indicated by γ-ray spectrometric data and geochemical analyses of potential sources	Which are more important U sources: basement rocks or sediments eroded from basement rocks? If basement U is important source, how do fluids from basement get into aquifer? Can you make a U deposit from a garden variety source?	District (camp) and terrane (basin)
3	Moderate temperature (~150-200°C), saline oxidised fluid derived through diagenesis in overlying basin	Fluids most suitable for high U solubilities	Essential	Fluid inclusion data; other methods of estimating temperature, diagenetic history, alteration assemblages[1]	Are there any other fluid types that could transport U in this setting? Is silica content of fluids important? Importance of Na vs. Ca in brines?	District (camp) and deposit
3	Source of highly oxidised fluids, e.g.: • Diagenetic fluids buffered by evaporites • Connate brines • Evolved meteoric waters • Seawater	Chemistry allowing high U solubility	Essential	O-H isotopes; alteration assemblages[1] (e.g. hematite-stable); distribution of evaporites (particularly gypsum, anhydrite) in basin	Are there other ways to get highly oxidised fluids?	District (camp)
3, 4	Preservation of redox state of fluids during migration controlled; low abundance of reductants	Chemistry maintaining high U solubility	Essential	Alteration assemblages[1], hydrology of fluid flow at time of mineralisation, distribution of reductants (e.g. FeO and organic matter) in sandstone above unconformity	Are evaporites important in maintaining redox state of fluids?	District (camp)
4	Lateral and vertical variations in permeability focussing fluid flow in aquifer: • Lithological variations. • Diagenetic destruction or creation of porosity/permeability.	Fluid conduits and aquicludes / aquitards	Essential	Litho- and sequence stratigraphy; facies distribution; structural mapping; mapping of shales/siltstone and other impermeable rocks; diagenetic cement history	How important are aquicludes, etc in determining size and grade of deposits?	District (camp)
4, 5	Regional to district alteration: • in basal sandstone aquifer, including regional illite-kaolin alteration, silicification and oxidation • along basement penetrating faults including chlorite, illite-kaolinite	Record of passage of uraniferous fluids through sandstone aquifer and into basement	Essential	Mineral occurrences and regional mapping of alteration assemblages[1] (particularly Fe-chlorite-sericite assemblages) and geochemistry[2] in basal sandstone & basement	Is this alteration zoned?	Terrane (basin) to deposit
4, 5	Presence of reductants, including: • Carbonaceous material (e.g. graphitic shale) • Hydrocarbons and/or H_2S in reduced fluids • Inorganic reductants (e.g., Fe^{2+}-rich rocks, sulphides and/or H_2S)	Reduction of uranium-carrying fluids and deposition of uranium	Essential	EM contrasts/conductors; drill hole logs from water and exploration drill holes; sedimentary facies analysis; structural mapping (including distribution and history of movement of second and third order structures, potential field data); alteration facies along permeable pathways; C-O and S isotopes of ore-related minerals	Is graphite really effective as a reductant at 150-200ºC?	District (camp)
5	Zones of faulting and brecciation, particularly in basement	Facilitate mixing, permeability & fluid-rock interaction	Desirable	Trace of faults as determined from geological, aeromagnetic and gravity data	What other mechanisms can produce secondary permeability?	Deposit
5	Association of calcareous rocks with reduced rocks in basement	pH neutraliser of the basinal fluids	Unknown	Distribution of carbonates in basement	Role re: Cu, Au, PGEs?	Deposit
5	Uranium deposition caused by water-rock interaction and fluid mixing from • Reduction (the major factor) • pH changes	Chemical gradient for uranium (and copper, gold and PGEs)	Essential	Mineral occurrences. Zoning of alteration assemblages from ore as follows: Ingress-type (basement-hosted ores): Fe-Mg chlorite → biotite±sudoite → sudoite±illite → illite±sudoite Egress-type (sandstone-hosted ores): biotite±sudoite Fe-Mg chlorite → sudoite±illite → illite±sudoite. Redox and related reactions may also be reflected in δD, $\delta^{13}C$, $\delta^{18}O$ and $\delta^{34}S$.		District (camp) and deposit
6	Presence of thick (~3-5km?) cover sequence above unconformity at time of mineralisation	Better chance of preservation; allows temps of ~150-200ºC to be reached in aquifer/source	Desirable	Thickness of cover sequence		Terrane (basin)
6	Preservation of sandstone above basement, particularly for ingress-type deposits	Preservation of ores	Essential	Distribution of preserved sandstone above unconformity		District (camp) to deposit

[#]Questions are as follows:
(1) What are the geodynamic and P-T histories (including timing of mineralisation) of the system?
(2) What is the structural and lithological architecture of the system?
(3) What and where are fluid reservoirs and metal sources for the mineral system?
(4) What are the fluid flow drivers and pathways?
(5) What are the metal (and ligand) transport and depositional processes?
(6) What are the effects of post-depositional processes on metal accumulations?

[1]Alteration assemblages can be mapped using rock colour, PIMA, whole rock geochemistry, isotope geochemistry, geophysical properties (aeromagnetics, radiometrics and gravity) at hand sample and regional scales) on outcrop and drill material, and using potential field inversion and hydrochemistry (including isotopes).
[2]Alteration geochemistry can be mapped using mineralogy, redox (e.g., $FeO/(FeO+Fe_2O_3)$, and S, C, Fe, Mo, V, etc. abundances.
[3]Particularly pH, Eh, carbon (CO_2 and CH_4) and sulphur (SO_4 and H_2S) contents, salinity, and stable and radiogenic isotopes.

Metasomatic uranium

Question[#]	Ingredient / process	Reason	Importance	Mappable/measurable characteristics	Outstanding questions	Scale
1	High T Low P orogen, possibly with anti-clockwise PTt path (Upper greenschist or higher) (syn-peak metamorphism)	Unknown	Unknown	Metamorphic facies, PTt paths, zones of high mica crystallinity (from ASTER/PIMA/HyMap)	Why is this ingredient important?	Continental to terrane
2	Crustal level at around the brittle-ductile transition	Creation of dilatant zones for fluid flow	Unknown	Metamorphic facies, style of deformation	Why is this ingredient important?	Continental to terrane
2, 4	Crust-penetrating shear/fault zones separating crustal blocks or orogens	Magma & fluid pathways from mantle & lower crust to near-surface	Unknown	PTt variations across crustal block boundaries, geophysical responses of deep crustal fault/shear zones, gradients in geophysical properties (magnetics, gravity), gradients in Pb and Nd isotopes	Not clear if this is necessary	Terrane to district (camp)
3, 4	Moderate to high temperature (~300-700°C?) CO_2-/F-/P?-rich Na-dominated magmatic-hydrothermal fluids, (H_2O-poor)	Carries U^{6+} and/or U^{4+} depending on redox of melt	Unknown	Look for carbonates, phosphates and fluorite, LOI, lack of abundant hydrous minerals, depth of water feature in PIMA spectra	How abundant are F and P?	District (camp) to deposit
3	Leaching of U from U-rich rocks (including (meta)granites, (meta)sediments)	Generates hydrothermal U ore fluid via leaching of pre-existing U-rich igneous rocks	Desirable	Th/U ratios from radiometrics (normalised to geology) and WR geochemistry	Magma vs host rock sources of U? Magmatic vs external source of fluid? Are U and Th co-transported in the same fluid?	District (camp)
2, 4	Regional to deposit scale flow of high- to moderate-T fluids	Large U deposits require very large volumes of fluid	Highly desirable	Regional to deposit scale albitic or carbonate alteration zones[1], loss of K (e.g., low K/Th in radiometrics), low abundance of hydrous minerals		District (camp) to deposit
4	Strong structural control	Focusing of fluid flow	Highly Desirable	Fault length (worms), fault density, seismic data, MT data		Terrane to district (camp)
5	U^{6+} deposition via fluid-rock reaction (reduction, pH change, activity of ligands, etc): • Fe^{2+} oxides, silicates, carbonates • And/or sulfides, H_2S • And/or reduced C, CH_4 • a_{Ca2+}	Fe^{2+}-bearing oxides, silicates, carbonates, sulfides or reduced gases may act as reductants for U^{6+}; deposition of U from U^{4+}-F complexes via fluorite formation	Desirable	Presence of Fe^{2+}-bearing oxides, silicates, sulfides, carbonates; presence of fluorite	Fluid inclusion characteristics?	District (camp) to deposit
5	U^{6+} or U^{4+} deposition via cooling, e.g. by fluid mixing/unmixing		Desirable	Evidence for cooling, fluid mixing		District (camp) to deposit
5	Progressive oxidation of alteration assemblage	Indicates gradients in physico-chemical environment	Unknown	PTt paths as indicated by alteration assemblages	Result of cooling and/or uplift? Is this reflected in PTt paths of alteration and ore minerals?	Deposit

[#]Questions are as follows:
(1) What are the geodynamic and P-T histories (including timing of mineralisation) of the system?
(2) What is the structural and lithological architecture of the system?
(3) What and where are fluid reservoirs and metal sources for the mineral system?
(4) What are the fluid flow drivers and pathways?
(5) What are the metal (and ligand) transport and depositional processes?
(6) What are the effects of post-depositional processes on metal accumulations?

[1]Alteration assemblages can be mapped using rock colour, PIMA, whole rock geochemistry, isotope geochemistry, geophysical properties (aeromagnetics, radiometrics and gravity) at hand sample and regional scales) on outcrop and drill material, and using potential field inversion and hydrochemistry (including isotopes).

Uranium-bearing iron oxide copper-gold

Question[#]	Ingredient / process	Reason	Importance	Mappable/measurable characteristics	Outstanding questions	Scale
1	Passive margin or intracontinental extension (pre-IOCG)	Sedimentary-volcanic rocks in subaerial to shallow water basin settings provide sources of metals and salinity, and maintain fluid redox at intermediate to high levels	Unknown	Passive margin or intracontinental extensional basins; (meta)evaporite sequences	Importance of pre-IOCGU setting? Can other settings provide similar sources & buffering?	Continental to terrane
1	Pre- to syn-IOCGU orogenesis on margin of craton; terrane accretion; multiple pre-IOCGU magmatic events	Pre-IOCGU orogenesis and/or terrane accretion provides crustal-scale fluid pathways; pre-IOCGU magmatism provides source for U-rich A-type syn-IOCGU magmas	Desirable	Syn-orogenic pre-IOCGU granitoids; metamorphic belts; crustal-scale faults/shears	Tectonic setting of orogenesis and A-type magmatism not well understood	Continental to terrane
1, 4	Major (mantle-driven?) thermal anomaly at IOCGU time; LPHT metamorphism	High geothermal gradients; formation of A-type U-rich melts including volcanics; mantle melts are source of some metals; LPHT indicative of high geothermal gradients regionally, needed to maintain high temps of fluids in near-surface; drives convection of brines deep into basement	Essential	A-type U-rich crustal melts emplaced at shallow levels; alkaline mafic magmatism; region may also have high-T I-type crustal melts & co-magmatic volcanics; LPHT metamorphic assemblages in syn-IOCGU orogens but not necessarily in shallow-crustal IOCGU districts	Tectonic setting of orogenesis and A-type magmatism not well understood; are U-bearing IOCG systems found only distally from regions of exposed highest grade LPHT metamorphism? Are thermal anomalies mantle-derived or radiogenic in origin? Not clear if convection was necessary, or if single-pass systems	Continental to district (camp)
1	Presence of shallow U-rich A-type granitoids and/or volcs immediately pre- to syn-IOCGU	Exposure of U-rich sources to shallow oxidised fluids	Essential	Cooling ages of exhumed basement same as intrusions & mineralisation (unless reset)	Exhumation of granites less important if volcanics or cover sandstones are source of U (?)	Terrane to district (camp)
1	Age of mineralisation younger than atmosphere inversion at ~2.5 Ga	Oxidising atmosphere	Essential	Age of mineralisation & associated magmatism	Is 2.5Ga the earliest that IOCG deposits formed (or could form)? Is <2.5Ga age required for U-rich IOCG?	Continental
2, 4	Crust-penetrating shear/fault zones separating crustal blocks or orogens; district scale fault networks reactivated during IOCGU	Magma & fluid pathways from mantle & lower crust to near-surface; permeability control on flow of deep-sourced and possibly meteoric fluids	Highly desirable	PTt variations across crustal block boundaries; geophysical responses of deep crustal fault/shear zones; IOCG-related alteration along faults; ages of fault movement	Is crustal block boundary universal to IOCGUs, or just Olympic Dam? (Mt Isa , Iberia?). Extensional or compressional or strike-slip?	Terrane to district (camp)
2	Close association of deposits with gradients of major gravity ridges	Gradients represent crustal block boundaries (major fluid pathways)	Desirable	Gravity data (upward continued); worms		Terrane

2	Brecciation at high crustal level; diatreme / maar volcanic setting	High permeability fluid pathways; maar volcanism indicative of high geothermal gradient & presence of groundwaters	Essential	Breccias of hydrothermal, and/or tectonic and/or phreato-magmatic origins; volcanological evidence for maar / diatreme setting	Not clear if breccias are essential for U-rich IOCG (OD cf. Wirrda Well, Oak Dam); drivers of hydrothermal brecciation unclear – CO_2 driven? Is diatreme/maar essential, or simply represents a thermal centre and topographic low in the hydrologic system?	District (camp) to deposit
2	Cover sequence of permeable, oxidised, U-rich sediments or volcanics, overlying basement with IOCG deposits/alteration	Source of U; pathways for meteoric fluid flow	Desirable	Clastic red beds; hematitic altered felsic volcanics /volcaniclastics; U-depleted where leached; U-rich where least altered; evidence of high permeability	Role of cover sequence versus basement as source of U unclear; potential for "unconformity-related" U hybrids?	Terrane to district (camp)
3, 4	Moderate to high temperature (300-550°C) Fe-rich (hyper)saline brine, magnetite- (to ?hematite-) stable	Carries Fe (±S, Cu) to form Fe^{2+}-bearing oxides, silicates, carbonate & sulfides, which may act as reductants for U^{6+}	Essential	Presence of fossil mod-high-T brines trapped in hydrothermal minerals	Is magnetite-stable brine necessary, or is the high-T brine only hematite-stable in some systems? Are U and REE carried in this brine? Magmatic versus non-magmatic contributions? Role of alkaline mafic sources of U, REE, Cu, Au?	District (camp) to deposit
3, 4	Low-moderate temperature (150-250°C) oxidised brines of variable salinity, hematite-stable; evolved meteoric waters	Assumed to transport U^{6+}	Essential	Presence of fossil low-mod-T brines trapped in hydrothermal minerals; evidence for preserved palaeosurface (IOCG time) close to current surface	Are these fluids what differentiate IOCGU from IOCGs? Could sandstones overlying basement be U source, in a post-IOCG U model?	District (camp) to deposit
3	Evaporite or ex-evaporite bearing sequences in basement and/or cover	Sources of Cl^- for complexing of Fe, Cu; source of CO_3^- and SO_4^{2-} for complexing of U; buffered redox state of fluids to moderate to oxidised levels	Unknown	Presence, extent and distribution of evaporite or ex-evaporite minerals (e.g. scapolite) and related rocks; fluid inclusion evidence (e.g. Br/Cl) suggestive of interaction of fluids with evaporites	Source of salts in either high- or low-moderate T brines poorly constrained; however, a non-magmatic contribution is present	Terrane (basin) to district (camp)
3	U-enriched granites or gneisses in basement or U-rich volcanic rocks and/or sandstones in cover	Sources of U	Essential	U enrichment indicated by γ-ray spectrometric data and geochemical analyses of potential sources	Not clear if source(s) of U are syn-IOCG granites and/or volcanics (syn-IOCG model) and/or overlying sandstones (post-IOCG model)	Terrane (basin) to district (camp)
3	Leachable U source, e.g. uraninite, metamict/altered monazite, allanite, etc.	U must be available for leaching, not locked in resistant minerals	Essential	Mineralogy and leaching characteristics of U sources	Mineralogy of U sources unknown; magmatic-hydrothermal vs host rock sources of U?	Terrane (basin) to district (camp)
3	Leaching of potential U sources	Indicates removal and uptake of U by fluids	Desirable	Loss of U associated with regional alteration of and/or palaeo-regolith development on potential source rocks; evidence of alteration of monazite and other U-bearing minerals in potential U source	Magmatic-hydrothermal vs host rock sources of U?	District (camp) to deposit
4	Topography	Drives flow of meteoric waters towards IOCG depositional zones, and possibly contributes to deep flow	Unknown	Palaeogeographic evidence for hydrological head, or evidence for deeper circulation	Essential if U introduced by (evolved) meteoric waters	Terrane to district (camp)
2, 4	Regional flow of high-T brines	Large IOCGU deposits require very large volumes of fluid	Essential	Mapping of regional magnetite-bearing albite or K-feldspar alteration zones[1]		District (camp) to deposit
2, 4	Regional flow of low-T evolved meteoric waters towards IOCG	Large IOCGU deposits require very large volumes of fluid	Essential	Mapping of proximal hematite-sericite-chlorite-carbonate alteration[1]; hematitic zones with U may be above or lateral to any magnetite-bearing zones		District (camp) to deposit
5	Reductant: • Fe^{2+} oxides, silicates, carbonates • And/or sulfides • And/or reduced C	Fe^{2+}-bearing oxides, silicates, carbonate & sulfides may act as reductants for U^{6+}	Essential	Presence of Fe^{2+}-bearing oxides, silicates, sulfides, carbonates; presence of alkali feldspars (albite in deeper zones, K-feldspar in shallower zones)	Is minor U introduced in early Fe oxide stage? Was U transported as F^- or other complexes in magnetite-stable brine?	District (camp) to deposit
5	Late stage oxidation of earlier alteration assemblages	Indicates influx of oxidised fluids, possibly carrying U^{6+}; deposition by fluid-rock reaction	Essential	Late stage overprint of hematitic alteration & U mineralisation; associated with chlorite, sericite, carbonate	What U complexes were critical, and how oxidised were fluids? How do (evolved) meteoric waters maintain high oxidation state? Significance of evaporites?	District (camp) to deposit
5	Fluid mixing	U deposition by reduction of U^{6+} via mixing with reduced fluid; can produce high grades	Desirable	Evidence for two fluids, e.g. barite, fluid inclusion evidence, isotopic evidence	Role of mixing versus two-stage fluid-rock reaction unresolved; can either produce ore-grade U?	Deposit
6	Cratonisation during or before IOCGU formation	Preserves near-surface setting of U-bearing IOCG systems, without excessive erosion	Essential	Lack of evidence for major tectonothermal events post-IOCG (i.e. require minimal erosion of IOCG setting)	If deeper IOCG systems also contain U (present answer is no), then this criterion is non-essential.	Continental to terrane
6	Basin formation over basement-hosted U-bearing IOCG	Minimises effects of weathering and erosion of IOCGU deposit	Desirable	Presence of basin not much younger than IOCGU systems	Is the basin an active part of U-bearing IOCG system, or simply a preserving blanket?	Terrane (basin) to district (camp)

[#]Questions are as follows:
(1) What are the geodynamic and P-T histories (including timing of mineralisation) of the system?
(2) What is the structural and lithological architecture of the system?
(3) What and where are fluid reservoirs and metal sources for the mineral system?
(4) What are the fluid flow drivers and pathways?
(5) What are the metal (and ligand) transport and depositional processes?
(6) What are the effects of post-depositional processes on metal accumulations?

[1]Alteration assemblages can be mapped using rock colour, PIMA, whole rock geochemistry, isotope geochemistry, geophysical properties (aeromagnetics, radiometrics and gravity) at hand sample and regional scales) on outcrop and drill material, and using potential field inversion and hydrochemistry (including isotopes).

Orthomagmatic uranium

Question[#]	Ingredient / process	Reason	Importance	Mappable/measurable characteristics	Outstanding questions	Scale
Q1	Pre-existing metasomatised mantle, eg via subduction	Fertile source for alkaline magma generation	Unknown	Mafic rock isotopic compositional variation at craton/province scale	Do provinces with magmatic-related U have distinctive mantle?	Continental to terrane
1	Melting of continental crust	Generates felsic magmas which may be enriched in U	Essential	Distribution of felsic igneous rocks		Continental to terrane
1	High temperature melting of the crust	Breaks down U-bearing phases, liberating U into the melt	Desirable	Geothermometry, zircon saturation temperatures	How much U can be liberated into the melt during low degree partial melting at low temperatures?	Terrane
3	Differentiation & fractional crystallisation in crustal magma chambers	Magmatic concentration of HFSE	Essential	Igneous fractionation geochemical trends; highly fractionated granitoids	How much magmatic concentration is required? Or are magmatic-hydrothermal processes sufficient to yield U ore fluid?	District (camp) to deposit
1, 3, 4	Orogenesis followed by extensional collapse	May result in shallow emplacement of HFSE-enriched magmas including volcanics	Desirable	Late-orogenic basins associated with alkaline or A- or I-type HFSE-enriched igneous complexes; high-level intrusives and volcanics	Not relevant to intracontinental rift-related alkaline magmatism (?)	Continental to terrane
1	Melting of U-rich basement	Basement with pre-existing high concentrations of U will produce melts which are enriched in U with partial melting	Desirable	Distribution of high U igneous rocks		Terrane
3	High U solubility in a magma accompanying fractional crystallisation	High U solubilities prevent the early crystallisation of U-bearing phases, allowing U to concentrate in the melt with progressive differentiation	Desirable	High concentrations of solubility-enhancing agents, peralkalinity		District (camp) to deposit
3, 4	Leaching of U from HFSE-rich igneous rocks by fluids	Generates localised enrichment in U	Desirable	Rock description which suggest high leachability (eg. “glassy”)		District (camp) to deposit
5	U^{6+} deposition via fluid-rock reaction (reduction, pH change, activity of ligands, etc): • Fe^{2+} oxides, silicates, carbonates • And/or sulfides, H_2S • And/or reduced C, CH_4 • a_{Ca2+}	Fe^{2+}-bearing oxides, silicates, carbonates, sulfides or reduced gases may act as reductants for U^{6+}; deposition of U from U^{4+}-F complexes via fluorite formation	Desirable	Presence of Fe^{2+}-bearing oxides, silicates, sulfides, carbonates; presence of fluorite; reactants for U deposition may be within igneous host itself or external, in wall rocks proximal to distal from intrusion/volcanic rocks		District (camp) to deposit
5	U^{6+} or U^{4+}deposition via cooling, eg by fluid mixing		Desirable	Evidence for cooling, fluid mixing		District (camp) to deposit
6	U enrichment	Produces localised zones of high grade mineralisation	Desirable	Enrichment of U relative to thorium, yielding Th/U ratios lower than those expected for typical fractional crystallisation		District (camp) to deposit

[#]Questions are as follows:
(1) What are the geodynamic and P-T histories (including timing of mineralisation) of the system?
(2) What is the structural and lithological architecture of the system?
(3) What and where are fluid reservoirs and metal sources for the mineral system?
(4) What are the fluid flow drivers and pathways?
(5) What are the metal (and ligand) transport and depositional processes?
(6) What are the effects of post-depositional processes on metal accumulations?

[1]Alteration assemblages can be mapped using rock colour, PIMA, whole rock geochemistry, isotope geochemistry, geophysical properties (aeromagnetics, radiometrics and gravity) at hand sample and regional scales) on outcrop and drill material, and using potential field inversion and hydrochemistry (including isotopes).

Magmatic-hydrothermal uranium

Question[#]	Ingredient / process	Reason	Importance	Mappable/measurable characteristics	Outstanding questions	Scale
1, 3	Source of U	U source provides metals for the mineral system	Essential	Distribution granites containing high average U	Can a granite with low U contents provide enough metal to form a deposit?	Terrane
2	Host rocks for mineralisation	Suitable host rocks are required for skarn formation	Desirable	Distribution of pre-intrusion carbonates	Are other lithologies amenable to forming magmatic-hydrothermal deposits?	Terrane to deposit
2, 4	Fluid flow pathways	Provide pathways for fluids for post-magmatic concentration of U	Essential	Faults		District (camp) to deposit
4	Fluid flow focusing	Focuses fluid flow to yield high U grades	Highly desirable	Contact metamorphic aureoles		District (camp) to deposit
3	Leaching of U from U-rich granites by magmatic-hydrothermal or metamorphic fluids	Generates hydrothermal U ore fluid via leaching of pre-existing U-rich rocks	Essential	??	Magmatic vs external source of fluid?	District (camp) to deposit
4	Regional to deposit scale flow of high- to moderate-T fluids	Large U deposits require very large volumes of fluid	Highly desirable	Regional to deposit scale albitic alteration zones[1]		District (camp) to deposit
5	U^{6+} deposition via fluid-rock reaction (reduction, pH change, activity of ligands, etc): • Fe^{2+} oxides, silicates, carbonates • And/or sulfides, H_2S • And/or reduced C, CH_4 • a_{Ca2+}	Fe^{2+}-bearing oxides, silicates, carbonates, sulfides or reduced gases may act as reductants for U^{6+}; deposition of U from U^{4+}-F complexes via fluorite formation	Desirable	Presence of Fe^{2+}-bearing oxides, silicates, sulfides, carbonates; presence of fluorite; reactants for U deposition may be within igneous host itself or external, in wall rocks proximal to distal from intrusion/volcanic rocks		District (camp) to deposit
5	U^{6+} or U^{4+}deposition via cooling, eg by fluid mixing		Desirable	Evidence for cooling, fluid mixing		District (camp) to deposit
1, 6	Metamorphic-driven fluid flow	Provides the fluids integral to forming large deposits	Highly desirable	Metamorphic grade maps		Terrane

[#]Questions are as follows:
(1) What are the geodynamic and P-T histories (including timing of mineralisation) of the system?
(2) What is the structural and lithological architecture of the system?
(3) What and where are fluid reservoirs and metal sources for the mineral system?
(4) What are the fluid flow drivers and pathways?
(5) What are the metal (and ligand) transport and depositional processes?
(6) What are the effects of post-depositional processes on metal accumulations?

[1]Alteration assemblages can be mapped using rock colour, PIMA, whole rock geochemistry, isotope geochemistry, geophysical properties (aeromagnetics, radiometrics and gravity) at hand sample and regional scales) on outcrop and drill material, and using potential field inversion and hydrochemistry (including isotopes).

Instructions for the CD-ROM

An assessment of the uranium and geothermal potential of north Queensland

This CD-ROM contains the above-titled Report as;
Record 2010/14.pdf

And plates;
p1_SHU_v2_300dpi
p2_SHU_channels_v2_300dpi
p3_unconformity_v2_300dpi
p4_metasomatic_v2_300dpi
p5_IOCGU_v2_300dpi
p6_orthomag_v2_300dpi
p7_mag_hydro_v2_300dpi
p8_hot_rock_v2_300dpi
p9_HSA_v2_300dpi

View this .pdf document using Adobe Acrobat Reader (click Adobe.txt for information on readers)

Click on: Record 2010/14.pdf to launch the document.